GCAGS JOURNAL A Publication of the Gulf Coast Association of Geological Societies www.gcags.org

The Smackover-Norphlet Petroleum System, Deepwater Gulf of Mexico: Oil Fields, Oil Shows, and Dry Holes

Theodore J. Godo

Huntsville, Texas 77340, U.S.A.

ABSTRACT

Exploration for oil in the Norphlet Formation of the deepwater Gulf of Mexico, has resulted in wells with major discoveries, economic tie-back discoveries, sub-commercial discoveries and dry holes. The Norphlet petroleum system is defined by the adjacent stratigraphic formations of the Norphlet reservoir with the overlying source rock and seal of the Smackover formation. The two formations lie directly on top of the Louann Salt, also an underlying seal. Examples of the Norphlet field sizes range between the giant Appomattox Oil Field (Mississippi Canyon [MC] block 392) and much smaller and economically challenged oil fields such as Gettysburg (De Soto Canyon [DC] block 398) and Shiloh (DC 269). Appomattox is the first Norphlet field to be producing oil with its first production having started in May 2019. The petroleum system has also yielded smaller volumes of only residual oil (Leesburg–MC 475), and residual oil columns below a thinner, live oil column (Titan–DC 178) and Antietam (DC 269). In other wells, the Norphlet is devoid of oil shows even when the overlying Smackover source rock is present and sufficiently rich and thermally mature.

Analyses of these wells indicate that three essential play components are required for discovering large oil fields and what limits field size. The aeolian dune facies of the Norphlet, is the only facies that has the required preserved permeability to create a pressure "sink" for oil to accumulate in today's subsurface. A "sink" is defined here as permeable sandstone with significant lateral continuity that is "under-pressured" relative to bounding stratigraphy. The Norphlet sandstone pressure sink provides the outlet for oil to enter from the overlying and higher pressured maturing Smackover source rocks. The Smackover source rocks must have a high enough threshold level of thermal maturity, measured by the vitrinite reflectance equivalent (VRE) level. A VRE level of 0.9 is the minimal level of maturity needed for oil migration to effectively fill a trap to an economic amount. Smaller "fetch areas" can also limit accumulations to smaller volumes especially at lower maturity levels. Higher maturity levels more effectively "squeeze out" Smackover oil creating more robust oil volumes charged downward into the permeable Norphlet reservoir. The timing of expulsion and migration from the source rock must occur from the recent to no older than 15 to 20 million yr ago. Otherwise, older formed traps will leak, leaving only residual oil. Only in older formed traps with a simple four-way basal Smackover closure component, will retain oil under this top-seal (e.g., Titan–DC 178 and Antietam–DC 269). All other trap components having any fault juxtapositions of other formations, will allow a slow leakage from the trap.

REGIONAL SETTING

The regional play setting for the deepwater Norphlet has been well described recently by both industry and academic institutions (Hudec et al., 2013b; Pilcher et al., 2014; Cunningham et al., 2016; Weber et al., 2016; Godo, 2017; Hunt et al., 2017; Steier, 2018). The Norphlet deepwater play in the eastern Gulf of Mexico is located outboard of the younger Cretaceous carbonate shelf margin (Fig. 1). The Norphlet Formation extends as a continental dryland sandstone and shale facies from northeastern Texas through Arkansas, Mississippi, Alabama, and northwestern Florida before continuing into offshore waters today (Godo, 2017) (Fig. 1). The Norphlet exploration wells are those drilled since 2003 in the deepwater Gulf of Mexico (Table 1). A history of these wells until 2010 is reported in Godo (2017).

Stratigraphic / Subsidence Model

The Norphlet Formation formed as continental sediments that spread around the margins of a broad, flat salt pan formed at is the Louann Salt. In Hudec (2013a), a model was proposed for a post salt crustal stretching (his phase 3 opening), where continental rifting continued for 7 to 12 yr after salt deposition ended. During this phase they claim that the salt basin widened by 62–155 mi (100–250 km) with extension or stretching tapering to zero at the edges of the basin where salt flowed laterally filling the widening basin. Just like salt flowing basinward, the Louann water's edge at Norphlet time, also flowed laterally into the basin

Manuscript received March 25, 2019; revised manuscript received May 28, 2019; manuscript accepted June 6, 2019.

GCAGS Journal, v. 8 (2019), p. 104–152.
DOI: pending

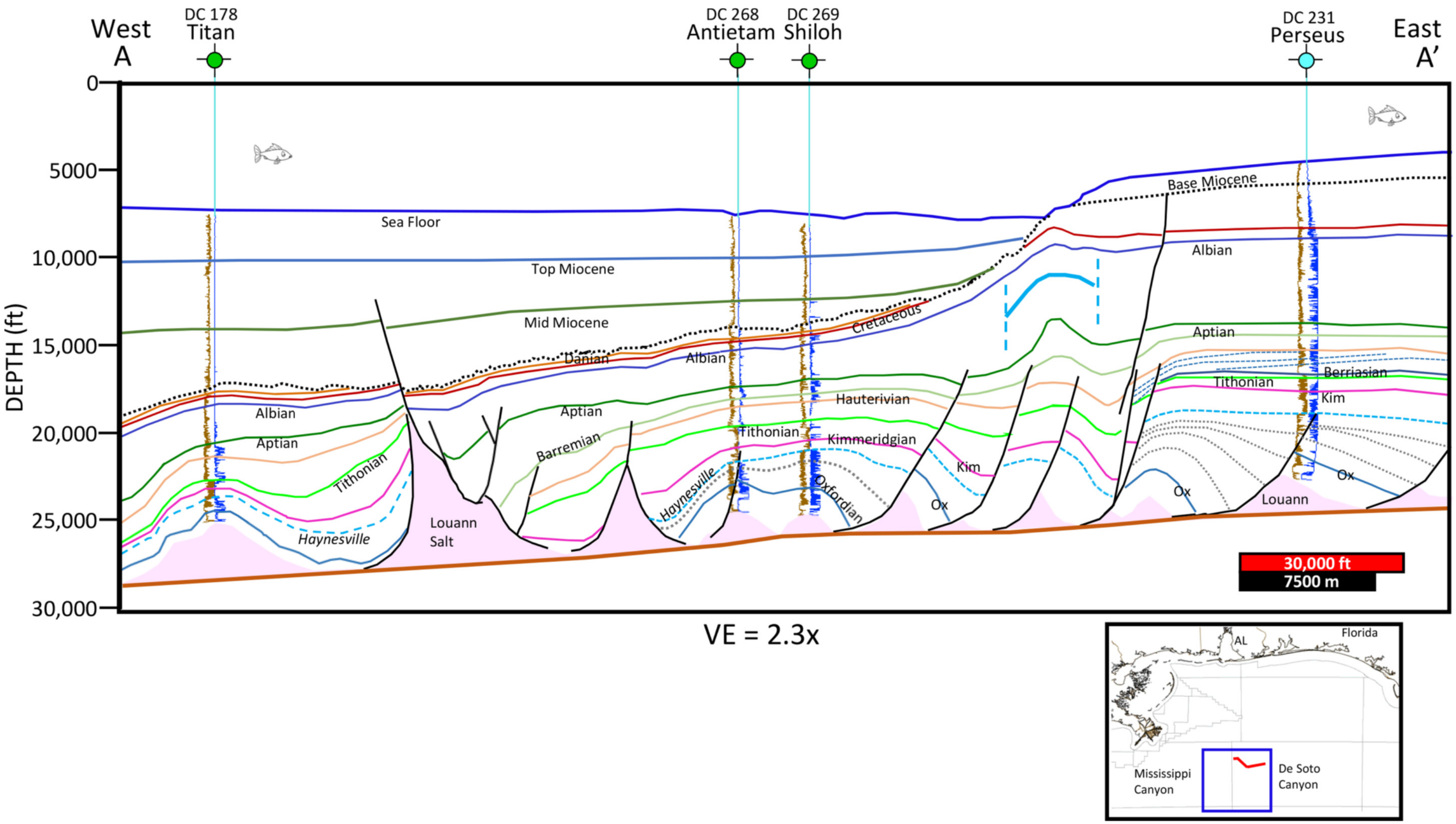

Figure 1. The structural cross section illustrates the position of the Jurassic Norphlet deepwater play relative to the Cretaceous and younger overburden thickness. The Norphlet play extends under the shelf waters and throughout the onshore area and lies beneath a thick burial of Cretaceous sedimentary rock (e.g., Perseus well). The reason for the thick Cretaceous burial is the depositional positioning of the Cretaceous shelf margins. There is a near vertical stacking of shelf margin sequences resulting in a rapid lateral change in thickness in the northeastern offshore Gulf waters.

Table 1. The table lists, in sequential drilling order, all wells drilled in the Norphlet deepwater play. The cross referencing of well locations and prospect names are also shown. Wells highlighted in yellow have well summaries and are discussed in the text.

Prospect Name	Location (Projection Area and Block Number)	Competion Date	Well Operator	Water Depth (ft)	API Identifying Number	Norphlet result--live oil, residual, or no shows
Shiloh	De Soto Canyon Block 269	09/0/2003	Shell	7509	608234000601	Live oil and residual
Vicksburg "B"	De Soto Canyon Block 353	09/0/2007	Shell	7457	608234001401	Live oil
Fredericksburg	De Soto Canyon Block 486	08/0/2008	Shell	7800	608234001500	No shows
Antietam	De Soto Canyon Block 268	08/0/2009	Shell	7400	608234001702	Live oil and residual
Appomattox	Mississippi Canyon Block 392	03/0/2010	Shell	7217	608174117203	Live oil
Vicksburg "A"	Mississippi Canyon Block 393	05/0/2013	Shell	7371	608174125300	Live oil
Petersburg	De Soto Canyon Block 529	05/0/2013	Shell	7625	608234002100	No shows
Raptor	De Soto Canyon Block 535	05/0/2013	Anadarko	8169	608234002000	No shows
Corinth	Mississippi Canyon Block 393	09/0/2013	Shell	7375	608174125302	Residual/color change
Sake	De Soto Canyon Block 726	09/0/2013	BHP	3575	608234002400	No shows
Madagascar	De Soto Canyon Block 757	12/0/2013	Marathon	8391	608234002500	No shows
Swordfish	De Soto Canyon Block 843	12/0/2013	Shell	8487	608234002200	No shows
Rydberg	Mississippi Canyon Block 525	06/0/2014	Shell	7456	608174128000	Live oil
Titan	De Soto Canyon Block 178	09/0/2014	Murphy	6560	608234002702	Live oil and residual
Gettysburg	De Soto Canyon Block 398	11/0/2014	Shell	7579	608234002800	Live oil
Perseus	De Soto Canyon Block 231	12/0/2014	Statoil	4495	608234002600	No shows
Fort Sumter	De Soto Canyon Block 566	02/0/2016	Shell	7015	608174131801	Live oil
Leesburg	Mississippi Canyon Block 475	05/0/2016	Shell	6590	608174132700	Residual/color change
Ballymore	Mississippi Canyon Block 607	12/0/2017	Chevron	6536	608174135802	Live oil

= Well summary described herein

much like "a swimming pool whose walls were moving apart" (Hudec, 2013a). This exposed area around the "pools edge" (Louann water), would produce a broader exposed salt flat pan for the surface on which fluvial outwash and aeolian systems could be deposited. This model is supported and used in this paper.

Initial downslope sliding movement of Norphlet sediments was noted by Hughes (1968), where he concluded that in Mississippi, the overburden load of the Norphlet caused a lateral push or flow of the underlying salt basinward. In Alabama, Sigsby (1976) reported that salt mobilization was initiated by progressive sediment loading during late Norphlet deposition through Late Oxfordian time. Mancini et al. (1985) also working in Alabama, stated that differential subsidence of salt by Norphlet deposition, resulted in locally thick Norphlet sandstone accumulations. In the East Texas Basin, Jackson and Harris (1982) stated that the lower Smackover transgression triggered initial salt movement. In other parts of the East Texas Basin, Harris and McGowan (1987) suggested that salt flowed basinward during Smackover deposition due to sediment loading and basin tilting via subsidence. Jackson and Galloway (1984) showed that less than 1970 ft (600 m) of overburden thickness is needed to initiate a downslope salt creep. Finally, Hudec (2013a) interpreted downslope movement to be from Oxfordian to Kimmeridgian time.

Regional subsidence in the Eastern Gulf of Mexico, is generally westward toward the Louann basin. Locally in the Norphlet deepwater play, the western-plunging basement arch known as the Middle Ground Arch (Fig. 2) was a paleo-high (Martin, 1978; Dobson and Buffler, 1997; Galloway, 2008; Hunt, 2013; Cunningham et al., 2016; Hunt et al., 2017). The Middle Ground Arch was both a sediment source exposing a terrane of lower Paleozoic sedimentary and metamorphic rocks and Mesozoic intrusive and extrusive rocks. This paleo-high would have also affecting paleo-wind directions. Louann Salt onlapped around the edges of this high thickening in a wedge shape. Northward, the Apalachicola Embayment is also called the De Soto Salt Basin. South of the paleo highlands, salt continued to be deposited in the Tampa Embayment (Dobson and Buffler, their figure 1; Wilson, 2011, his figure 2; Marton and Buffler, 2016). West of the Middle Ground Arch, the highest subsidence rate occurred as the area was more central to the axis of the subsiding Gulf of Mexico. Different subsidence rates allowed for different thicknesses of Louann Salt around the three flanks of the paleo-high. Thicknesses of the Norphlet sediments also vary around the Middle Ground Arch paleo-high as different sediment delivery points provided different amounts of ephemeral waters carrying sediments onto the salt flat. Winds which also blew around the highland edges focusing sand dune fields with varying thickness due to varying sediment supply and wind directions.

The structural axis of the Middle Ground Arch plunges westward and separates three adjacent salt basins. Sedimentary rock packages which onlapped the high, broke apart, and slid basinward off the arch axis. The initial breaks that defined the rafts edges occurred after the Norphlet and early Smackover formations were deposited. The lateral side movement began by Oxfordian and continued into the Cretaceous. These raft blocks slid along a divergent radial spreading pattern off the arch axis. The directions of early raft movement spread apart from one another further basinward around the plunging arch like fingers spread off a hand. Sliding or "rafted" blocks along these paths, could also be called sediment "chips," with younger mainly Kimmeridgian sediments filled the enlarged slide gaps. These same raft blocks are described by Pilchar et al. (2014), comprising the additional rocks of the Norphlet, Smackover, Haynesville, and Cotton Valley formations. McDonough et al. (2008) described the rafted blocks as "floating" on top of the Louann Salt. Pilchar et al. (2014), stated that the main raft movement took place after deposition of the Haynesville Formation with raft sizes ranging from 1.2–24.9 mi (2–40 km) in length and 1.2–9.3 mi (2–15 km) in width.

During Norphlet deposition, differential vertical loading even over short lateral distances initiated salt withdrawal beneath the sediments while rising to the surface around depositional edges, creating a positive topographic bulge. At Appomattox, dramatic lateral thickness changes in the Norphlet over short distances, can be shown in early appraisal wells (Fig. 3). As a general depositional model for the area, formations of these early salt bulges defined depositional corridors or created barriers by "walling-off" other areas from sediments. Salt walls provided depositional boundaries for basins to collect fluvial facies that washed in through openings in the salt walls and more broader corridor areas for winds to create dune fields.

Ings and Beaumont (2010) described local depositional basins between salt highs which they call viscous pressure ridges (VPRs). VPRs occur as a first response to the initial sediments loaded on the salt. Ridges then continue to form because of "uneven sedimentation" or differential loading which later became the break points for lateral rafting (Goteti et al., 2012). Goteti et al. (2012) used isostatic balancing to argue that lateral thickness changes in sediments caused lateral pressure differences large enough to initiate salt movement. Sediment loading by ponding (or blowing) against the ridge provided further uneven sediment loading. Subsequently, the sediment load became sufficiently thick and dense enough for Rayleigh-Taylor instabilities to add to the salt ridge formation (Goteti et al., 2012; Ings and Beaumont, 2010). Goteti et al. (2012), reported that under optimal conditions, uneven sedimentation against topographic salt relief can initiate mini-basins with salt walls in as few as 50,000 yr.

In the Paradox Basin, Utah, salt walls have been shown to divert fluvial delivery and shield some areas for aeolian dune formation from further fluvial access (Banham and Mountney, 2013). Mapping these salt walls, revealed polygon shaped bounded basins for dryland deposition (Banham and Mountney, 2013), similar to many polygonal shaped Norphlet basins. Trudgill (2011) stated that the salt walls, were probably at or very close to the surface during deposition. Subaerial exposure of the salt wall has been described by Lawton and Buck (2006) where diapir derived detritus of the salt wall was incorporated into sediments that onlap the salt wall (Castle Valley, Utah). Salt walls in an aeolian environment may also influence and deflect wind speed thus affecting construction of dune fields. Salt walls may also block or redirect fluvial waters from areas where winds blow dune fields.

Norphlet reservoir oil fields in the deepwater Gulf of Mexico play only become oil charged if there is effective permeability to receive the downward charge from the Smackover source rocks. This is based on evaluation of all wells in the study area that are dry holes that have overlying mature Smackover source rocks. Effective permeability that can receive oil charge is only found in the aeolian dune facies. The better permeabilities are found in dryer, taller dunes above a deeper water table. The best reservoirs would be a dune field with a high sediment supply and slow enough subsidence to preserved multiple stacking of dune trains. Having broader areas of deposition between salt walls would enable the dune field to traverse without being stacked vertically causing local subsidence to increase. Too rapid of subsidence, limits the amount of repeated rainwater events which wash clay particles downward through the dune, percolating through the sand grains "basting" grain surfaces. These repeated washings (or bastings) of clays around framework grains, provide a more effective coat to resist later cementation with burial. Where areas that sand dunes were subjected to a paleo-water table that rose quickly into the dune, clay particles would enter the otherwise dry dune and modify depositional texture. Kocurek and Havholm (1993) stated that wet sand dunes imply that the paleo-water table was closer to the dune base in wetter times. In these times, the water table would be drawn up into the lower portion of the dune while the top was still above the water table. Dry dunes stood above the rising water table for longer periods of time and thus have more time for repeated downward washing of rainwater to distribute the clay coats then evaporite. Both wet and dry dunes produce the needed permeability preservation, but drier dunes may have built a higher relief thus also producing longer/thick avalanche beds which individually have the best permeability (Kocurek and Havholm, 1993).

Norphlet Sandstone Properties and Diagenesis

Porosity-versus-depth curves are commonly used to estimate sandstone porosity in exploratory wells. Rice et al. (1997) stated that the Norphlet aeolian facies have porosity values significantly higher than porosities at the same depth than most other sandstones around the world. Taylor et al. (2010) suggested that porosity-versus-depth curves are not a robust way of predicting reservoir quality for sandstones. For example, sandstones do not follow a simple porosity degradation trend in Tertiary aged rocks at depths between 14,750 and 24,600 ft (4500 and 7500 m). Because porosity variability is due to the occurrences of quartz cementation that begin occurring when temperatures are greater than 212°F (~100°C) (Taylor et al., 2010).

Porosity in the Norphlet is mostly primary intergranular porosity. Dixon et al. (1989) stated that porosity evolution in the Norphlet was controlled by inhibition of cementation (see also Taylor et al. [2010]). In the deepwater environment, the Norphlet has experienced less overburden over a shorter time span, compared to Norphlet inboard of the Cretaceous shelf margin (Fig. 1). Predicting Norphlet dune sandstone (in practice) in the deepwater play can be better approximated if wells use only the overburden thickness from the base Miocene. This is assumed process, because more "recent" burial and compaction effects may not have been fully equalized at the Norphlet level. Porosity depth trends are very different for dune sands versus the water-lain fluvial wash facies due to less quartz cementation and depositional clays in aeolian dune sands.

The Norphlet stratigraphically lies directly on salt and is overlain by a clean carbonate (low argillaceous content). This stratigraphic position would isolate the Norphlet to other formation waters that would otherwise pass through older sediments an might cause more variations in cementation/diagenesis found in the Norphlet. Isolation from other dewatering formations allow a cement type such as halite to occur in the Norphlet (Hartman, 1968; McBride, 1981; McBride et al., 1987; Kugler and McHugh, 1990; Thomson and Stancliffe, 1990; Schenk and Schmoker, 1993). Water salinities in the Norphlet reservoir are very high compared to other Gulf of Mexico reservoirs. For example, Gettysburg had a measured water salinity of over 240,000 ppm while Titan has a salinity measurement from a water sample at over 350,000 ppm. Norphlet salinities can be especially high without the presence of the basal anhydrite (Pine Hill member of the Louann Salt) or a more extensive basal fluvial shale. The

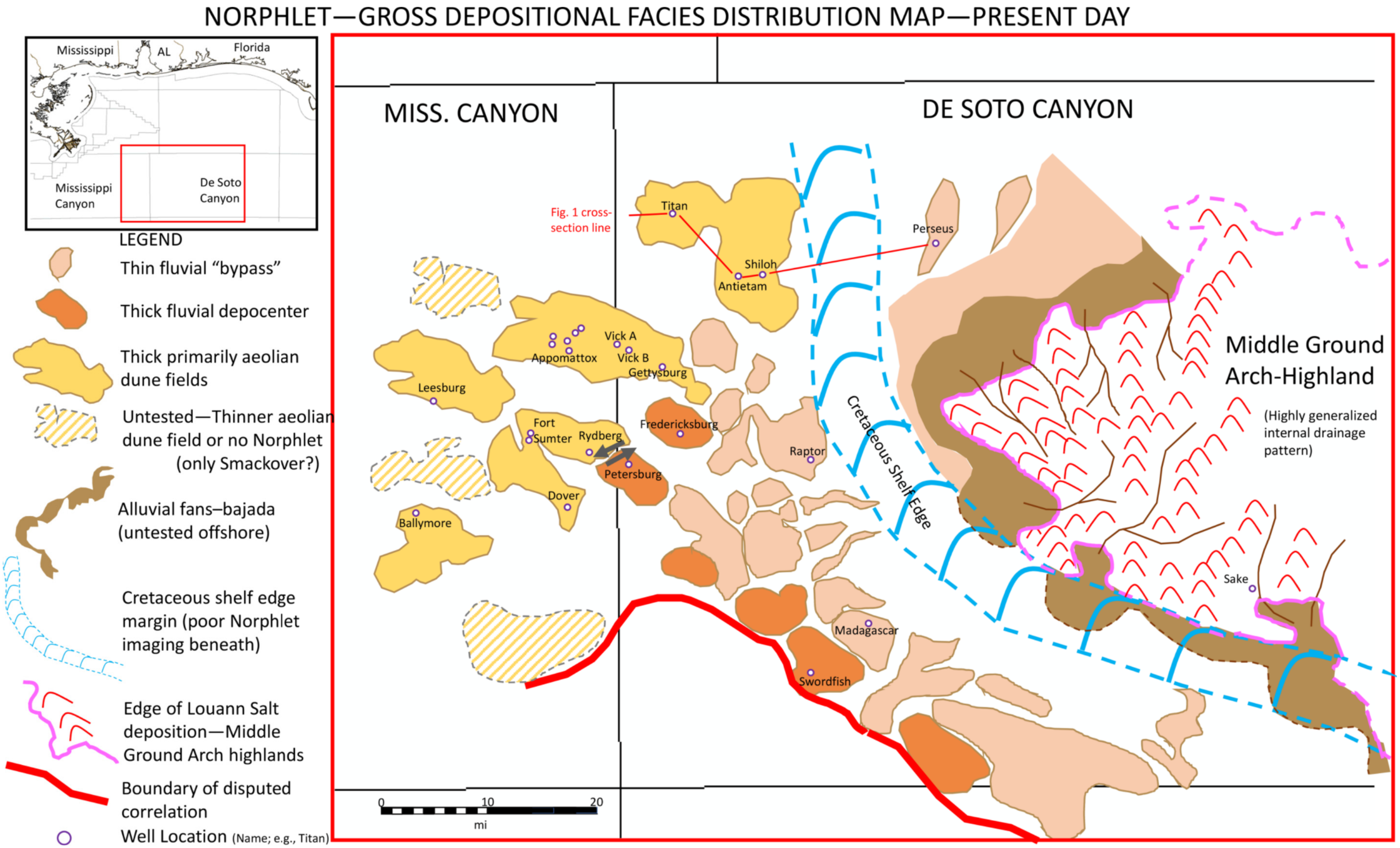

Figure 2. The map is a present-day location map (unrestored) of the Norphlet deepwater play. Each Norphlet depobasin is colored by the generalized and dominant facies types found in the well and projected across the basin or interpreted with seismic and a geologic model. The Norphlet deposited in the depobasins lie directly on a Louann Salt pan. The Louann water is likely to have existed near the mapped basinward limits of the Norphlet. Each depobasin was likely completely or nearly completely bounded by salt walls. Salt walls were pushed upward and around the Norphlet depobasin as a result of just the weight of the Norphlet. The Middle Ground Arch was an exposed highland creating both a local sediment source and affecting wind directions. In general, aeolian dunes formed more outboard away from the limits of ephemerally flowing waters off the Middle Ground Arch. The area marked with blue arcs and bounded by blue dashed lines represent an area of vertically stacked Cretaceous reef margins. Beneath the reef edge, seismic imaging is poor yielding a low confidence of Norphlet depobasin identification.

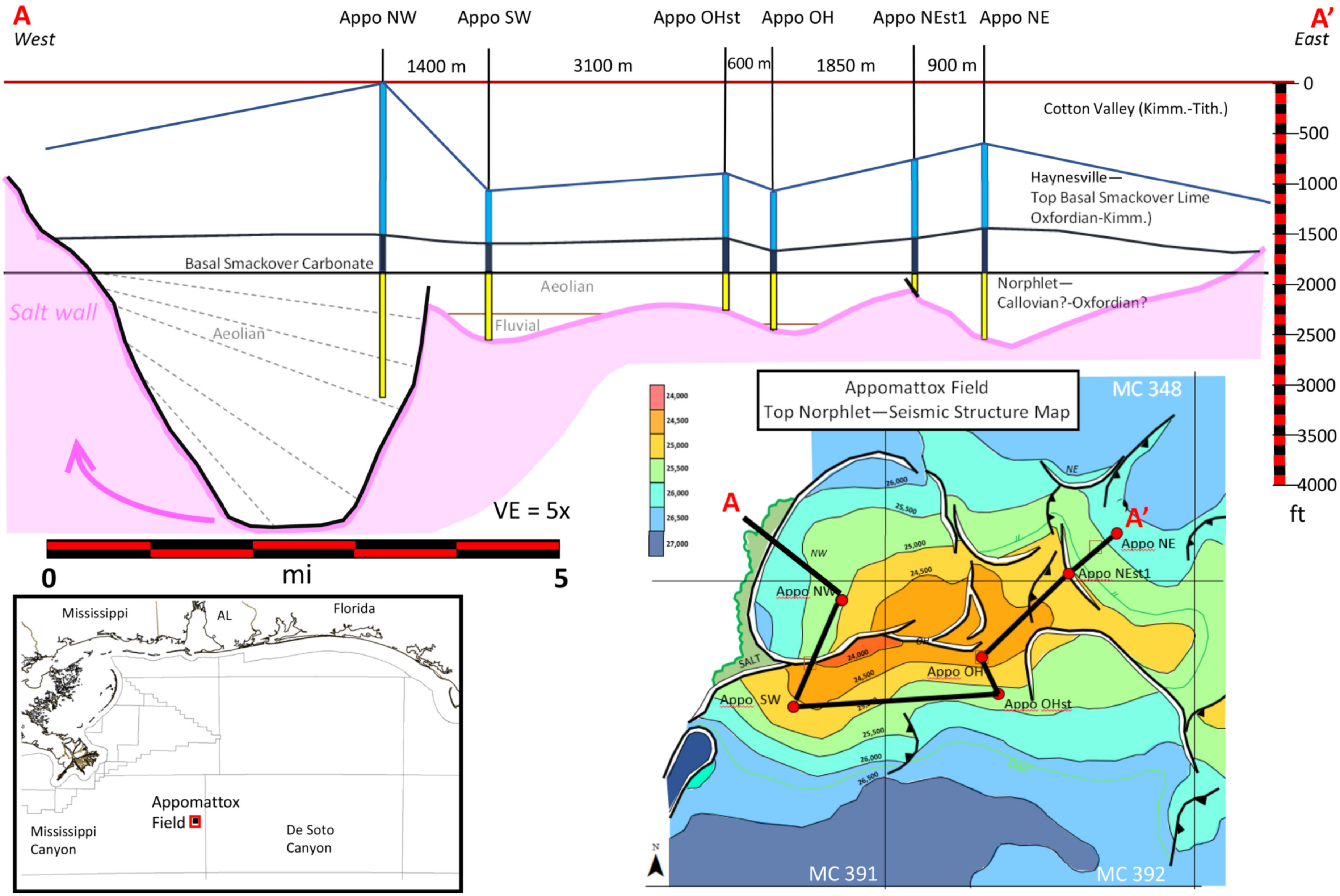

Figure 3. This “stick” cross section illustrates thickness variations in the Norphlet of Appomattox Field. The cross section is flattened on the top Norphlet Formation. Thickness variations result from early salt subsidence caused by differential Norphlet sediment loading. 1 mi = 1.61 km and 1000 ft = 304.8 m.

presence of an anhydrite or a basal fluvial shale may provide a stratigraphic barrier from the Louann Salt which yields high salinity water that can result in halite cement. Norphlet traps bounded by salt flank traps, may have the highest salinities well above 250,000 ppm.

Porosity and permeability values are initially controlled by the depositional facies of the Norphlet Formation. The first order type of depositional facies is whether deposition occurred by wind or water. Aeolian wind deposits have the best porosity and permeability values and can be oil bearing. Sands deposited in dry dunes with the largest dune heights, form the best subfacies called avalanche beds (Kocurek and Havholm, 1993; Schenk, 1983; Net, 2003). These beds are deposited by gravity through grainfall down the lee side of the dune face. Taller dunes have longer fall distances and form the thickest and most porous facies. The next best subfacies are wind ripple beds that are deposited up the windward side of dune slopes. Sand sabkha and sand sheets are next with interdune deposits having the poorest initial porosity values (Marzano et al., 1988; Dixon et al., 1989; Schenk, 1981; Ajdukiewicz et al., 2010; Douglas, 2010). Porosity and permeability in other aeolian systems in literature show the same ranking of subfacies (Ahlbrandt, 1979; Lupe and Ahlbrandt, 1979; Fryberger et al., 1983; Lindquist, 1983; Net, 2003).

In each subfacies of the aeolian dune deposits, nearly complete grain coatings of clay, typically chlorite clay grain coatings are present. Despite exposing the Norphlet to temperatures from 320°F (160°C) to over 392°F (200°C) at Mobile Bay, this nearly complete grain coating is responsible for maintaining intergranular porosity by inhibition of quartz cementation. (Dixon et al., 1989; Taylor et al., 2004; Ajdukiewicz et al., 2010). Grains need up to ~98% of the grain coated by clay to prevent extensive quartz cementation (Taylor et al., 2004, 2010). Also present, but less common and pervasive as chlorite coating, are microcrystalline quart overgrowths that can also be an effective mechanism for inhibiting the formation of pore-filling quartz overgrowths (Aase et al., 1996; Taylor et al., 2010; French and Worden, 2012).

All dunes in this environment are characterized by periodic wetting and drying (evaporative pumping) in a highly oxidizing environment (Dixon et al., 1989). Repeated "washings" of dust and clay by via infiltration by rainwater through the dune mechanically (Walker, 1979). The most complete grain coatings of clay result from repeated infiltration events that occur the longer the dune is above the water table. More opportunities for repeated wetting and drying cycles will occur in taller dunes which sediment supply is one factor, but also slower subsidence of the dune into the water table. Within the dune, early diagenetic reactions can include incipient hydration and solution of the most unstable labile grains (such as volcanics; e.g., see Thompson [1979] and Taylor et al. [2004]) with precipitation of clay/iron oxide rims on framework grains (Dixon et al., 1989). These rims are precursors of authigenic grain-rimming chlorite. Rimming clay particles dry flat onto grains and along fluid menisci as rain water evaporates from the pores (Crone, 1975). By orienting flat against a grain, the clay would adhere to more of a grain's surface to insure a more complete grain coating (Walker, 1979; Matlack et al., 1989; Turner et al., 1993; Shammari et al., 2011). Coarser sand sizes which are found in the avalanche beds forms, have more effective permeability for emplacement of the most infiltrated clay (Matlack et al., 1989).

Waterlain sandstone facies deposited by ephemeral fluvial outwash have the lowest porosity and permeability of facies types in the Norphlet. In the fluvial facies, permeability is so low that the entry pressure for oil appears too high to overcome. Low permeability does not allow for fluid movement to occur within the Norphlet and without lateral flow in a geopressured environment, no hydrodynamic underpressured "sink" forms. It is one of the premises of this paper to provide evidence and a model, where low permeability in the Norphlet sandstone cannot be charged with oil and will not yield any oil shows. This phenomenon occurs despite the Norphlet sandstone being adjacent to a relatively over pressured, maturing source rock. In the early days of Norphlet exploration, the porosity was mainly used to consider as the critical reservoir parameter. After all, some of the thick, Norphlet blocky shaped, high net to gross sands say in Fredericksburg, seemed acceptable to hold oil. It was only later realized that permeability is the critical parameter needed to produce a pressure sink needed for a downward oil charge to occur. As an example of low permeability in the Norphlet, see the values in the Petersburg well that are generally well below 0.25 md.

Smackover Source Rock and Hydrocarbon Charge

The Smackover source rock is made up of two lithologic types, a basal carbonate and an overlying more argillaceous marl section (Godo, 2017, his figure 3). The basal carbonate source rock is dominated by source rock laminations. Brand (2016) also further breaks this unit into 2 units, a "Shaley Limestone" and "Massive Limestone." In both units there are intervals with algal in laminations and other more disseminated organic rich material. Solid hydrocarbons found in the Norphlet are sourced from the more carbonate rich microlaminated facies of the Smackover (Sassen, 1988; Sofer, 1988; Dixon et al., 1989; Godo et al., 2011; Godo, 2017).

Tissot and Welte (1984) described how carbonate source rocks will compact to further concentrate even any disseminated bitumen and clays into laminations and fine layers. The concentration of organics in laminated carbonates allows for more effective expulsion resulting in an earlier petroleum generation with a lower thermal maturity threshold. In the case of the Smackover source rock, there is an initial expulsion of a low maturity bitumen, rich in asphaltenes, from the basal carbonate facies. Bitumen is mainly based on its solubility in carbon disulfide solvent as originally defined by Herbert Abraham's book titled *Asphalts and Allied Substances*, with subsequent editions culminating in 1960 (Abraham, 1960; see also Hunt et al. [1954]; Jacob [1989]). In the Norphlet, the solid hydrocarbon (SHC) has components that are both soluble and insoluble in carbon disulfate (Godo et al., 2011). The soluble portion, as Abraham's (1960) chart shows, is a bitumen derived product with some fusiblity (refractory materials) and is in the asphaltites (e.g., gilsonite) category. As the thermal maturity increases in the trapped hydrocarbon column, there is a transition to pyrobitumen, insoluble in carbon disulfate (e.g., impsonite category). The solid hydrocarbons have a much greater proportion of pyrobitumen in more thermally mature oil columns such as in Titan, Vicksburg, Appomattox, Shiloh, and Antietam (F. Mosca, 2019, personal communication). Other Norphlet hydrocarbon accumulations have also described solid hydrocarbons in Mobile Bay and in onshore accumulations (Sofer, 1988; Sassen, 1988; Dixon et al., 1989, Kugler and Mink, 1998, Mankiewicz et al., 2009).

Solid hydrocarbons initially injected downward from the Smackover into the permeable Norphlet sandstone would have entered pores with larger pore throats (Rogers et al., 1974). From there the migration path would have concentrated and focused flow paths toward the crest of the structure. The path would follow structural bends or "noses" up the flanks toward the structural trap. Hydrocarbon charge entering the Norphlet from downdip positions, would migrate near the top seal toward the crest. Migration could most easily follow through larger pore spaces in the avalanche bedding and likely follow shifting pathways of this pore system up the structure. At the structural crest, oil would enter the Norphlet reservoir and fill the structure down the structural flanks.

After the initial charge, a second phase of Smackover hydrocarbons were expelled and followed a downward path of the initial asphaltene-rich bitumen and mixed with this oil in the reservoir. The source of this better-quality oil originated in the middle Smackover middle marl member (Godo, 2017, his figure 3). Publicly released geochemical reports on wells in this report, show the kerogen type in the middle marl section to be largely type II/IIs of Tissot and Welte (1984). This same kerogen type can be described as organofacies A and B of Pepper and Corvi (1995).

Quantifying porosity reduction degree caused by bitumen presence in a reservoir is difficult. Reservoir bitumen is not readily detectable on logs because of the lack of significant density contrast between crude oil and bitumen (Frydl, 1989; Lomando, 1992). Dutton et al. (1991) estimated that 90–99% of bitumen volume occurred in the reservoir pores Travis Peak Sandstone (Cretaceous) in East Texas. Bitumen presence, as measured by log evaluation, will show as oil-filled porosity because of the composition, density, and corresponding hydrogen indices of bitumen. The incorrect calculation of reservoir bitumen using common log suites will result in erroneous net pay amounts, recovery factor, original oil in place, and estimated recoveries (Lomando, 1992).

Solid hydrocarbons in reservoirs are not readily identified on typical log suites, where it is read as open porosity (Lomando, 1992). Lomando (1992) suggested that immovable SHC's located in the pore spaces should be evaluated as a diagenetic product that has affected pore space. More recent tools such as nuclear magnetic resonance (NMR) can establish the presence of SHC's but may not measure a correct porosity. Tucker (2013) used SHC in the Norphlet and defined in his work a new term called "paleo porosity" to deterministically solve for fluid and solid phase pore volume fractions. Paleo porosity would better estimate the original pore volume fraction of rock available for oil to fill and provide better calculations in basin modeling.

Sandstone Color and Alteration by Hydrocarbon Charge

The Norphlet dryland environment was likely a highly arid and oxidizing environment, characterized by the red color in all the lithologies likely due to iron oxide in hematite rich clays. Fluvial sandstones, shale and aeolian dunes existed in various proportions and thicknesses around the edges of the salt pond depositing the Louann Salt. The Norphlet extent is best known from northeastern Texas through Arkansas, Mississippi, Alabama, and Florida and extended southward into the present-day deepwater Gulf of Mexico. Mancini et al. (1985), Kugler and McHue (1990), and Dixon et al. (1989) described the red onshore sedimentary rock and Godo (2017) described the deepwater portion of the trend. Descriptions of color and grain sizes from Norphlet well cuttings are found in the mudlogs in all the deepwater wells (Table 1) and are available from the Bureau of Safety and Environmental Enforcement (BSEE, 2019).

Red color in sedimentary rock is a common characteristic of a highly oxidizing environment developed at the time of deposition due to a red pigment in the ferric oxide hematite (Walker and Honea, 1969; Walker, 1979; McBride, 1981). The iron ions in hematite were likely transported as an amorphous ferric hydrate and/or finely crystalline goethite, both of which are metastable and convert to hematite upon aging (Berner, 1969; Langmuir and Whittemore, 1971; Turner, 1980). In the finer grain sizes, there is an increased iron content of both Fe^{+} and Fe^{3+} (Van Houten, 1961, 1973; Picard, 1965; Walker and Honea, 1969; Turner, 1974). For enough pigment to color the sediment red to reddish-brown, Walker and Honea (1969) and Turner (1980, his table 6.5) suggested that an exceedingly small amount of pigmentary material (0.1 to 2.1%; avg. 0.7%) is needed. The foundational and excellent summary work on continental redbeds, like the facies in the Norphlet, is provided by the work of Walker (1967), Folk (1976), Walker et al. (1978), and Turner (1980).

Three factors alter the degree of redness or reddish-brown in sediments (Folk, 1976). First, a source needs to supply the iron by either heavy minerals or ferruginous clay. Heavier minerals, especially if derived from primary source rocks, equals greater potential for red to develop (Miller and Folk, 1955; Walker, 1974). Deposition above the water table would be primarily in sand dunes where periodic rainfall could wash down and distribute iron material through the dune (see also Walker [1967] and Walker et al. [1976, 1978]). Thirdly, little organic matter present on the desert floor to begin with or the condition of dryness is necessary to oxidize and destroy organic matter. Given these three prerequisites, red will still vary locally due to the varying amounts of moisture, residence time in the oxidizing environment and higher temperatures (Folk, 1976). Some moisture is necessary to alter the original iron minerals to hydroxides. Folk (1976) suggested as little as 5 in/yr (12.7 cm/yr) is needed, based on work in present-day deserts. Increased heat speeds the chemical reactions. Finally, enough time is required to alter the initially brown iron hydroxides through weathering with enough heat into red iron oxides (Folk, 1976). Walker (1976) described how dunes sands get redder even within thousands to tens of thousands of years. He stated that mechanically infiltrated clay percolates downward through the dune in highly permeable sediments frequently are recharged by influent, oxygen-bearing surface water (a key feature described by Folk [1976]). Walker (1976) continued by saying alteration of framework silicates by heat and water can release additional iron resulting in more hematite formation and more intensive reddening.

Geologists have described a "bleaching" or removal of red or hematite pigmentation from sandstone by the migration of oil through the rock. A few widespread locations and geologic ages of this phenomena are given in the Lyons Sandstone of Colorado (Levandowski et al., 1973; Weimer et al., 1985), the Sespe Formation of California (Rarey, 1990), Jurassic sandstones in Utah (Chan et al., 2000; Parry et. al., 2009), the Rotliegendes Sandstone of the North Sea (Pudlo et al., 2011) and the Norphlet Formation of Alabama (Dixon et al., 1989). Migration of hydrocarbons with the presence of organic acids, creates a decarboxylation and release of iron (Crossey et al., 1986; Surdam et al., 1993). Rainoldi et al. (2015) also described the bleaching of Cretaceous aged red sandstone in Argentina via removal of hematite grain coatings dissolved by acid oil migration. The acidic content of the oil appears cause a redox reaction thus reducing the iron in hematite into a soluble ferrous iron state and precipitating it as iron sulfide or as a constituent of the clay mineral in the sandstone. Other workers such as Dixon et al. (1989) and Crossey et al. (1986) also characterized the bleaching by the iron first released or reduced within the clay structure itself and released as ferrous iron. They both described that the resultant diagenetic minerals containing the ferrous iron most commonly are chlorite and ankerite. Freeing of ferrous iron from migrating oil brine might be a source for additional thickness of chlorite coatings often found in the oil saturated columns of Norphlet accumulations. Turner (1980) suggested that free iron might also be adsorbed onto clay minerals as amorphous material which would not readily be detected by X–ray diffraction. At prospect Gettysburg, a whole core across the oil-water contact, illustrates the increase of chlorite in the oil column and a color change in the sandstone across the oil contact. X–ray diffraction of the minerals in the Gettysburg core show loss of hematite at the oil-water contact. X–ray data also show the mineral change from hematite below the oil contact to pyrite within the oil column.

The oldest publications to describe the removal of red hematite pigmentation by oil and associated reducing brine fluids is by Moulton (1926), who studied the Triassic Chugwater Formation in the Bighorn Mountains, Montana. He described the formation as having "brilliant red sandstone, sandy shale and shale". Moulton (1926) observed that the red in the sandstones was removed leaving an "untinted white" color. He claimed the red is due to an iron oxide framework grain coating and that an oil moving through the sandstone altered the ferric state of iron to a ferrous state and removed the red. He used the word bleaching to describe red color removal and described rocks near faults and joints where oil moved through this conduit and bleaching the sandstone from red to white. Moulton (1926) also showed where sandstone bleaching occurred over a 10 ft (3 m) vertical section beneath oil saturated sandstone. Moulton (1926) advised that "the bleaching of redbeds [in such circumstances] has a significance to the oil geologist which should not be overlooked." His advice of observing a color change became more obvious to the author in a whole rock core, such as at Gettysburg, that displays the gradual color change. The color change across other Norphlet oil accumulations can be noted by the color of cutting descriptions as described in the mudlogs.

By understanding that oil causes this color change, a key observation can be made for evaluating both a present-day oil column or a residual oil column resulting from trap leakage. The normal red, reddish brown, to brown in the Norphlet sandstone dune facies, becomes a light gray to gray brown, using the color as described by mudlogging companies. With a whole core taken across the oil-water contact, the color description can be made uniformly and consistently described in a vertical view by using the Munsell color chart of Goddard et al. (1948) (see Gettysburg core photos in Figure 7). Using the color change from reds and browns to shades of light and dark gray, is useful when combined with presence or absence of oil shows or solid hydrocarbon descriptions. Summarizing, if no oil charge ever entered the Norphlet sandstone, then the color described in cuttings or cores will be red to reddish brown. Only if oil is currently, or once was, contained in the Norphlet, sandstone color will be only shades of gray. If there is no live oil recovered in the well, and the sandstone color are shades of gray, then the well likely encountered a residual oil column.

Norphlet Charging and Trap Leaking

Reasonable basin models made across the Norphlet play show that prospects received their peak oil fill in one of two distinct time ranges. Some Norphlet prospects show that peak fill occurred in the late Cretaceous at approximately 65 Ma. Other Norphlet prospects show peak oil fill occurring during middle Miocene (15 Ma) to more recently (Fig. 4) (Weimer et al., 2016a). Peak generation spikes resulted from rapid burial of some prospects by thick Cretaceous sediments (Harding et al., 2016), while others not buried by thick Cretaceous, remained buried shallow enough, not maturing the source rock, until the mid-Miocene and recent sediments.

There are four examples of Norphlet traps that were charged early during Cretaceous using well temperatures (for the gradient) and burial history (Antietam, Shiloh, Titan, and Leesburg). All four of these wells held a larger oil column that what is present today. Three of the four still have some remnant oil preserved, Antietam, Shiloh, and Titan. Leesburg, however, is interpreted to only have a residual oil column. All four leaked traps are speculated to have experienced a slow leak via capillary breakthrough of previously sealing lithologies. The peak oil charge in early-charged traps was about 65 Ma and they all have evidence of residual oil columns. Traps that filled with a peak oil charge of less than 15 Ma, appear fully charged, with no residual oil column. It is proposed then, that traps can hold a maximum oil charge for at least 15 million yr but not 65 Ma. Therefore, leakage may have begun to occur 65–15 Ma with only a live oil column remaining beneath the only longer-term top seal trapping component. This longer-term top seal component is a simple four-way dip closure of the basal Smackover carbonate top seal. Between 50 and 15 Ma, the Paleogene and Lower Miocene time frame deposition yielded 350 to 700 ft (106.7–213.4 m) isopachous sediment thickness and occurred during a time of minimal salt movement. The lithologic types that dominate the Paleogene and Lower Miocene sediments are chalks, marls, and shales with few silts and sands. Prospects that received their peak oil charge more recently, all appear to retain their maximum oil fill. Their maximum fill of oil is based on a color change and absence of any shows below the oil-water contact. There is no evidence that fields which received their peak oil charge in the last 15 million yr have residual oil columns. Therefore, it is assumed that the residence time for traps to retain their maximum fill is at least 15 million yr. With a geologically recent time since the trap was oil-filled, even small subseismic faults or deformation bands appear to trap and hold hydrocarbon columns. These features may be leaking today, but at a rate that preserves significant oil columns such that they can be produced today.

Macgregor (1996) analyzed 350 giant oil fields proposing that these oil fields are a "dynamic short-lived phenomena." The median residence time since oil filled the reservoirs is 35 million yr. Macgregor (1996) suggested that a combination of post-entrapment destructive processes limited the residence time of hydrocarbon charge. His post-entrapment destructive processes include, but are not be limited to, fault leakage, top seal erosion, gas flushing, and/or biodegradation. Miller (1992) also studied the global oil system and proposed a half-life for oil fields, invoking a model of exponential decay with time. Miller (1992) indicated that a residence time for oil to be retained in a trap have a median age of 29 million yr.

Hermanrud et al. (2005) and Aplin and Larter (2005) proposed a slower leakage of trapped oil through progressive hydrocarbon permeability over time across formerly through sealing lithologies, such as mudrock. Aplin and Larter (2005) stated that hydrocarbon leakage is accomplished by changing the wettability from originally water wet pore to an oil wet pathway providing the evacuation route of oil. Aplin and Larter (2005) stated that mudrock seals "do not act as permanent seals but simply retard the inexorable flow of petroleum to the basin surface."

Some oil discoveries in Norphlet although filled to their maximum level (at any time), appear to be underfilled with respect to structural closure. That is, there appears no structural reason why the oil-water contact could not be filled to a deeper level assuming an unlimited amount of oil charge. Discoveries such as Gettysburg, Rydberg, and perhaps both Vicksburg's "A" and "B" all seem to be underfilled. It is suggested that these examples are underfilled of oil because the fill contact is not constrained to or controlled by, any mapped spill points (see structure maps in the section on wells). What may limit the amount of oil that fills these traps is a source rock not rich enough to generate a larger volume of oil to fill the traps. The factors affecting the amount of available charge are source rock richness, thermal maturity and effective fetch areas. Richness of the Smackover source rock is adequate to fill traps such as Appomattox, but it appears to require, most importantly, a high maturity. For example, at Gettysburg, Rydberg and possibly Vicksburg "B," these VRE measurements range from ~0.75 at Gettysburg to likely 0.9+ down the flanks at Vicksburg "A." At these maturities, the oil contacts do not appear to be controlled by a spillpoint, hence underfilled. Fetch areas for Norphlet oil discoveries are not all large, so features such a lack of a permeable dune sands extending across the structural fetch area, would lessen effective fetch. Prospects such as Gettysburg and Rydberg thin quite dramatically into the structural fetch which might suggest part of the fetch area is composed of non-permeable waterlain facies. Also, fields with post mid-Miocene charge have effective seals such as small faults and deformation bands, which if blocking a charge path, might also limit an otherwise effective structural fetch area.

PROSPECT SUMMARIES

The following summaries of wells illustrate the critical concepts based on well data availability to reveal critical components

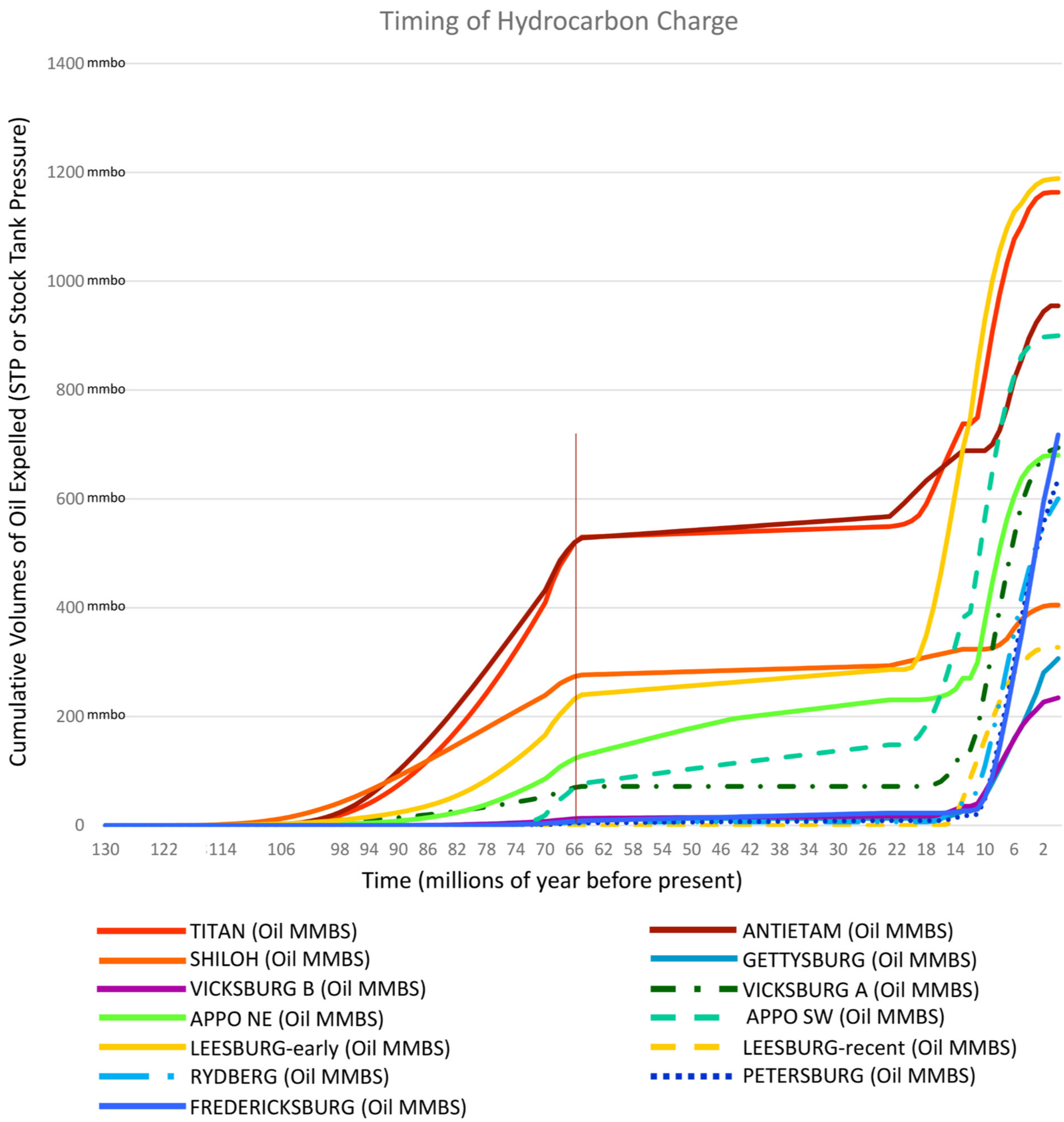

Figure 4. Plot of geologic time versus the amount of cumulative volume of oil expelled from the Smackover source rocks. The graph is an output from a basin model made regionally across and calibrated to wells in the deepwater Norphlet play. The volume of oil was measured using polygons around the structural fetch area for each prospect. The thin vertical line at the end of the Cretaceous (66 million yr) marks the time of peak oil generation for four of the wells in the play that found residual oil columns.

to finding successful and commercial oil fields. Gettysburg, Rydberg, and Vicksburg illustrate a range of smaller subcommercial to economic "tie-back" sized accumulations. The Appomattox field illustrates how maximizing all factors result in forming a major oil field. Shiloh, Antietam, Titan, and Leesburg, show that large oil fields leak with time if the charge-timing is too distant. The dry holes at Fredericksburg and Petersburg show the importance of reservoir permeability allow an oil charge.

Gettysburg

Gettysburg was drilled in late 2014 by Shell in block 398 of De Soto Canyon (DC). The exploration well targeted Norphlet aeolian sandstone reservoir. Structurally, Gettysburg is a faulted, four-way dipping anticline (Fig. 5). The Gettysburg well is located at the eastern boundary of the Norphlet depobasin that includes Vicksburg and Appomattox. In this end of the Norphlet depobasin, fluvial sediments likely entered through an open salt wall extending southwest to northeast across Mississippi Canyon (MC) block 399. This salt wall feature currently wraps around the east end of one of the larger Norphlet depobasins. The salt wall south of the Gettysburg well, presently has a thick likely Norphlet, windblown sands that stacked against the salt. The lateral loading of this salt wall pushed southward and continued sediment loading through Oxfordian time based on reconstructions. During Kimmeridgian time, the salt wall had pushed south far enough to cause the Gettysburg south flank to roll into its present anticlinal position.

The Gettysburg well found porous and permeable aeolian Norphlet sandstone charged with oil. The oil-water contact is at 23,835 ft (7265 m) (true vertical depth [TVD]) and shows a transitional decrease in oil saturation to the water contact. No evidence exists that the oil in the trap has ever leaked and the oil contact is at its maximum level today. Toward the base of the well, approximately 75 ft (22.9 m) TVDT [TVD thickness] of red siltstone is present above the top Louann Salt that was just penetrated at total depth. Average porosity from core plugs is about 22% with a range from 19 to 26%. Permeabilities are in the several 100s of md with a range from less than 50 to 650 md. Two oil samples were taken at 23,784.8 ft (7249.6 m) and at 23,826.9 ft (7262.4 m) (Fig. 6). The shallower oil is 33.4° American Petroleum Institute (API) gravity with a viscosity of 1.35 centipoise (cP) (1.35 mPa-s) where reservoir temperature was measured at 299°F (148°C) with a pressure of 16,792 psi (115.8 MPa). The deeper oil is 32.5° API gravity with a viscosity of 1.46 cP (1.46 mPa-s) where reservoir temperature was measured at 300°F (149°C) with a pressure of 16,806 psi (115.9 MPa). Two water samples were collected below the oil-water contact at 23,979.9 ft (7309.1 m) and at 23,981 ft (7309.4 m) TVD. The total dissolved solids (TDS) in the shallower water sample is 240,716 ppm. The deeper water sample has TDS at 239,677 ppm.

The photographs of the Gettysburg core allow comparisons of selections from the Munsell color chart (Goddard et al., 1948), next to core from the water leg and from the oil leg (Fig. 7). The colors assigned by the mudlogger, can also be compared with the core and color samples. X–ray diffraction on the core plugs shows that hematite is removed in the oil column (Fig. 6). Conversely, the ferrous state of iron represented by pyrite is present only in the oil column and not in the water leg (see also Gomes et al. [2018]). Finally, the amount of chlorite has increased in the oil column compared to chlorite in the water saturated core. The color change and the measured amount of hematite, pyrite and chlorite support the concept that acidic components in the oil are responsible for these changes. Hence, using the color change in evaluation might jump start evaluation of future well results.

At Gettysburg, components necessary to find oil in the Norphlet were met. However, the amount of oil was deemed not commercial. The volume of oil at Gettysburg is not filled to a spill point suggesting this field is charge limited. What are the limiting factors that did not allow the oil to form a larger oil column and make the field larger? Gettysburg has a limited fetch area, likely because of a very thin fluvial section with low permeability rock extends over a large part of the deeper structural fetch area. The area in green dash (Fig. 5) is qualitatively based on a Norphlet thickness map and within this circle only permeable facies might exist. Even with higher maturity levels in the syncline, if no permeable facies allow a downward migration into the Norphlet, then that part of the fetch area is not effective. That leaves only lower maturity levels on and near the crest to expel oil into the reservoir which limits the total volume expelled. The crest of Gettysburg is shallower than at Vicksburg "A," which lies just west of Gettysburg. Based on the basin model, likely maturity of the Smackover at the crest of Gettysburg is less than 0.9 VRE, perhaps 0.85. Summarizing, lower thermal maturity of the source rock coupled with a potentially limited fetch area, yields a sub-commercial oil accumulation in the Norphlet play.

Rydberg

Prospect Rydberg was drilled by Shell in 2014 in MC 525 (Weimer et al., 2017). The structure is a faulted dipping nose trapped against a salt mass (Fig. 8). Prospect Rydberg is located at the easternmost end of a Norphlet depobasin that also has been penetrated at Fort Sumter (Fig. 2). The subsidence history at Rydberg was local deposition of Norphlet dunes, loading against a salt wall and evacuating more of the salt southward. The northern most portion of Rydberg in the synclinal flank likely contains only a thin fluvial wash section in the Norphlet based on seismic thickness. With an impermeable Norphlet, no downward charge would occur with no subsequent lateral oil movement toward the crest. In risking a prospect like this, one could discount the effective fetch area, if no permeable dune facies exist.

The Rydberg well drilled 1260 ft (384 m) (in measured depth [MD]) of total Norphlet section with good permeable dune facies (Fig. 9). In the lower Norphlet, the well encountered approximately 260 ft (79 m) of fluvially deposited red shale and siltstone. Above this fluvial base, aeolian dune sequences built to the top of the Norphlet. The dip meter log shows the steeper bedding within the dune facies. The oil-water contact is at 25,535 ft (7783.1 m) MD. There is a nice resistivity transition stage, decreasing in oil saturation to the water contact, indicating that the trap was never filled more than is present today (Fig. 9).

Rydberg does not appear to be filled to an observable spill point (Fig. 8). Obviously, the timing of recent charge was favorable, but what were the limiting factors that caused an underfilled Norphlet trap? Using structural contours, the fetch area for Rydberg is not very large (Fig. 8). Effective fetch area may be even more reduced considering how much of the area might be unable to be oil charged. A qualitative green dashed line may highlight the area of permeable facies, based on a seismic thickness map (Fig. 8). While there is some thickness of Norphlet north and east of the prospect crest, the basal Smackover lies essentially on basement, indicating that no dune section is present. Without a permeable dune facies, no downward and lateral migration of oil would occur, limiting the fetch area. Another critical factor needed to more effectively fill Norphlet traps, is higher maturity of the Smackover source rock. Filling structures completely to a spill point requires the maturity of the Smackover to reach VRE levels of at least 0.9 equivalents. Based on calibrated basin models, the VRE level at Rydberg is perhaps 0.9 in the syncline where limited effective fetch might exist. Downward charge from the structure flanks and at the crest might be less than 0.9. Rydberg has been announced as commercially viable likely tied back to Appomattox (Beaubouef, 2018).

Vicksburg "B"

Prospect Vicksburg (location B) was the second well drilled to target the Norphlet aeolian sandstone in the deepwater play (Weimer et al., 2017). This well was drilled in 2007, 4 yr after finding oil in the Norphlet at Prospect Shiloh. The Vicksburg structure has multiple culminations and each culmination was labeled A, B, C, and D. The map in Figure 10 shows the structural culminations at A and B. Vicksburg "B" was chosen to be drilled first over location Vicksburg "A "(the larger structure culmination) because of more certainty that the well would find a thick Norphlet section to test. This certainty rose from that fact that a base Norphlet could be defined. Seismically, the rather homogeneous aeolian sand adjacent to the top of homogeneous salt, provides no boundary seismic event to detect base Norphlet. In 2007, most of the nearby analogs were in the Destin Dome protraction area. This area has a few wells with no Norphlet as the basal Smackover sits depositionally directly on the Louann Salt. In addition, the first well to drill the deepwater Norphlet play was at Shiloh which found a relatively thin Norphlet section (~250 ft [~76.2 m] TVDT), compared to wells finding aeolian sands in Destin Dome. The risk of not finding a Norphlet section at Vicksburg, had to be reduced. Fortunately, at location "B," but not in location "A," is a seismically hard event was present that likely marked the base of the Norphlet. The hard event was thought to be either a fluvial shale/silt section or a local anhydrite deposit. Both lithologies, if thick enough, will create a seismic hard event at the base Norphlet. Location "B" was drilled and the seismic hard at the base is fluvial shale.

The Vicksburg "B" structure is a culmination of closing contours on the hanging wall of a small thrust sheet (Fig. 10).

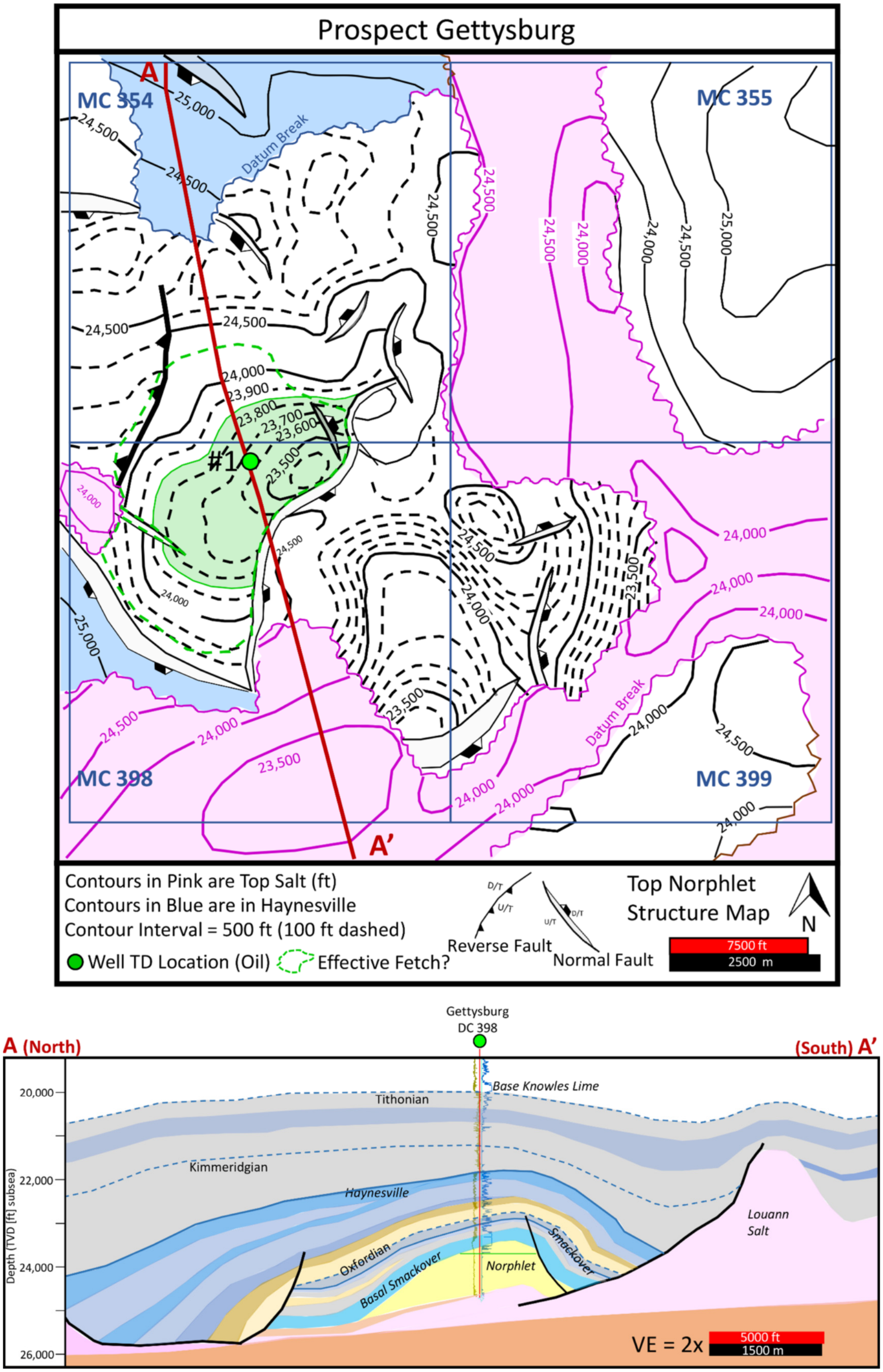

Figure 5. The map on the top Norphlet illustrates the simple closure at the Gettysburg prospect. The cross section shows the rapid lateral thickness change in the Norphlet as dune facies stacked vertically and loaded against a now evacuated salt wall. During upper Smackover and Haynesville deposition, this salt wall evacuated, rolling the base Smackover/top Norphlet. The green dashed circular area on the map outlines the likely extent of aeolian facies based on a sesimic gross thickness change away from the well. 2000 ft = 609.6 m.

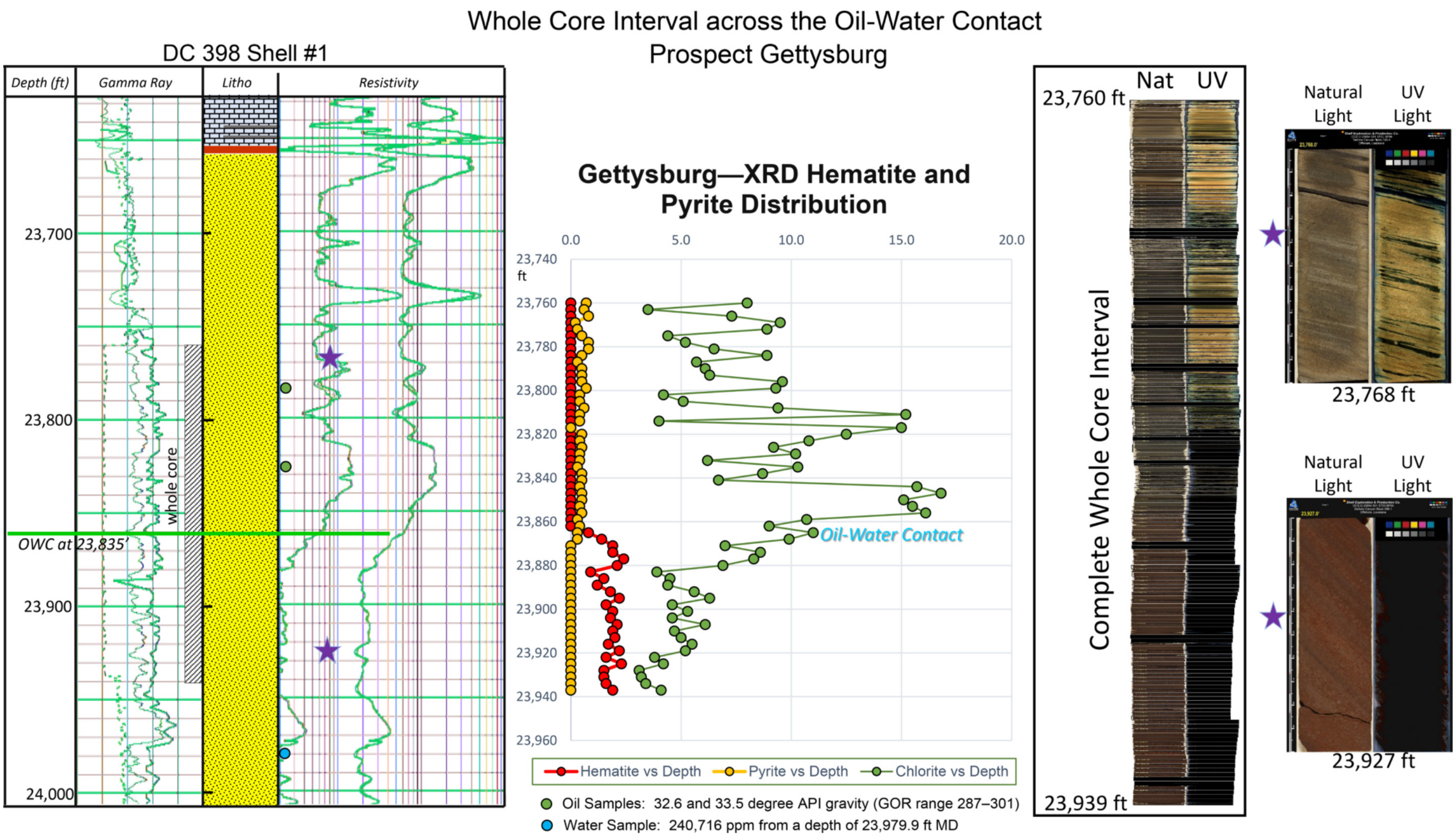

Figure 6. A TVD log from the Norphlet at Gettysburg is on the left. It illustrates the resistivity and gamma ray profiles over the cored interval between 23,760 and 23,900 ft (7242.0 and 7284.7 m) which spans the oil-water contact at 23,835 ft (7264.9 m). The resistivity level decreases gradually through a transition zone reacting to a decreasing oil saturation at the contact. Photographs of the whole core are shown on the right. The color change and lack of florescence in the core photos is shown in natural and ultraviolet light. The middle column is a plot of X–ray diffraction values of hematite, pyrite and chlorite. Hematite presence in the red sandstone is responsible for its color and in the oil column, the hematite is gone and pyrite appears along with an increase in chlorite resulting from the bleaching process described in the text. 100 ft = 30.5 m.

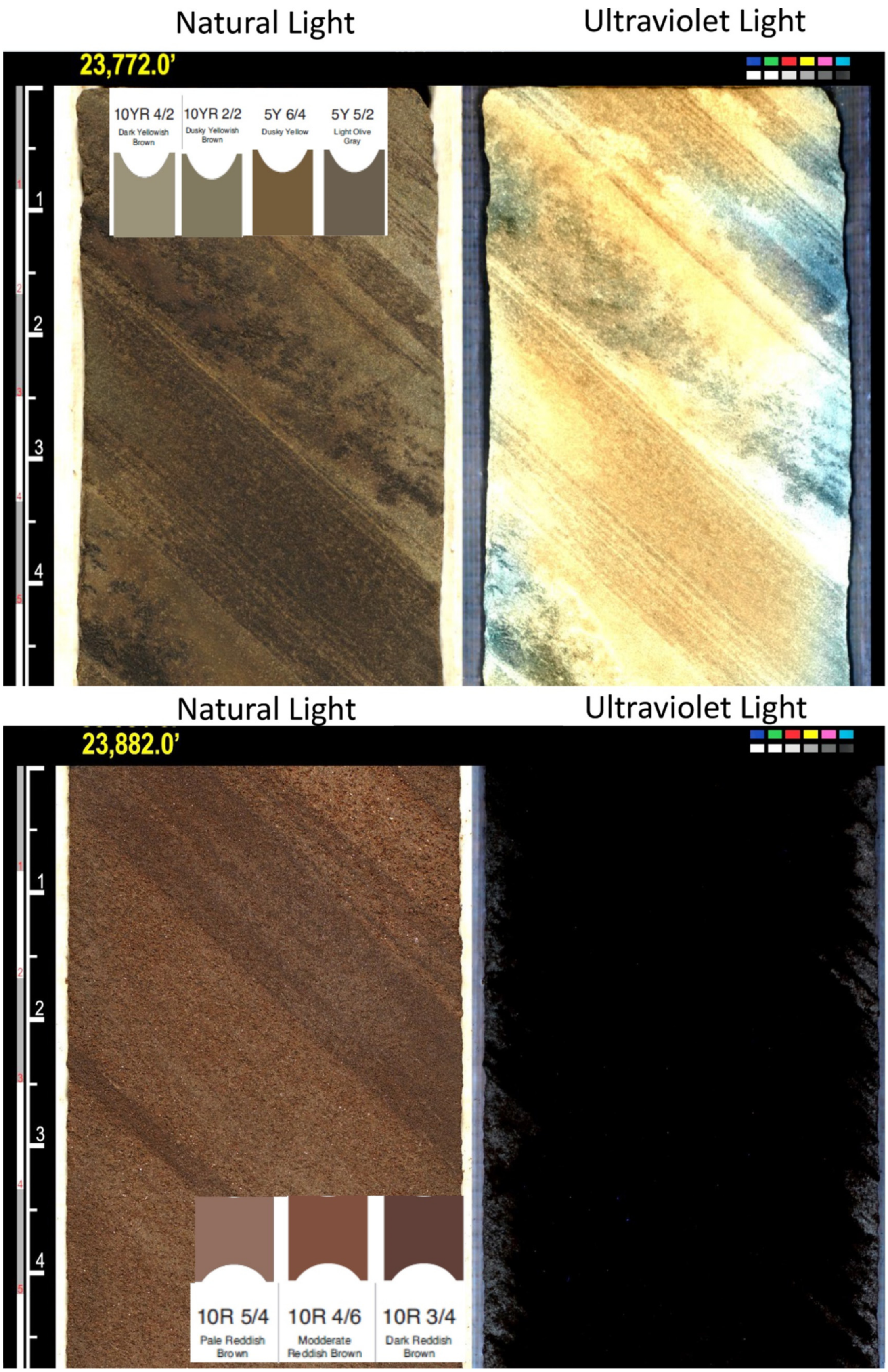

Figure 7. The two pictures are from the Gettysburg Norphlet core and are approximately 6 in (15.2 cm) in long. The depth scale is marked in tenths of inches. These Norphlet cores are a closer look at the avalanche bedforms and colors typical of the complete core. The upper core is taken in the oil column and under ultraviolet light shows fluorescence. The lower core is from the water leg and has no ultraviolet fluorescence. Sandstone color is best observed in natural light (a true color palette taken with the photo is shown in the upper right). Selected color samples from the Munsell color palate (Goddard et al., 1948), facilitate more detailed comparisons of red and gray shades. 0.1 in = 0.254 cm.

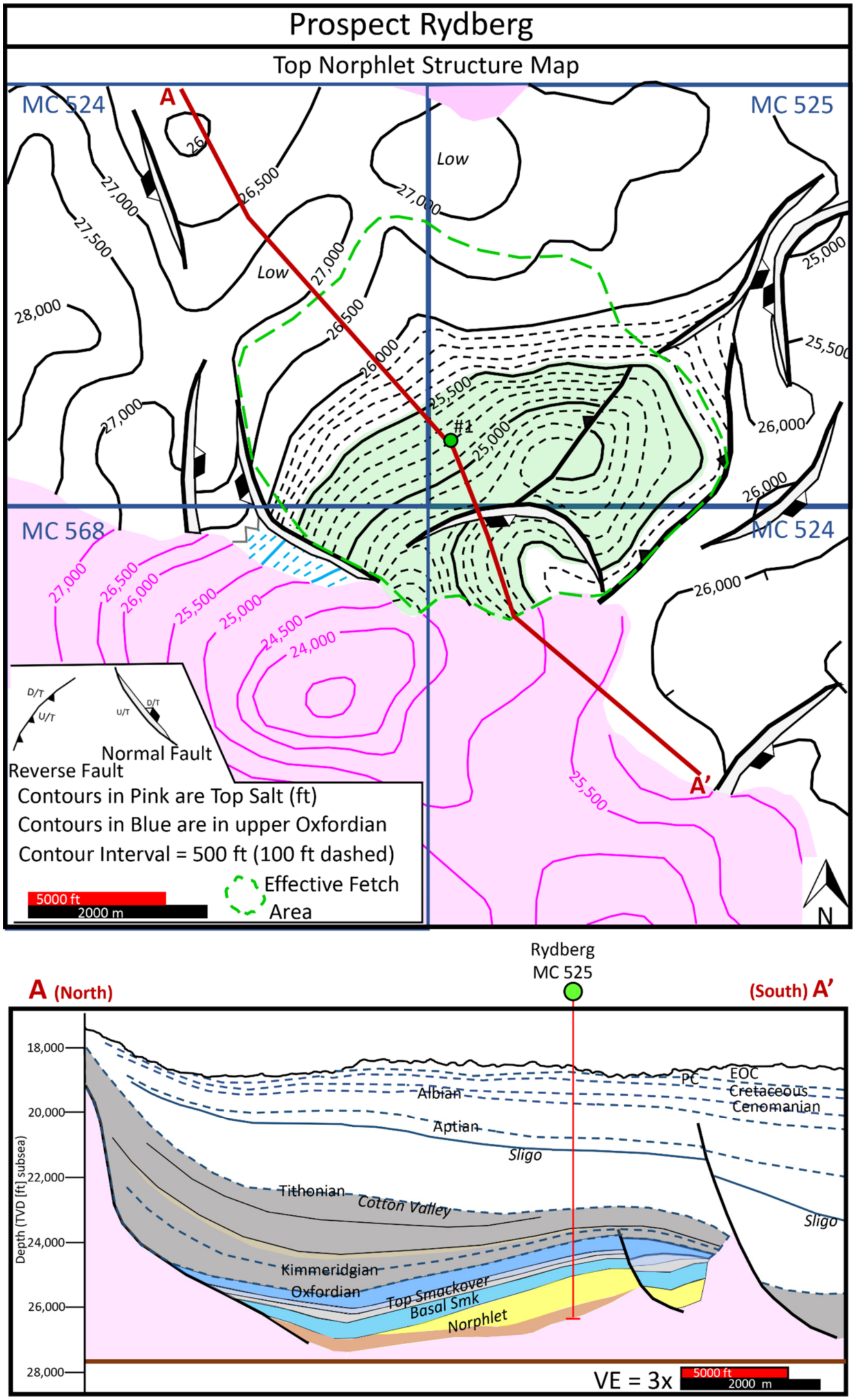

Figure 8. The structural map at Rydberg is made at the top Norphlet. The structural type is a three-way dipping faulted nose. The updip trap requires both the salt flank and upthrown faults to seal an oil accumulation. Across the fault, the Norphlet is adjacent to upper Oxfordian which spans to upper Smackover and into lower Haynesville marls. Aeolian sands were stacked against a salt flank, which evacuated southward as sediment continued to load the salt flank and further its moving. 2000 ft = 609.6 m.

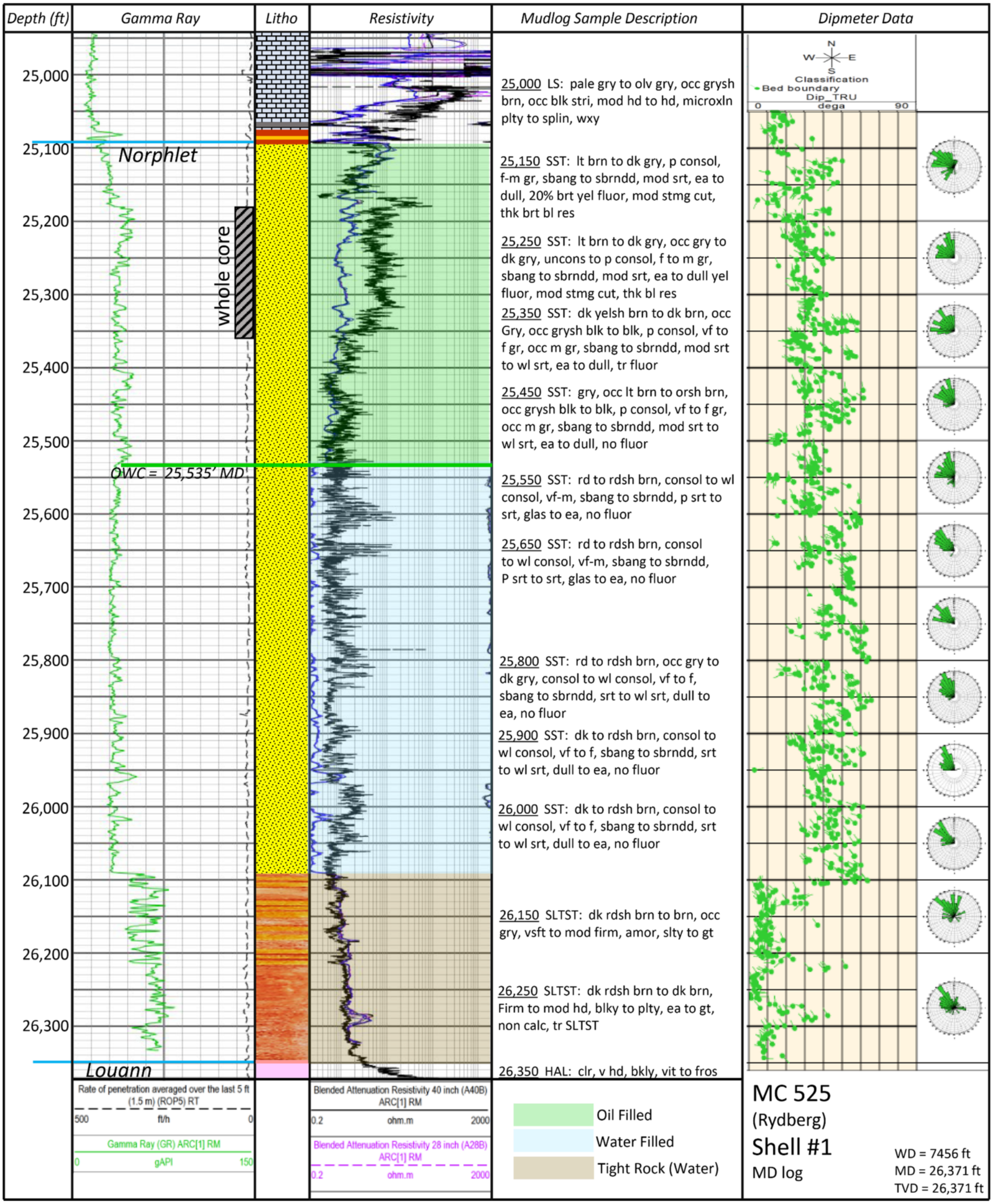

Figure 9. The measured depth (MD) well log from the Rydberg prospect shows a resistivity profile (blue curve) with typically high resistivity values representing the highest oil saturation at the top of the pay. Over the interval from about 25350 to 25,535 ft (7726.7 to 7783.1 m), the resistivity values gradually decrease, indicative a normal transition zone from oil to water saturations. The color change recorded from the mudlog description indicates that the red sandstone beneath the oil column has never received an oil charge. Therefore, the oil contact is likely at its maximum level today. The Norphlet section is dominated by aeolian sands supported by the dipmeter data. Below the aeolian facies are waterlain siltstone and sandstone. The well reached the top of the Louann Salt at the well bottom. 100 ft = 30.5 m.

The basal Smackover carbonate lies both directly on the footwall section and above the Norphlet in the hanging wall crest. The thrust fault is interpreted to cut the Norphlet at 24,950 ft (7604.8 m) TVD and likely caused a granulation of cemented quartz grains in the fault zone. Granulation will abrade grains removing delicate chlorite grain coats that otherwise prevent cementation. Fault location in the well is inferred by the presence of a (high resistivity) cemented zone and by seismic dip projection of the obvious fault cut which offsets the basal Smackover limestone.

At Vicksburg "B," the Norphlet section has five large-scale depositional intervals (Godo et al., 2011). These intervals are fluvial interbedded mudrock with silty/sandy units, overlain by stacked aeolian sheetsand facies and large-scale drying upward barchanoid dune deposits topped by waterlain sabkha facies. Average log porosity for the cored interval is 17% and for the entire aeolian sand sequence, is 20%. Porosity and permeability increase in the water wet section below the oil zone (Fig. 11). These measurements often increase in the water leg most likely due to an absence of any SHC lining that would reduce porosity and thinner chlorite rims for same reason. An increased thickness of clay (chlorite) rims is common in the oil leg (see Gettysburg chlorite content change across the oil-water contact; Fig. 6). Chlorite thickness apparently increases in the oil column by additional iron remobilization from its ferric state (hematite) in the water wet section as acidic oil displaces the water. The converted iron to a ferrous state might be reincorporated into the clay rims, thus increasing clay rim thickness and reducing effective porosity and permeability. The oil-water contact is at 24,650 ft (7513.3 m) and below this are the typical red colored sands of the water leg.

The amount of SHC in Vicksburg "B" is very large and was a huge concern because they are immovable (Godo et al., 2011). SHC reduced the porosity and permeability to such a degree that it was questionable whether the Norphlet would flow at economic rates. The question still remains as to what the distribution of SHC is vertically and laterally away from the well. The SHC source is likely the more asphaltene rich kerogen type in the algal carbonate laminae of the Smackover lower member (F. Mosca, 2019, personal communication). Vicksburg "B" is somewhat uniquely positioned from all other wells with the basal carbonate in the footwall block and overlying the Norphlet depositionally in the hanging-wall block. With the "sandwiching" of the Norphlet in the crestal position seen by the well, the early asphaltenes product would have greater area to fill the Norphlet section. This is just one purposed model.

Vicksburg "A"

Vicksburg "A" was drilled in 2013 by Shell. The faulted four-way dip closure is a short distance east of the Appomattox discovery made in 2010 (Fig. 10). Vicksburg "A" drilled the entire Norphlet section and reached total depth (TD) immediately after reading Louann Salt. The Norphlet section is approximately 745 ft (227.1 m) TVDT of aeolian sand with no fluvial section at the base (Fig. 12). A whole core was taken in the oil column and the column and displayed a normal transitional zone decreasing in oil saturation to the oil-water contact. Pressure gradients measured in the oil column all align to illustrate a continuous column (Fig. 12). The Norphlet also had a gradual color change from grays to red sandstone below the water contact at 24,823 ft (7566.1 m) TVD.

The oil-water contact in Vicksburg "A" is deeper than found in Vicksburg "B" by some 173 ft (52.7 m) (24,823 ft [7566.1 m] versus 24,650 ft [7513.3 m]) (Fig. 10). The trapping element that separates the contacts, is the north trending fault marking the culmination of the Vicksburg "B" structure (Fig. 10). The trapping element appears a continuing sealing element in the fault zone that has a mappable displacement of approximately 100 ft (30.5 m). The Norphlet sand thickness found in the wells on both sides of this fault are several hundreds of feet thick of aeolian sand without shale interbeds. If similar thicknesses are found on both sides of a fault with a displacement of 100 ft (30.5 m), it would not prevent sand juxtaposition. It is likely that cemented and sealing deformation bands exist in the fault and prevent oil to spill across the fault.

Appomattox

Appomattox in MC 392 was drilled by Shell in 2010 (Godo, 2017; Weimer et al., 2017). The four wells are labeled MC 348 #1, MC 348 #1 st1, MC 392 #1 and MC 392 #1 st2 bp1 and are in the eastern half of the Appomattox structure (Fig. 13). These wells are used to: (1) show the variable Norphlet thicknesses and (2) the change in the sandstone color in the oil column and in the water section. The discovery well log labeled MC 392 #1 is shown and discussed by Godo (2017). A cross section is shown in Figure 13. The most striking revelation at Appomattox is the difference in the oil-water contact on the northeast structural flank from the contact in the south flank. The depth of the oil spillpoint is defined but a bigger question is what seals this long column at the structural crest. At the crest of the structure, faulting is either not apparent or has minimal offset. Yet at the crest, the south flank has an oil column height of between 1700 and 1800 ft (518.2 and 548.6 m) which is not in communication with the northeast flank (Fig. 13). Along the crest of the Appomattox anticline, it is not clear what features combine to seal hydrocarbon communication across the crest. Some possibilities are (1) deformation band occurrence and frequency along the crestal fold axis, (2) subseismic faulting or (3) sand pinch out or an aeolian facies change.

Deformation bands may project into the unfaulted section beyond fault tip lines of mapped faults (Hesthammer and Fossen, 2001) and extending below seismic resolution. The formation of deformation bands occurs prior to fault formation (Aydin and Johnson, 1978; Fossen and Bale, 2007). The idea at Appomattox is the tighter folding along the crest, cause grain slippage or grain catalases, thus initiating a deformation band (Aydin and Johnson, 1978). With higher temperatures, these bands would become cemented (Walderhaug, 1996). Across the deformation bands, six orders of permeability reduction can occur (Fossen and Bale, 2007). Further permeability reduction in deformation bands might also occur caused by contribution and concentration of fine-grained material from the smearing/dissolving of lithic fragments (Knipe et al., 1997).

To help quantify permeability reduction associated with deformation bands, a reservoir model was constructed based on outcrop measurement in the Jurassic Navajo Sandstone in the San Rafael Monocline, Utah (Zuluaga et al., 2016). Their reservoir modeled a simulated fluid flow across the limb of a contractional fold using the outcrops of the San Rafael swell monocline. Multiple simulations all used a two-phase flow model where water is displacing oil. Modeled different orders of permeability reduction were made across deformation bands varying from 1–5 orders of magnitude less permeable than the host rock. Results showed that at least 3 orders of magnitude permeability reduction were needed to have a noticeable effect and produce flow barriers. Deformation bands with 4–5 orders of magnitude less permeability had significant water break through delays (Zuluaga et al., 2016).

Norphlet thickness variations can occur locally even on the scale of field development. An example of thinning is seen between the two wells drilled on the northeast flank in block 348. The MC 348 number one well, drilled off the structure looking for an appraisal oil-water contact, found 700 ft (213.4 m) TVDT of Norphlet (Fig. 14). The sidetrack drilled updip from the original well only found about 160 ft (48.8 m) TVDT (Fig. 15). The sidetrack penetration cut a small normal fault with about 150 ft (45.7 m) of offset in the Norphlet before drilling into salt. Areas

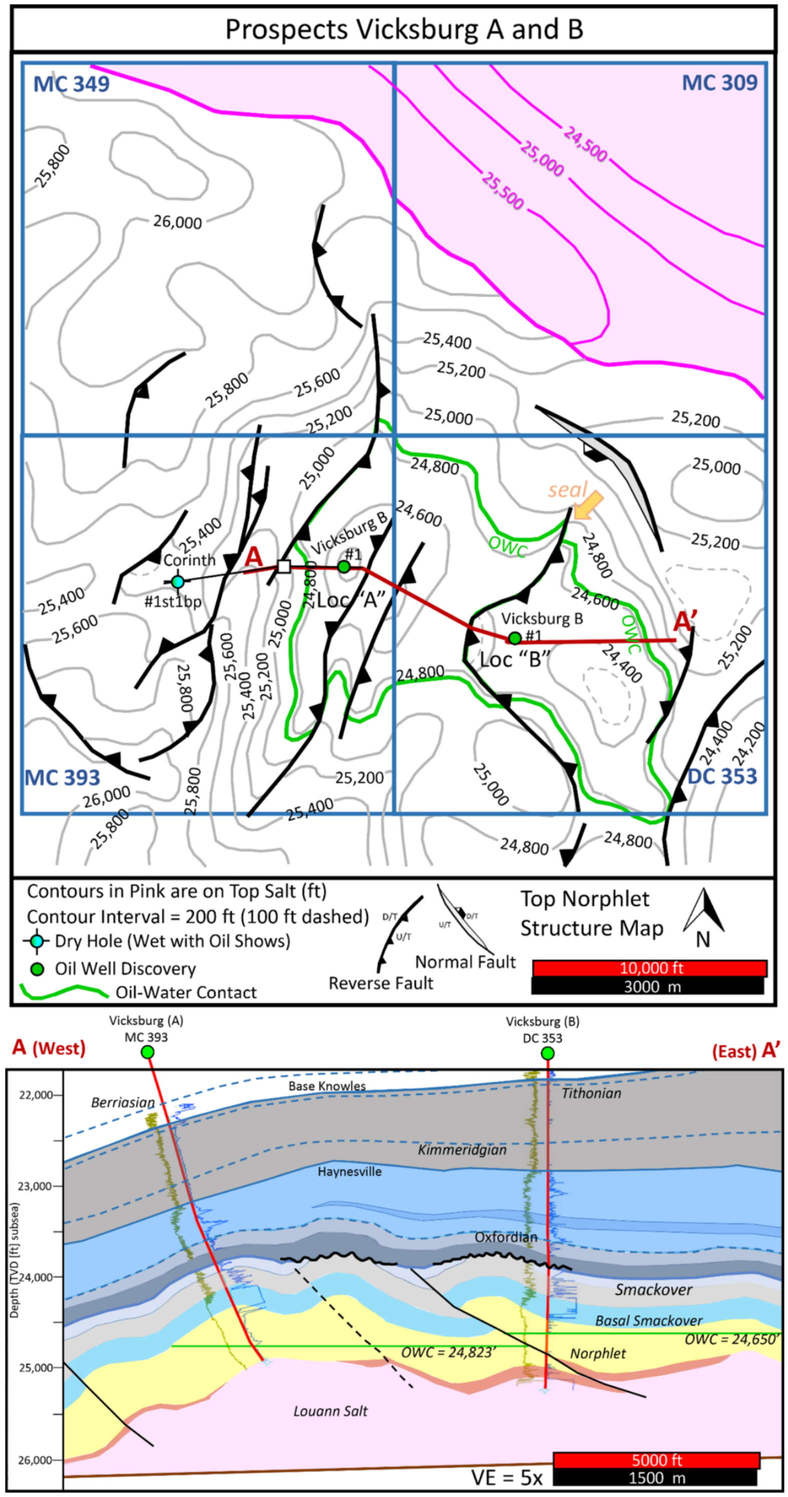

Figure 10. The top Norphlet structure map at the Vicksburg wells illustrate the compressional structural style. Horizontal compression by early translational sliding of the Norphlet and basal Smackover are seen by the thrust faults moving toward the basin. Timing can be seen by the local unconformity as there was erosion or non-deposition of basal Smackover on the structural highs. These highs may have been exposed shoaling areas during basal Smackover. Highlighted in dashed green lines, are the oil pools with the different oil-water contacts seen in both Vicksburg fault blocks. Offset of the contacts at the northern edge of a dying displacement fault (orange arrow labeled "seal") is interesting as an effective seal. Interesting because if the Norphlet aeolian sandstone has similar thicknesses as in both wells, then the small fault displacement would likely juxtapose permeable sandstones. Deformation bands that are likely within this fault and extend northward some beyond the fault tip, are one mechanism to temporally seal both accumulations. At Vicksburg "B," the proximity basal Smackover both underly and overlie the Norphlet. The Norphlet in the Vicksburg "B" well is surrounded or sandwiched between the carbonate rich source rock. It is this carbonate source rock member that is responsible for expelling the early asphaltenes. The largest amount of solid hydrocarbon derived from asphaltenes sourced in the carbonate source member. By having the thrusted Norphlet crest sandwiched by this source rock, it may be reasonable to see why there is so much solid hydrocarbon in the well. 1000 ft = 304.8 m.

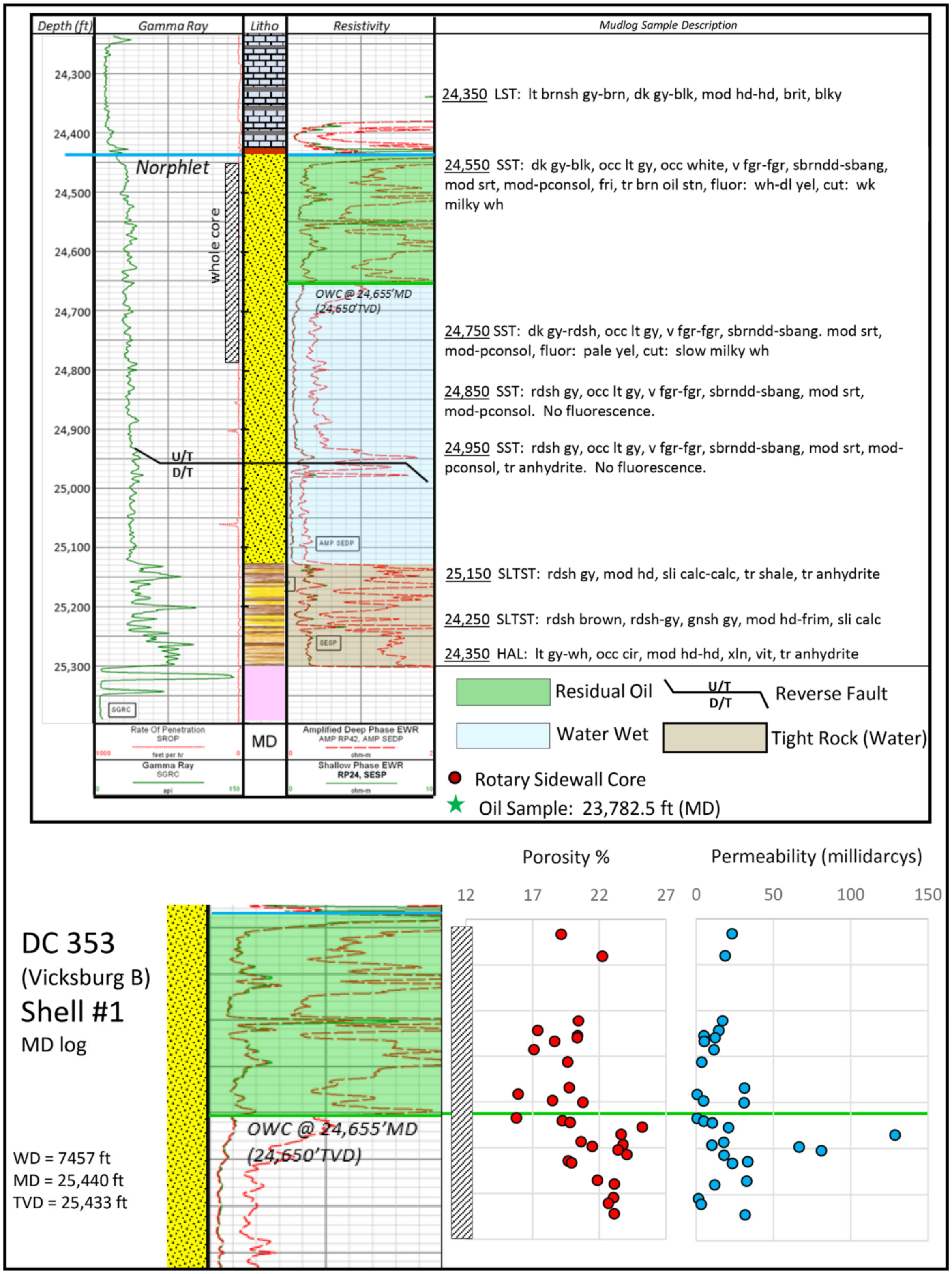

Figure 11. The Vicksburg "B" discovery well shows the oil pay logged in the Norphlet Sandstone. The oil column has an oil-water contact at 24,650 ft (7513.3 m) TVD. A color change recorded from the mudlog description indicates that the red sandstone beneath the oil column has never received an oil charge. Therefore, the oil contact is likely at its maximum level today. The well entered porous and permeable aeolian sandstone at the top of the Norphlet. Porosity and permeability values measured from core plugs are shown on the diagram. Porosity and permeability increase in the wet zone is likely due to having larger pore spaces with wider pore throats due to lesser amount (thickness) of chlorite grain coating. Chlorite amount has been seen to be increased in the sandstone found in the oil leg (see the X–ray diffraction data from Gettysburg [Fig. 6]). Internal analyses of thin sections made from many thin sections in wells from taken in the oil leg sand water leg have greater thickness of chlorite coats in the oil leg. A thrust fault defining the fault block boundary and providing a seal between the two wells is at approximately 24,955 ft (7606.3 m) MD in the zone of higher resistivity. The high resistivity zone is interpreted to result from crushed and cemented grains in and near the fault slip surface. The well reached its total depth in Louann Salt. 100 ft = 30.5 m.

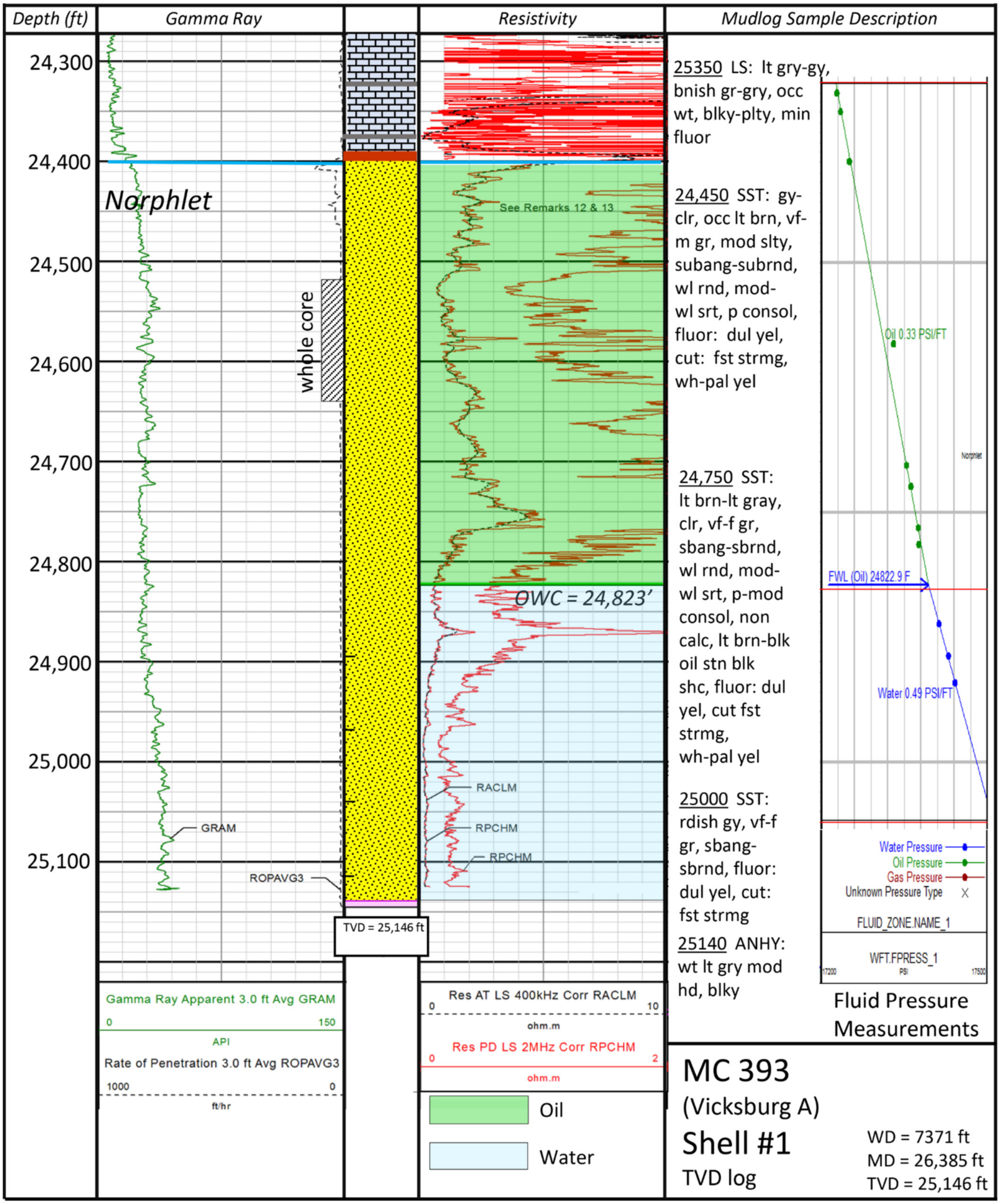

Figure 12. The Vicksburg "A" discovery well found the Norphlet to be entirely composed of aeolian sands with a complete penetration down to salt. With all aeolian sands, the velocity between these sands and salt are very similar, so the is no seismic reflection to define the Norphlet. The oil column appears to have a typical oil saturation zone into to the wet section as seen by the decrease in resistivity readings. The well log shows that the resistivity curves are highest at the top of the oil section in the well. The resistivity curves decrease in value gradually over the interval from 24,750–24,823 ft (7543.8–7566.1 m) TVD representing a normal transition zone from oil to water saturations. The pressure gradient plot on the right define the oil-water contact depth at 24,823 ft (7566.1 m) TVD. The color change recorded from the mudlog description indicates that the red sandstone beneath the oil column has never received an oil charge. Therefore, the oil contact is likely at its maximum level today. 100 ft = 30.5 m and 1 psi/ft = 0.0226 MPa/m.

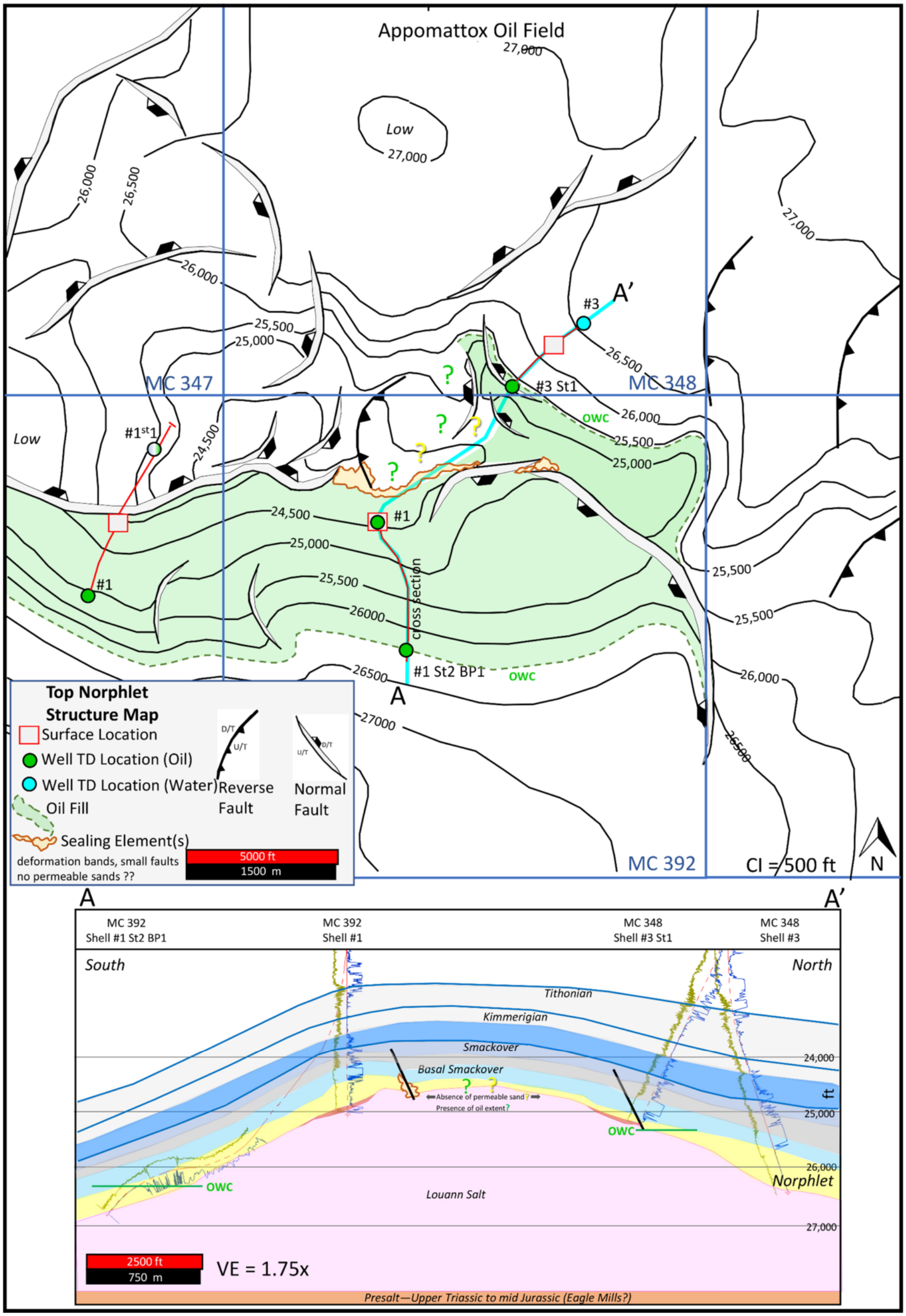

Figure 13. The structure map at Appomattox focuses on the eastern half of the structure. The map shows no faulting across the entire crest. The small tan irregularly-shaped polygons that extend across unfaulted areas suggest where there must be additional sealing elements, other than mappable faults, which separate the oil columns from the northeast flank and the south flank. The cross section at the bottom shows the variable sandstone thicknesses. 1000 ft = 304.8 m.

on the structure map along the crestal position are marked with question marks. An unknown element is how thin the Norphlet might be depositionally (Fig. 13). Early salt movement caused by subsidence resulting from Norphlet thickness variations, cause salt to bulge locally leaving areas of thinner Norphlet deposition.

If Norphlet sands are present across the structural crest, then what element creates the seal to separate the oil columns? The sealing element(s) might be deformation bands in small faults and deformation bands along the fold axis of the structure. Having recent charge enables most discontinuities (e.g., faults, deformation bands) to be effective seals. How long seal integrity is maintained for each type of discontinuity or sealing lithology is critical for evaluating the timing of peak oil charge for other Norphlet prospects. Retention time of traps holding oil is limited perhaps up to 20 million yr in the Norphlet play. Oil leakage occurs when the retention time of oil held in the trap exceeds a suggested 20 million yr (e.g., Shiloh, Antietam, Titan, and Leesburg). Only the basal Smackover carbonate appears to have longer retention time in its ability to hold an oil column, albeit a small column. Salt may also be a strong candidate as a seal maintaining oil columns for a longer retention time. To date however, the only prospect completely trapped on all sides against salt is probably Ballymore and from basin modeling the peak charge is more recently. So, to summarize, most sealing elements and lithologic juxtapositions other than the basal Smackover and possible salt are temporal seals. This is the case at both Vicksburg and Appomattox fields where subtle features such as deformation bands appear to be effective seals.

In the pre-drill stage of Appomattox, the spill point for the south and northeast flank were at the same location, the synclinal low on the east flank (Fig. 13). Because there was no fault to separate the north from the south across the crestal position. With the drilling results this east flank synclinal low is the likely spill point for the northeast flank only (MC 348 #3 st1) where the oil column is approximately 1050 ft (320.0 m). The oil column on the south flank is over 1700 ft (518.2 m). If there was no separation of the oil columns a common oil contact would be at about 25450 ft (7757.2 m) TVD.

On the cross section (Fig. 13, the water wet sections are in the MC 348 #1 and MC 392 #1 st2 (Figs. 14 and 16). In the Norphlet, we see the typical reddish-brown in the water leg and gray Norphlet in the oil column.

Shiloh

Shiloh was discovered in 2003 and was the first well drilled to test the Norphlet in deepwater. The exploration well stacked three Jurassic objectives in the pre-drill plan: Cotton Valley, Haynesville and the Norphlet aeolian sands (Fig. 1) (Godo, 2006, Godo, 2017). Shiloh was recognized as a paleohigh during Cotton Valley deposition and found thin oil sands within a Tithonian source rock package in simple closure. The Haynesville section drilled interbedded marls and carbonaceous shale. Upon entering the Norphlet interval, gray sandstones having a strong streaming cut florescence shows and other mudlogged gas shows were abundant. Drilling continued through to the base of the Norphlet penetrating the Pine Hill Anhydrite reaching its total depth in the Louann Salt (Fig. 17). A decision was made after reaching total depth, to plug back into the Smackover and kick off a new well bore in a bypass hole to take a whole core. The 180 ft (54.9 m) core barrel had complete recovery of 100% aeolian sand taken across the high resistivity drop at 23,860 ft (7272.5 m) TVD, interpreted to be the oil-water contact. Oil samples were taken had API gravity measurements of 42.2 and 45.1°. A very sharp transition from the oil column to the water leg exists (Fig. 17). Below the oil contact, continued spotty or patched fluorescence is present in the core. The sandstone is not red, but rather only gray, indicative of hydrocarbon bleaching. The fluid inclusion report shows hydrocarbon inclusions to the base of the well and petrographic examinations reveal grain rimming SHC are present in the pore spaces.

The present-day oil contact appears to coincide with the edge of simple closure beneath the basal Smackover carbonate seal (Fig. 18). This critical leak point appears to be where the Norphlet and Smackover formations were laterally rafted or pulled apart from the upthrown block (Fig. 19). As the raft moved laterally at the end of Smackover time, Hayesville marls and shales filled the gap of accommodation space. These sediments became juxtaposed laterally against the Norphlet. Sediments that were juxtaposed, once held a larger oil column but later leaked with increased residence time in the trap. Leaked oil rose up to a level and stopped leaking, where the basal Smackover carbonate continued to seal the remaining oil. Below the present-day oil-water contact is residual oil and SHC's in a bleached reservoir that remains juxtaposed with Haynesville marl and shale. Shiloh received it peak oil charge during the Cretaceous time, then at least the oil in the trap today, resided over 65 million yr. The current suggestion is that the trap held the maximum oil column for perhaps 20 to maybe 30 million yr before partial drainage occurred. The trap likely followed an imbibition type drainage by the oil overcoming the capillary entry pressure of the rocks (Aplin and Larter, 2005). The leak(s) likely were in the fault gouge or adjacent Haynesville marls and shale. Only the overlying basal Smackover carbonate maintained its seal integrity, preserving the remaining oil column found today.

Antietam

Prospect Antietam was drilled in 2009. Both Shiloh and Antietam lay under the same closure of the Haynesville carbonates and the Tithonian clastics and therefore had a very similar burial history (Fig. 1). At Antietam, there is a larger displacement at the crest, which juxtaposes the Norphlet against the clastics and marls of the middle Smackover (Fig. 19). At the structural crest of Antietam, is there a small trap component of simple four-way dip closure at the top Norphlet section. The basal Smackover is the top seal for this simple closure.

Drilling through the Haynesville in Antietam, two major mudlogged gas shows were encountered at 22,410 ft (6830.6 m) and 22,660 ft (6906.8 m) TVD (just above and below the top Smackover, respectively). After the first gas show, mud weight was increased by 0.3 ppg (pounds per gallon), then after penetrating an additional 250 ft (76.2 m) TVDT, the second gas show was encountered. Mud weight was again increased by an additional 0.2 ppg and a liner had to be set, before drilling deeper. After setting casing, the well drilled on and entered the Norphlet section. Immediately, the mudlog indicated good fluorescence with oil cut fluorescence in brownish gray to dark gray sandstone. Initial resistivity readings in the top Norphlet are high but after about 30 ft (9.1 m) of penetration, the resistivity measurement decreased very rapidly to a low reading indicating an abrupt oil-water contact had been penetrated. Drilling continued in the lower Norphlet section finding about 130 ft (39.6 m) TVDT of ephemerally deposited fluvial sediments. The well reached a total depth upon encountering halite of the Louann Salt (Fig. 20). The upper Norphlet aeolian sand at Antietam is logged with some 600 ft (182.9 m) TVDT with good porosity and permeability values. Log measured porosity averages about 20%. The fluvial section in the lower Norphlet is mostly red colored shale, siltstone and two thin sandstones with porosity less than 10%.

A structural map at the top Norphlet/base Smackover was made with 3D seismic data from Tomlinson Geophysical Services (TGS) 3D (Fig. 21). A thin oil column at the top of the Norphlet has a spill point coincident simple closure at the base of the top seal (basal Smackover). Below this simple closure of the basal Smackover, the Norphlet is fault juxtaposed to younger rocks. It is interpreted that a paleo oil column had extended to the base of the aeolian section. The Norphlet sandstone below

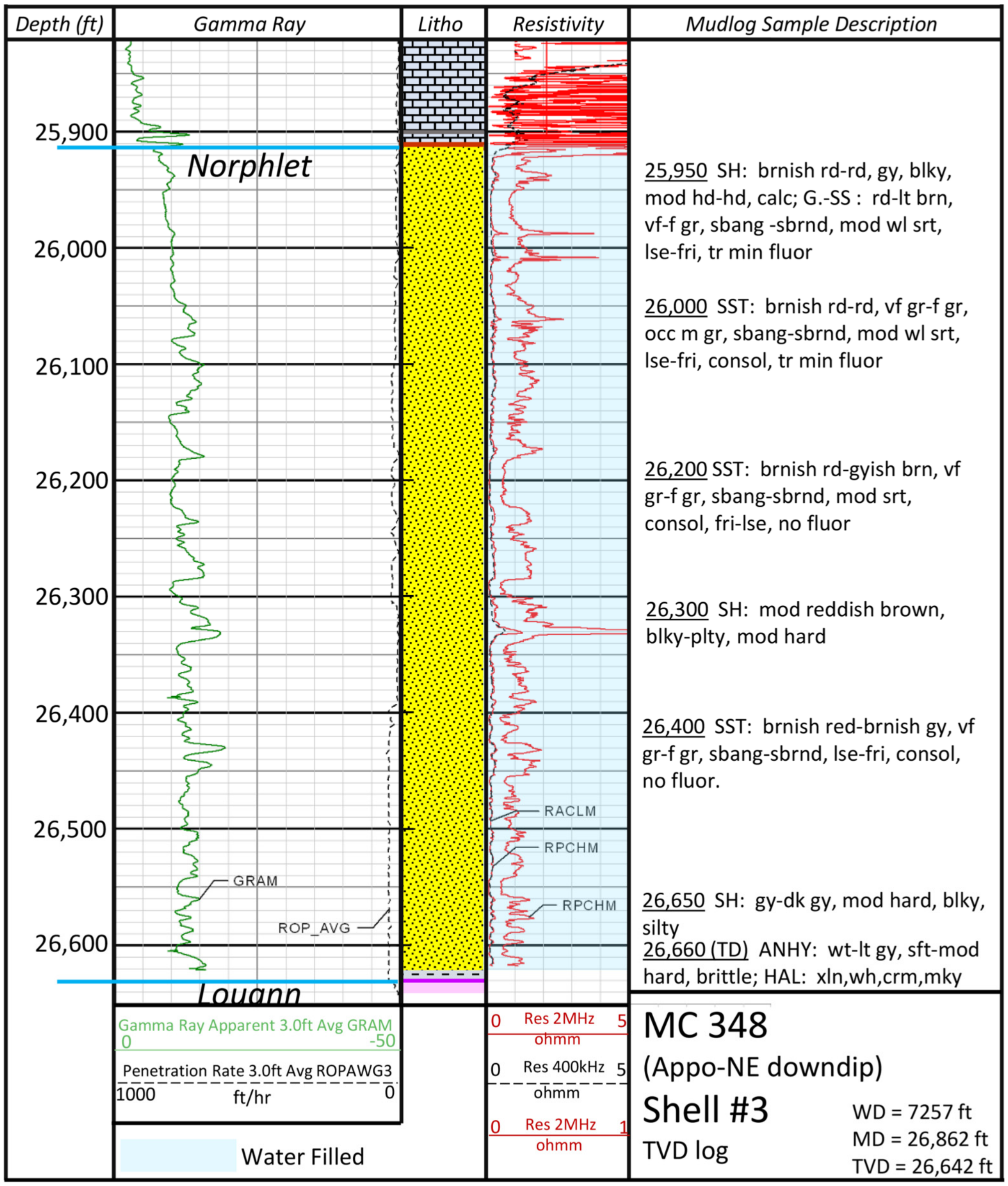

Figure 14. The MC 348 #3 well at Appomattox has a penetration with approximately 700 ft (213.4 m) TVDT of aeolian Norphlet brownish red, wet sandstone. No evidence of either present-day or paleo oil fill is in the well. 100 ft = 30.5 m.

the oil contact is all gray with SHC residue in the pore space as shown in photomicrographs (Figs. 22 and 23). Fluid inclusion reports oil to the base in support of the paleo oil column (F. Mosca, 2019, personal communication). Leakage of the larger oil column is suggested to have occurred as capillary entry pressure was overcome in sediments juxtaposed the Norphlet section or along the fault itself. Hydrocarbon seepage occurred due to an excessive residence time in the trap. This leakage occurred, draining the Norphlet, until the only oil preserved lie beneath the simple closure of the top seal. The mechanism for this and all the Norphlet leaked traps is hypothesized to have leaked slowly as trapped oil seeped through previous seals by overcoming their capillary entry pressure. Aplin and Larter (2005) stated the based on field and experimental data, that once a water-wet cap rock is breached, the leak path will become oil wet. Thus, loss of petroleum through this cap rock or seal, increased it relative permeability for oil to pass, limiting any meaningful formation of a hydrocarbon column. Aplin and Larter (2005) further characterized this scenario of changing the wettability from water wet to oil wet in the seal lithology representing "low-permeability chokes to petroleum systems instead of capillary seals."

Titan

Prospect Titan was drilled by Murphy Oil in 2014 to explore for oil in the Norphlet sandstone in DC 178. Structurally, the Titan location is on a long and narrow south-plunging nose flanked on the east and west by thick Cretaceous filled synclines (Fig. 24). The crest of the structural nose rises more gently northward and is trapped against a salt mass. Also local along the nose crest, is a small salt high that pierced upward through the Norphlet. The thick Cretaceous flanks on the east and west sides of the nose, buried the Smackover source rock and maturing it during the Late Cretaceous (Weimer et al., 2016b, their figure 8A). The Titan structure is but one of the three separate Norphlet traps within the fetch area of the greater Titan area of which the Titan "ridge" is the shallowest. Not all the hydrocarbons would have migrated to Titan without being trapped in two other Norphlet traps. These three traps are shown on the structure map with the Titan #1 (Titan ridge), the #1 st well (downthrown Titan) and a simple four-way dipping structure. The four-way simple dip closure of the basal Smackover carbonate seal is located southeast of the Titan wells mostly on

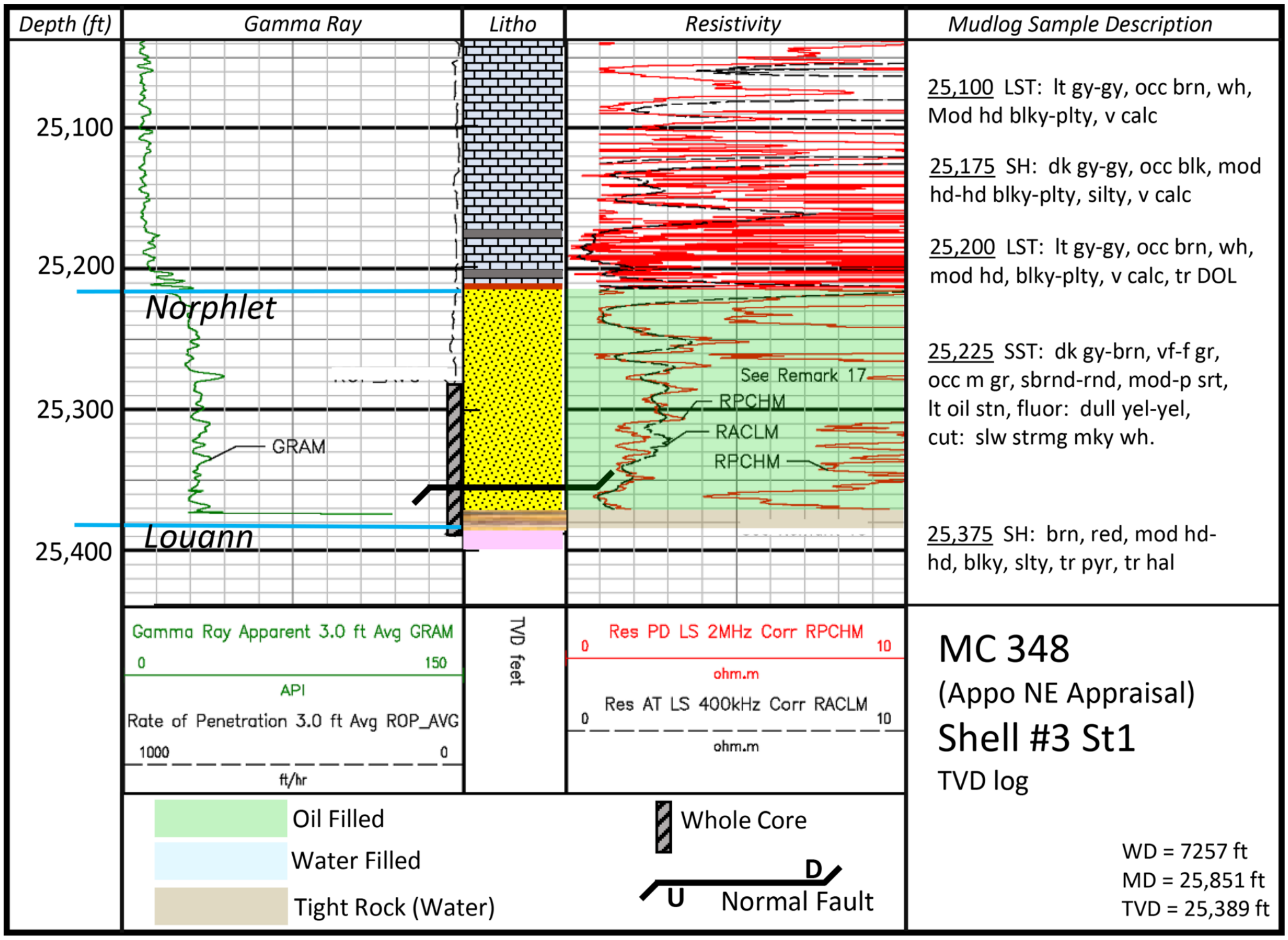

Figure 15. The MC348 #3 st1 well is a sidetrack well targeted to find oil updip from the MC 348 #3 well on the northeast flank of Appomattox. The well drilled a thinned Norphlet sandstone section that is filled with oil to the base of the permeable aeolian facies. The wellbore cut a normal fault where penetrated the Norphlet in the downthrown block. While taking a whole core, the well cut the fault, reducing the Norphlet thickness before penetrating the Louann Salt with about 10 ft (3.05 m) TVDT of shale on top of the salt. The water contact was not penetrated. 100 ft = 30.5 m.

block 179. On the large Titan structural ridge, the #1 well drilled into a very small four-way dipping simple closure beneath the Smackover basal carbonate (Figs. 24 and 25). For any significant column height to exist on the ridge structure, fault juxtaposition with younger rock on the east flank would have to seal. This fault juxtaposition exists along a general north-south trending extensional fault just east of the #1 well. This juxtaposition along this fault places the Norphlet sandstone in fault contact with rocks of upper Smackover and Haynesville. Retention of trapped oil against this juxtaposition, would have to remain for 65 million yr after peak oil expulsion (Fig. 4). Hydrocarbons likely leaked from trap either up the fault plane itself or directly into Upper Smackover/Haynesville rocks. Once hydrocarbons began to leak across through these adjacent rocks, migration likely continued vertically without a presence of a top sealing lithology. The hydrocarbon shows in the overlying Haynesville and Smackover may be isolated pockets of hydrocarbons, as oil may have leaked into the shallower depths and formations.

While drilling of the Titan well, upon entering limestones at the top of the Hayneville, mudlogged gas increases were incoming and mudweight was increased to control the gas. Internal reports indicated that fractures were seen with higher pressured fluids likely traveling up faults from deeper formations. Unusually high resistivity measurements were recorded at the top Haynesville around 22,600 ft (6888.5 m). The mudweight required to control the increased gases required setting an intermediate casing before drilling deeper. A fluid inclusion report highlighted a significant increase over the entire Haynesville and upper to middle Smackover of some 800 ft (243.8 m) (22,688–23,523 ft [6915.3–7169.8 m]). Throughout this interval, fluid inclusion work indicated that this zone was gas-rich associated with oil. The zone probably represents diffusion of oil and gas through otherwise tight but also fractured carbonate, marl, mudstone, shale and limestone.

Upon entering the Norphlet interval, light gray aeolian sandstone was present which have florescence shows from 23,780 to 23,900 (7248.1 to 7284.7 m) (Fig. 26). The resistivity profile initially was high indicating oil pay in the first 10–15 ft (3.05–4.6 m) below the top Norphlet. Then, the resistivity quickly dropped to very low level indicating an oil-water contact was present without any gradual resistivity decrease typical in a transition zone. Below the contact at 23,792 ft (7251.8 m), light gray to black, thick aeolian sand continued. A color change from gray to reddish brown sandstone occurred around a depth of 24,000 ft (7315.2 m). Drilling continued below the top red sandstone for an additional 134 ft (40.8 m) before reaching a total depth of

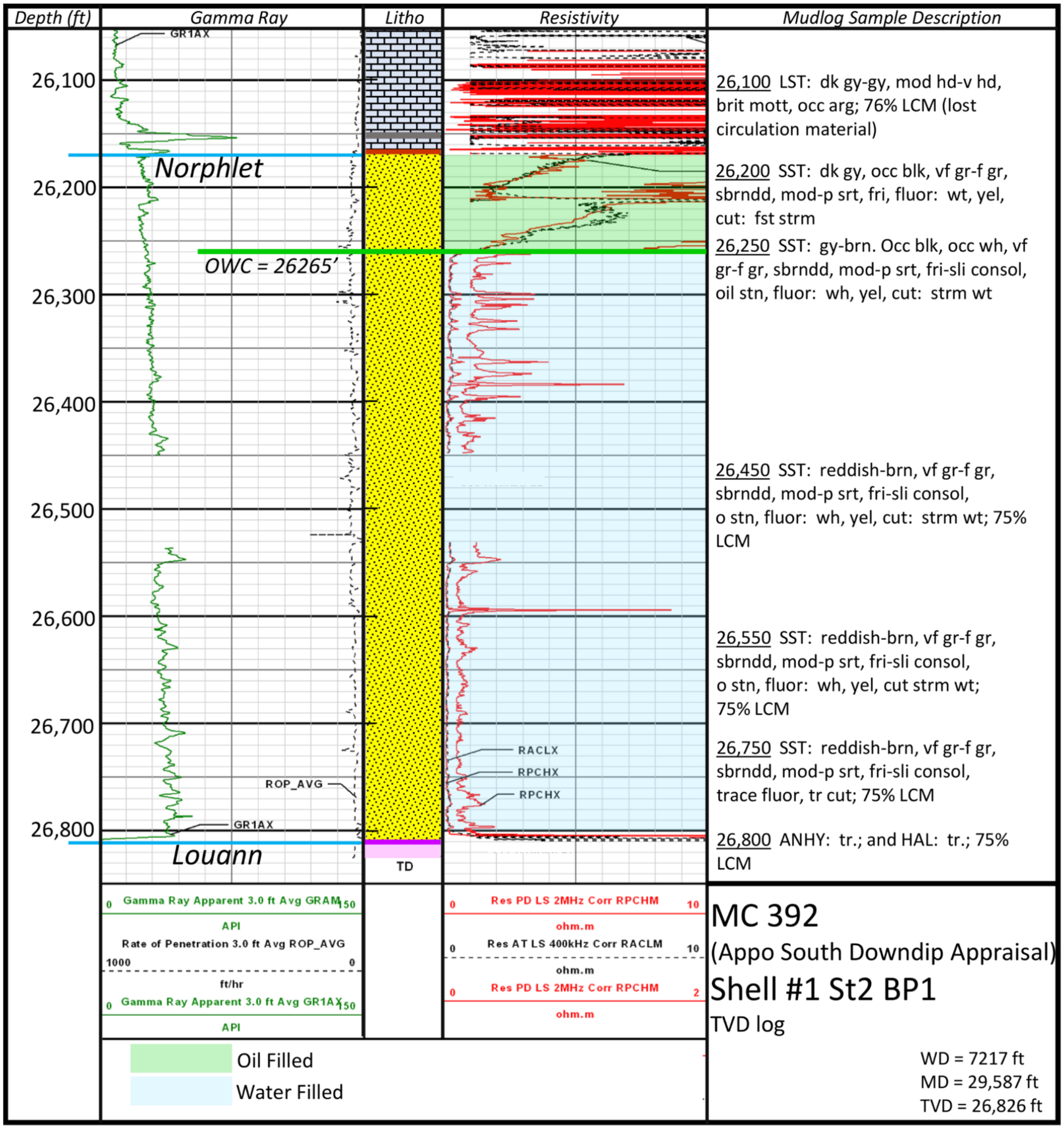

Figure 16. The MC 392 #1 st2 bp1 well at Appomattox is a complete Norphlet penetration with approximately 650 ft (198.1 m) TVDT of aeolian Norphlet sandstone. The oil-water contact at 26,265 ft (8005.6 m) TVD is at a structural depth whose structural contour may is close to the deepest level before leaking at a structural spill point. Based on the structure map (Fig. 13), there is a couple more hundred feet of closure below the depth of the oil-water contact in this well. The resistivity level in the oil column is high and drops very quickly from 26,240 to 26,265 ft (7998.0 m to 8005.6 m) TVD. This rapid drop in resistivity over a seemingly short interval might suggest that the transition zone from an oil to water saturation is too abrupt and some leakage has occurred. There are strong oil shows reported in the mudlog below the oil contact. Also, the sandstone is still reported as gray to brown up to 150 ft (45.7 m) below the oil. 100 ft = 30.5 m.

24,534 ft (7478.0 m), still in Norphlet aeolian facies. An oil sample was taken at 23,782.5 ft (7248.9 m) that has an API gravity of 43.7° and a viscosity of 0.7 cP (0.7 mPa-s). Several rotary sidewall cores were taken up to 164 ft (50.0 m) below the live oil zone (Fig. 27). In these deeper sidewall cores, thin section examination reveals oil bitumen (SHC) lined and partially filled isolated pore spaces in the sandstone. The model of a leaked trap is supported by presence of SHC in the pore spaces below the present oil contact. Further support for a leaked trap uses the model that hydrocarbons bleached an originally red colored sandstone to now gray colored. Most of the larger amount of oil escaped laterally into the Haynesville then upward. The vertical loss of hydrocarbons was only slightly limited, remaining trapped beneath the small simple dip closure in the basal Smackover top seal (Fig. 25).

A water sample was taken at 23,805 ft (7255.8 m), which had a very high salinity that measured above 350,000 ppm. At this high salinity, it might be anticipated that some halite precipi-

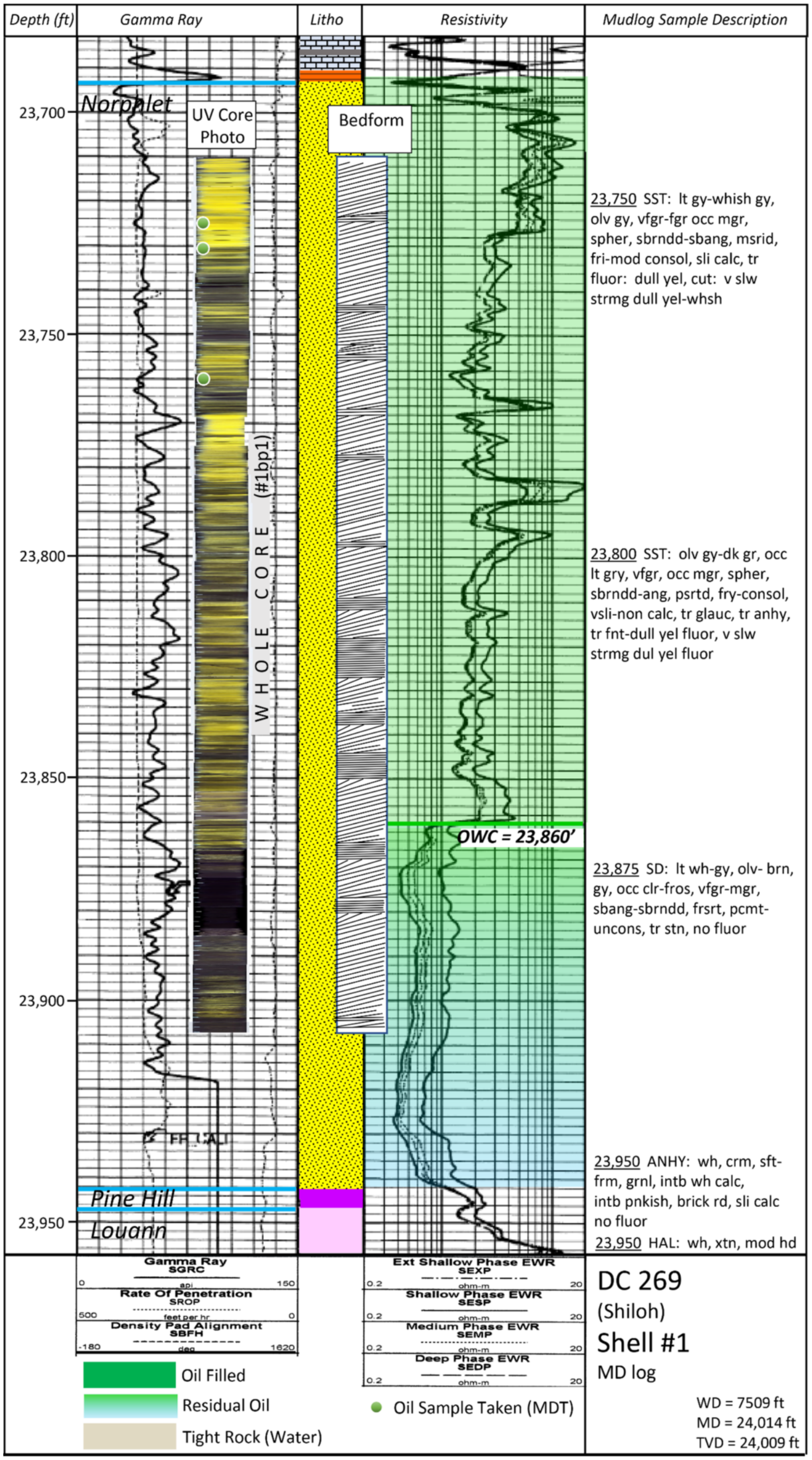

Figure 17. The Shiloh discovery well penetrated about 250 ft (76.2 m) TVDT of all aeolian sand before penetrating anhydrite then halite. The whole core was taken in a bypass well (DC 269 #1 bp1) drilled very close by the original #1 borehole (~15 ft [~4.6 m]). Shown with the log of the #1 well are the core photos, taken un ultraviolet light and with a general bedform log made from the bedding on core photos. The ultraviolet light photos show intervals of fluorescence from oil below the oil-water contact. Resistivity values decrease very abruptly across the present oil-water contact and it does not look like a normal, more gradual decrease in a transition zone from oil to water. Mudlog sample descriptions describe only olive gray to dark gray sandstone, with no shades of red. 100 ft = 30.5 m.

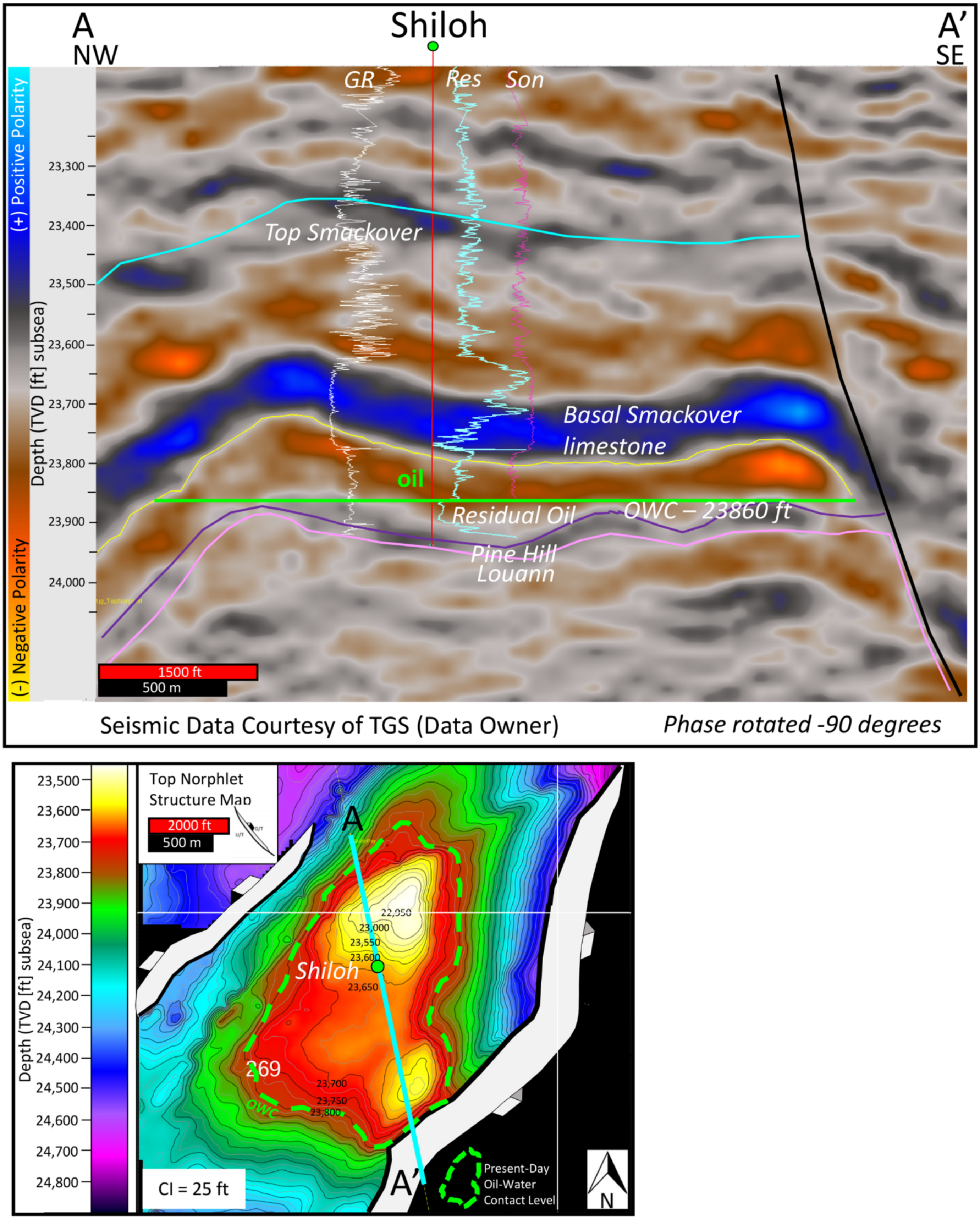

Figure 18. The structure map at Shiloh shows a small but simple four-way dip closure at the top Norphlet/basal Smackover contact. The simple closure flattens southeastward, then terminates against a hanging wall of a normal fault. This normal fault formed to accommodate thickened Oxfordian aged sediments that filled the space created by the lateral sliding of the Shiloh block. The depth of the oil contact in Shiloh matches closely the depth level at the terminal end of the sealing basal Smackover closure. 100 ft = 30.5 m.

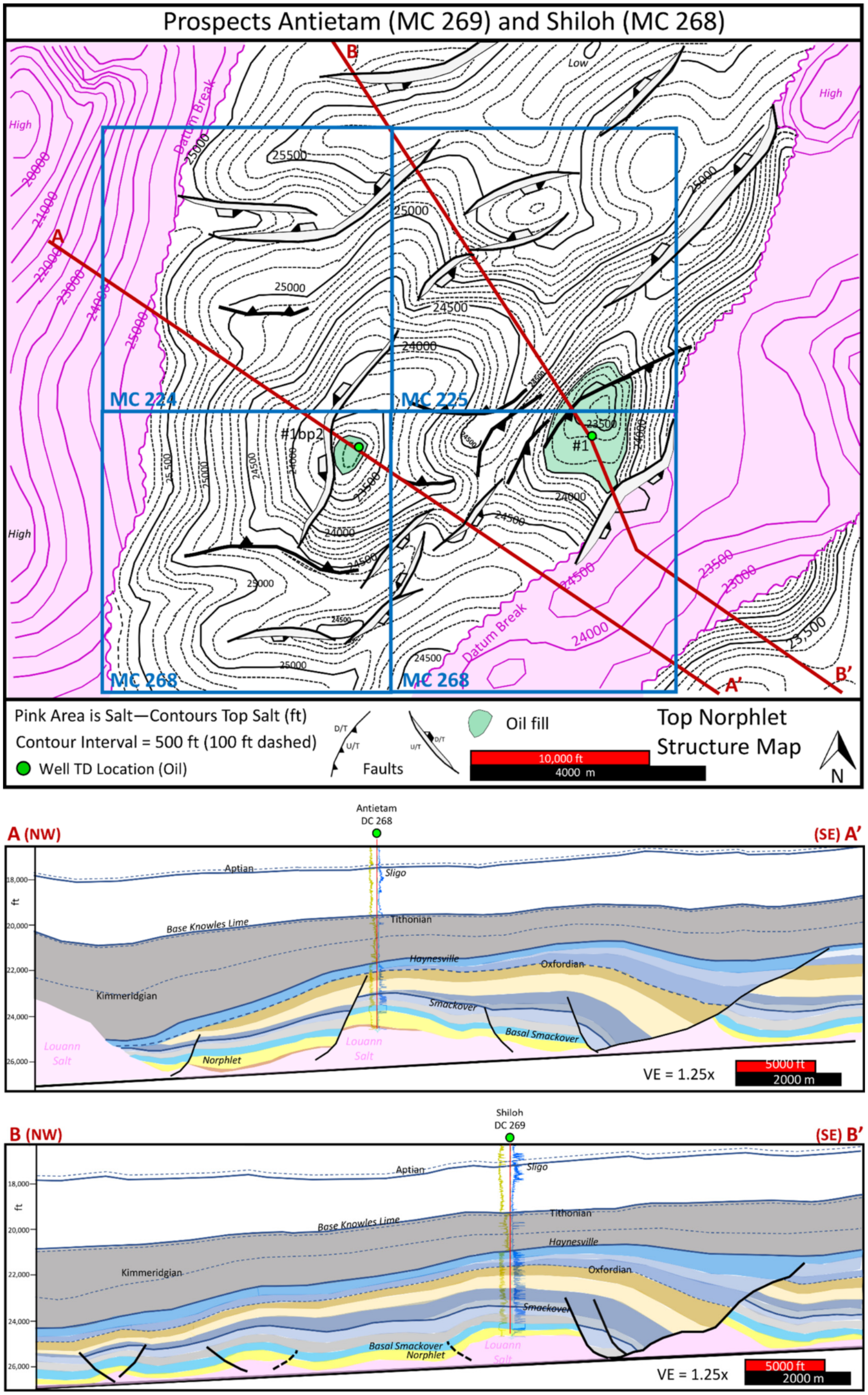

Figure 19. The cross sections over Shiloh and Antietam illustrate the early lateral sliding of the Norphlet and lower Smackover rocks. This package of rocks laterally slid or rafted, during the upper Smackover (Oxfordian) and lower Haynesville (Kimmeridgian) as these younger sediments filled in the vacated space of earlier lateral sliding. Salt contours in pink are a datum change from the contours on the Norphlet to a change at the same depth to salt contours. The map highlights the oil accumulation of Shiloh and Antietam in the Norphlet (green filled contours). 2000 ft = 609.6 m.

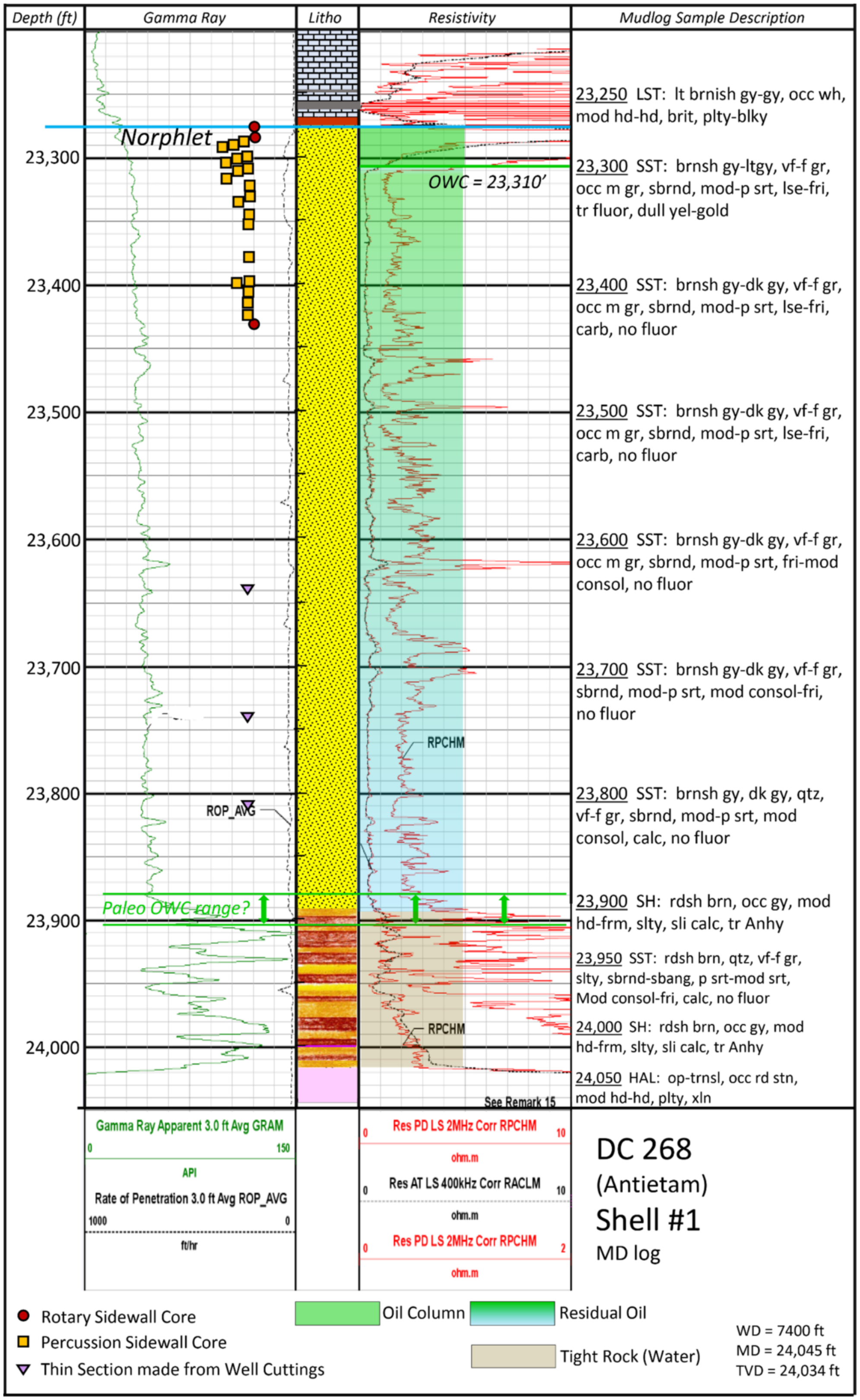

Figure 20. The gamma ray and resistivity log at Antietam show that the well penetrated a complete and much thicker Norphlet section than found in Shiloh. The Norphlet thickness in Antietam is nearly 750 ft (228.6 m) TVDT. The lower Norphlet has a fluvially deposited shale, siltstone and sandstone thickness that combine to form a seismically fast (hard) event that defines the base Norphlet. Above this fluvial section is just over 620 ft (189.0 m) TVDT of repeated sequences of aeolian dune sands. Depths of rotary and percussion sidewall cores taken from the well are show as well as the points where available thin sections photomicrographs are publicly available. Resistivity values decrease very abruptly across the present oil-water contact and it does not look like a normal, more gradual decrease in a transition zone from oil to water. Based on the absence of red aeolian sandstone, solid hydrocarbon residue, and resistivity profile, Antietam is interpreted to have once been filled with oil to the base of permeable Norphlet and since leaked. 100 ft = 30.5 m.

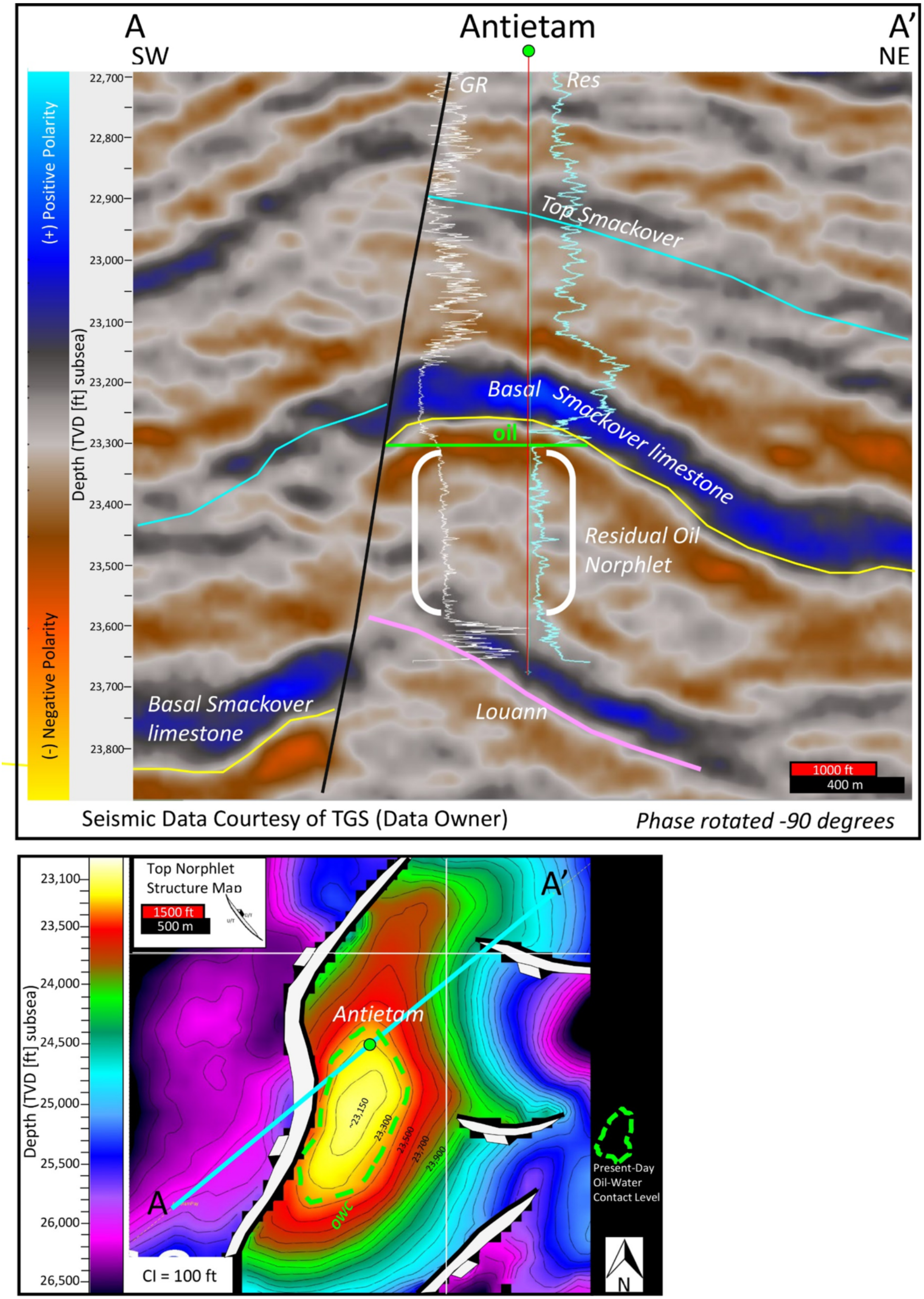

Figure 21. The spill point and simple closure level of the basal Smackover top seal is shown on this seismic well tie at Antietam. The Norphlet oil column once extended much deeper as the fault seal/juxtaposition of the Upper Smackover held the paleo oil column. With residence time in this trap exceeded, upward leakage across the fault occurred rising the oil column to the basal Smackover top-seal. The smaller structural map made on 3D data, illustrates the conformance of the oil-water contact to that of the simple closure. 100 ft = 30.5 m.

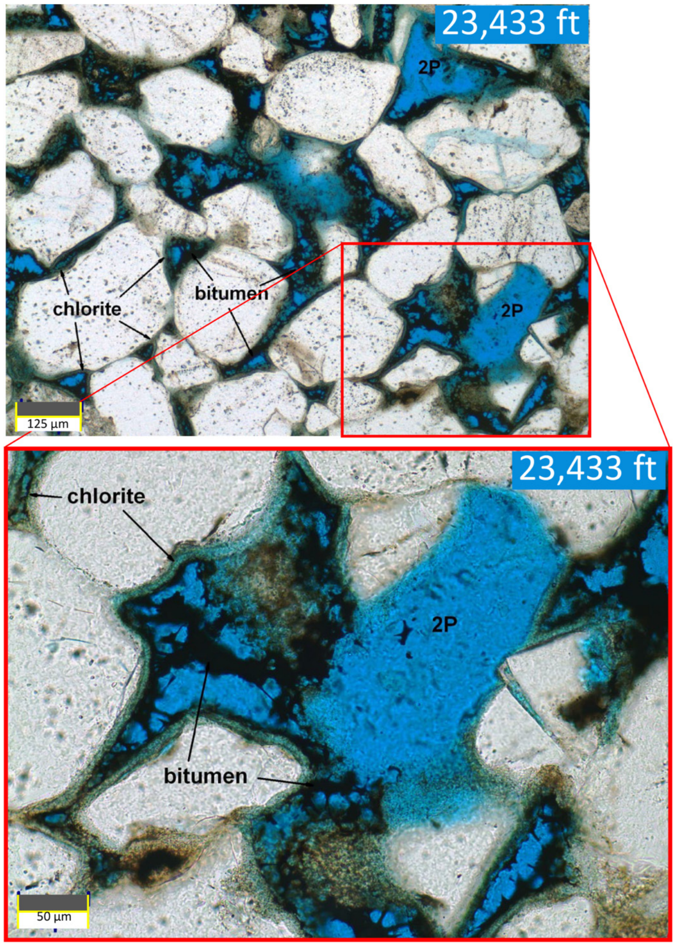

Figure 22. Top: Rotary sidewall core from Antietam at 23,433 ft (7142.4 m) MD. The diagenetic sequence of cements includes moderately early precipitation of pore-lining Fe–rich chlorite, followed by precipitation of microporous asphaltene. Isolated areas of secondary porosity (2P) may in some cases reflect grain plucking during thin section grinding (lower right pore). Bottom (Inset Enlargement): The "suspect" secondary pore has a small remnant of quartz in the pore and there is an absence of a preserved grain-rimming chlorite coating. This suggests that the clay coating was plucked away with the missing grain. There are moderately thick, continuous films of grain-rimming Fe–rich chlorite.

tation would form as a cement, but no evidence of halite cement was reported.

Leesburg

The exploration well for prospect Leesburg was drilled in Mississippi Canyon Block 475 by Shell Oil in 2016. The objective was the Norphlet aeolian sandstone facies located on a faulted structural nose (Fig. 28). Leesburg is the first well to penetrate the Norphlet in this polygonal depobasin (Fig. 2). Named the Leesburg Norphlet depobasin, this basin is also likely bound by salt walls from adjacent basins. The closest Norphlet basin lies to the east and named the Vicksburg basin for its first penetration (Fig. 2).

At the top of the Norphlet there was not any movable oil, but it did find cut fluorescence in gray sandstone. With continued drilling, thick apparently aeolian facies are present, having good log porosity and permeability. The gamma ray log represents a thick section of sand. Near the bottom 40 ft (12.2 m), the mudlog describes red shale (Fig. 29). The last bottoms up sample at total depth, described a trace of halite. This may indicate that the well may have just scratched the Louann Salt at total depth.

The trapping elements of Leesburg are the footwall sides of three normal faults against which the closing Norphlet structural contours. In fault juxtaposition with the Norphlet on the hanging wall are sediments of the Haynesville in the eastern fault and Lower Cretaceous on the western fault. Only in a small crestal area, is the Norphlet trapped against salt. There does not appear to be any trap component of simple closure (Fig. 28).

The Leesburg structural nose was first formed by the end of Cretaceous time when peak oil was expelled (Fig. 4). A Norphlet map viewed at Cretaceous time is obviously not possible, so an isopach made between the top Norphlet and the top Cretaceous is used as an approximate top Norphlet map from the Cretaceous time (Fig. 30). The crestal area of both top Norphlet maps are similarly shaped and in a similar position. In other words, the crestal area at Cretaceous time, is generally the same crestal area of the present top Norphlet. The Norphlet structure map at the end of the Cretaceous, if charged then, would have trapped oil filled 65 Ma. For the next 45 million yr, the trap was not buried much as the Paleogene and Lower Miocene was relatively thin. At middle Miocene time, the eastern flank became deeper buried, altering the east flank of Leesburg. This eastern flank became buried deep enough to mature the Smackover source rocks generating a second charge and migration path into the previous crest. Oil shows and a sand color change at 26,850 ft (8183.9 m) TVD from red in the lower section to gray in the upper, suggest Leesburg may be a leaked oil field.

Fredericksburg

Fredericksburg was drilled in 2008 by Shell in Block 486 of De Soto Canyon. The exploration well targeted Norphlet aeolian sandstone reservoir on an unfaulted four-way simple dip structural closure (Fig. 31). This structure formed soon after rapid Norphlet deposition as seen by the middle and upper Smackover thickness change (900 ft [274.3 m] to 300 ft [91.4 m]) across the structure from north to south (Fig. 31). The Norphlet basin at where Fredericksburg is located, is a relatively small confined polygonal salt basin. The limits of Norphlet deposition in this basin was confined and surrounded by likely positive salt highs. The basin had at least one sediment entry point for sediments that flowed downdip from the eastern highlands localizing deposition at Fredericksburg. Rapid and thick deposition of Norphlet sedimentary rocks increased the rate of subsidence responding to this initial load of Norphlet. The thickest part of the Norphlet in the basin subsided faster than the basin flanks. Upon the completion of salt evacuation, the base Norphlet rested on the basement and stopped subsiding. Next, the basin flanks continued their subsidence in the remaining salt until Norphlet sediment touchdown on the basement. With the basin inversion complete, the Norphlet basin became inverted or "turtled" (Peel, 2014). A turtle is marked by the thickest Norphlet section (previous syncline) that now forms the structural crest with a simple closure. The present -day salt weld at base Norphlet, is observed near the well's total depth. Below the halite section in Fredericksburg, is an interpreted eroded basement consisting of basalt clasts in a shale matrix (Fig. 32). This type of early Norphlet basin inversion, located in other small confined salt polygonal depobasins, are common in the play area based on internal mapping. The term "pothole basin" is used here to describe this type of localized Norphlet turtle structure. The distribution of these structures aligns themselves in a rather linear belt oriented from northwest to southeast with Fredericksburg located at the northwest end. Two others of these turtles have been drilled at Petersburg (DC 525) and Swordfish (DC 843). Other undrilled turtle structures are in DC 573, 663, 753, 799/843, and 935/979.

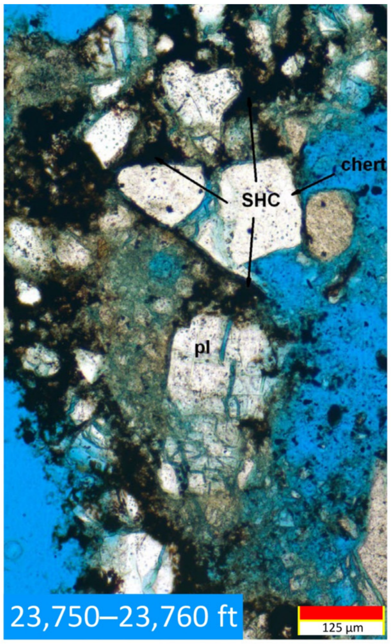

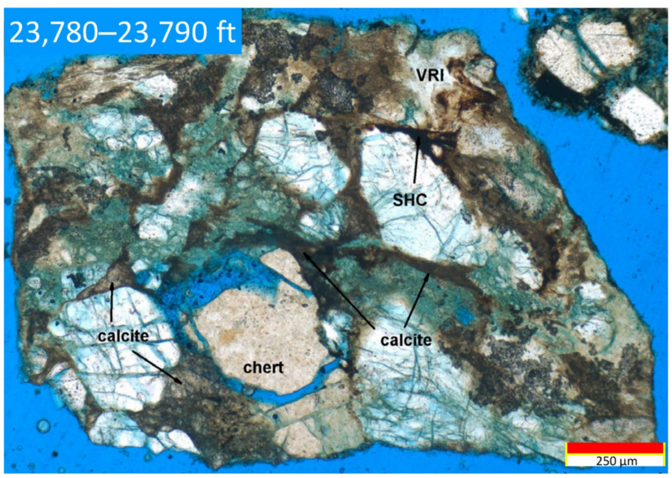

Figure 23. Top: Antietam thin section made from cuttings over the interval from 23750–23760 ft (7239.0–7242.0 m) MD. Sand grains consist of plagioclase (pl), chert, quartz, and altered volcanic rock fragments. The dark material is interpreted as SHC in the pore space. The textural features show the asphaltene resting on top of grain-rimming chlorite, which suggests residual asphaltene. Bottom: Thin section made from Antietam drill cuttings over the interval from 23780–23790 ft (7248.1–7251.2 m). Cutting consists of calc-cemented, med-grained, lithic sandstone with low amounts of pore-filling asphaltene. Asphaltene found in the center of a tightly cemented sandstone fragment suggests that the hydrocarbon is not related to invasion of mud around the edges of the cuttings.

Norphlet facies found at Fredericksburg are dominated by fluvially deposited sediments confined to a basin rimmed by salt bulged highs where sediments thickly accumulated in a relatively small area. Locally some of the sand when dried out from the ephemeral flow episodes, may have form small dunes not rising far above the paleo-water table. All Norphlet lithofacies display shades of red to reddish brown colored, hematite-rich, sandstone, silty sandstone, sandy siltstones and claystones (Fig. 32). The finer grained clay and siltstone are found in the lower portion of the Norphlet in the well. Two intervals of Fredericksburg have the most sand content around 23,600–23,650 ft (7193.3–7208.5 m) MD and the other between 23,710–23,810 ft (7226.8–7257.3 m) MD. The lower interval appears to have a thickening upward trend as shown on the log by the curve drawn next to the gamma ray log. Although this gross overall trend, likely reflects smaller wet aeolian dunes close to the water table. With a rising water table, there is redistribution of fine grain muds which block pore throats and modifies or destroys primary sedimentary fabric in the dune. The upper interval starts at the base just above a marked shale break at 23,690 ft (7220.7 m) MD. This interval may indicate more small dunes between minor shale breaks or possibly sand sheets that could not build topographically. Toward the top of this sequence, the gamma ray increases indicating that either subsidence rate increased as the thicker, basal Smackover shale began to transgress the area.

Norphlet fluvial sandstones and small height aeolian dunes are unable to retain permeability over time due to pore throat openings that became clogged early during deposition by the introduction of clays via fluvial waters and by a rising water table. Aeolian dune sands that can have more open pore throats that resist later cementation do not do so if the dunes cannot stay dry above a water table for longer periods of time. Dryer sand dunes allow two major items to occur: (1) no modification of dune fabric by rising water table and (2) more time for rainwater introduction of clays coats via percolation through dunes. Downward percolation of rainwater and clay particles “baste” framework grain surfaces with clay coats, essentially “armoring” or protecting grain surfaces from later syntaxial quartz cementation. Preventing quartz cementation in sand dune fabric (e.g., coarser grained avalanche bedding with wider pore throats) maintain a good permeability.

The Fredericksburg sandstone log-derived porosities, range average from 10% to 17% with very low permeabilities. Rotary sidewall cores were taken primarily from middle to lower portion of the Norphlet unfortunately not in the better sandstone toward the top. In these rotary cores, the porosities are generally 6 to 12% and up to 19.8% in one core. Corresponding permeability measurements, in even this best porosity point, is less than 1 md. In practice, microporosity is very abundant as seen in Norphlet thin sections.

Microporosity is porosity associated with texture and composition of clay minerals. Especially relevant is diagenetic clay coats reducing permeability at pore throats by increasing the surface area of grains (Pittman, 1979). Evaluating total porosity in sandstones will likely overestimate porosity values by adding microporosity (ineffective for fluid flow) and intergranular (effective for fluid flow) porosity (Pittman, 1979; Hurst and Nadeau, 1995; Dutton et al., 2016; Giannetta et al., 2016). As an example, in the Wilcox (Fandango Field, Texas), Dutton et. al (2016) have porosimeter data averaging 13.4% total porosity and in 57 of these samples, the average microporosity is 7.6%. The clays described in these sandstones are chlorite coats, detrital clay matrix, and altered grains (feldspars) and volcanic rock fragments.

The Norphlet had no hydrocarbon shows in the red sandstone despite having a thermally mature Smackover source rock, with oil shows even at the base of this formation. The low permeability fluvial Norphlet sandstone was unable to produce a less pressured environment relative to the overlying maturing source rocks. As a result, a downward oil charge into the Norphlet reservoir was not produced resulting in a dry hole.

Petersburg

Petersburg was drilled in 2013 by Shell in Block 529 of De Soto Canyon. The exploration well targeted the Norphlet Sandstone. Structurally, the well penetrated a small four-way dipping simple closure on a larger three-way dipping faulted nose structure, adjacent to a salt wall (Fig. 33). The Petersburg structural

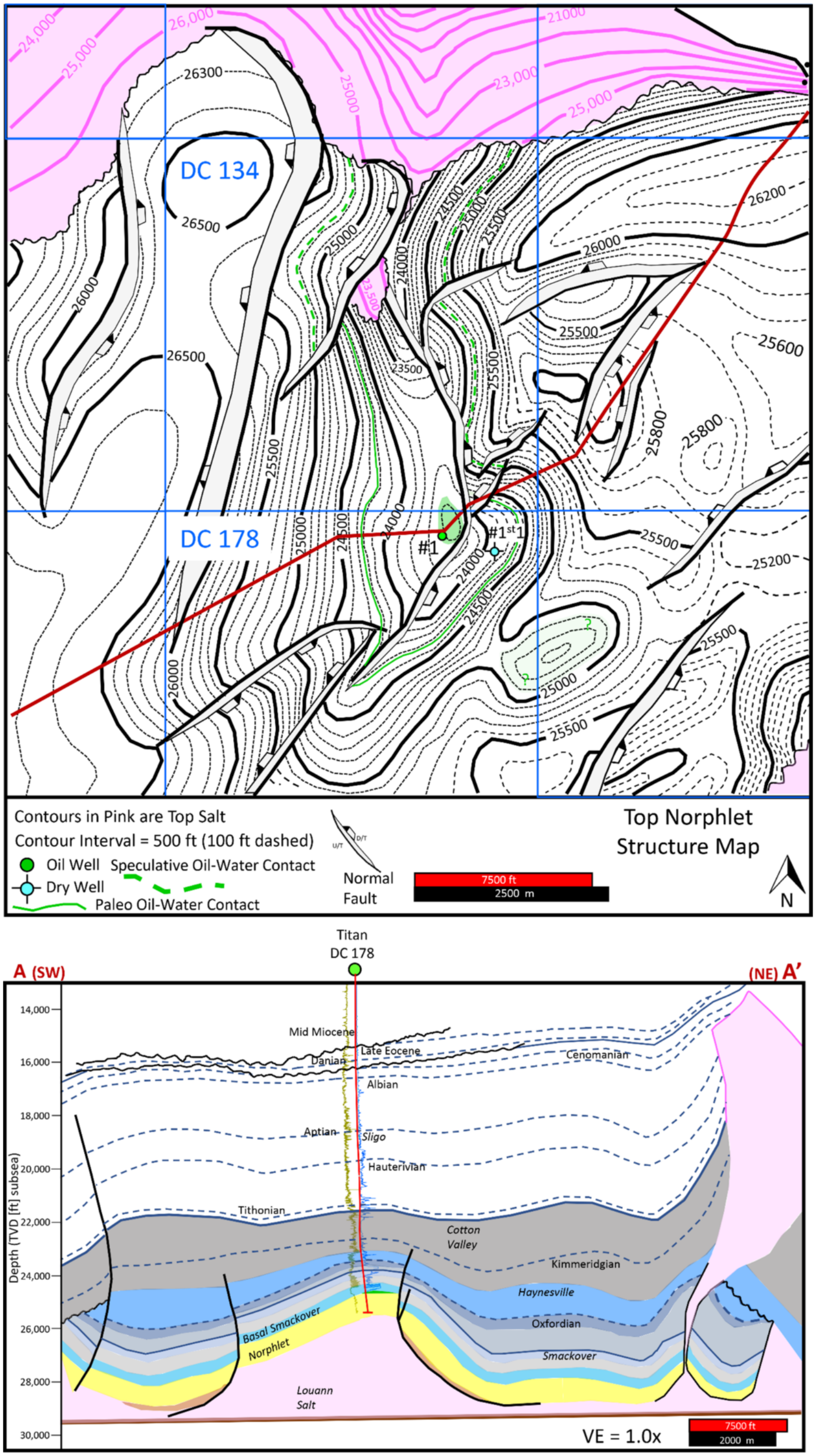

Figure 24. The top Norphlet map at prospect Titan is shown with the long and narrow south-plunging structural nose flanked on the east and west but thick Cretaceous filled synclines. The present-day oil column is colored in green covering the very small area of simple closure found in the #1 well. The paleo oil column is suggested in the solid green colored line. Other likely traps with unknown but also likely paleo oil columns, are highlighted by the possible dashed orange colored line. 2000 ft = 609.6 m.

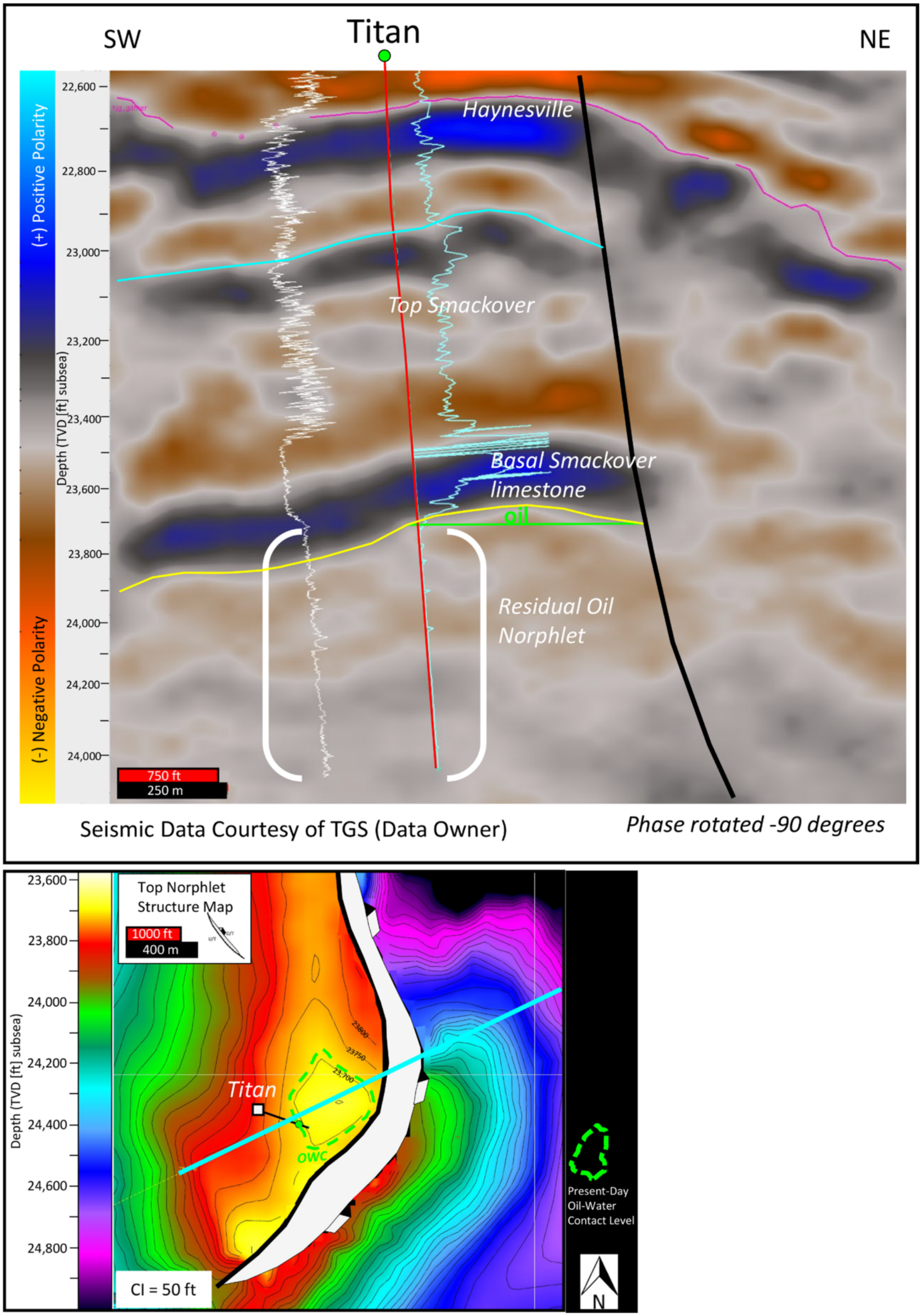

Figure 25. The Titan well tie to seismic data shows the oil-water contact depth matching the base of the top seal spill-point. Below this top seal closure, Norphlet is in a fault juxtaposition with a Haynesville rocks that over time, allowed oil to migrate through draining the trap of oil. The smaller structural map made on 3D data, illustrates the conformance of the oil-water contact to that of the simple closure. 100 ft = 30.5 m.

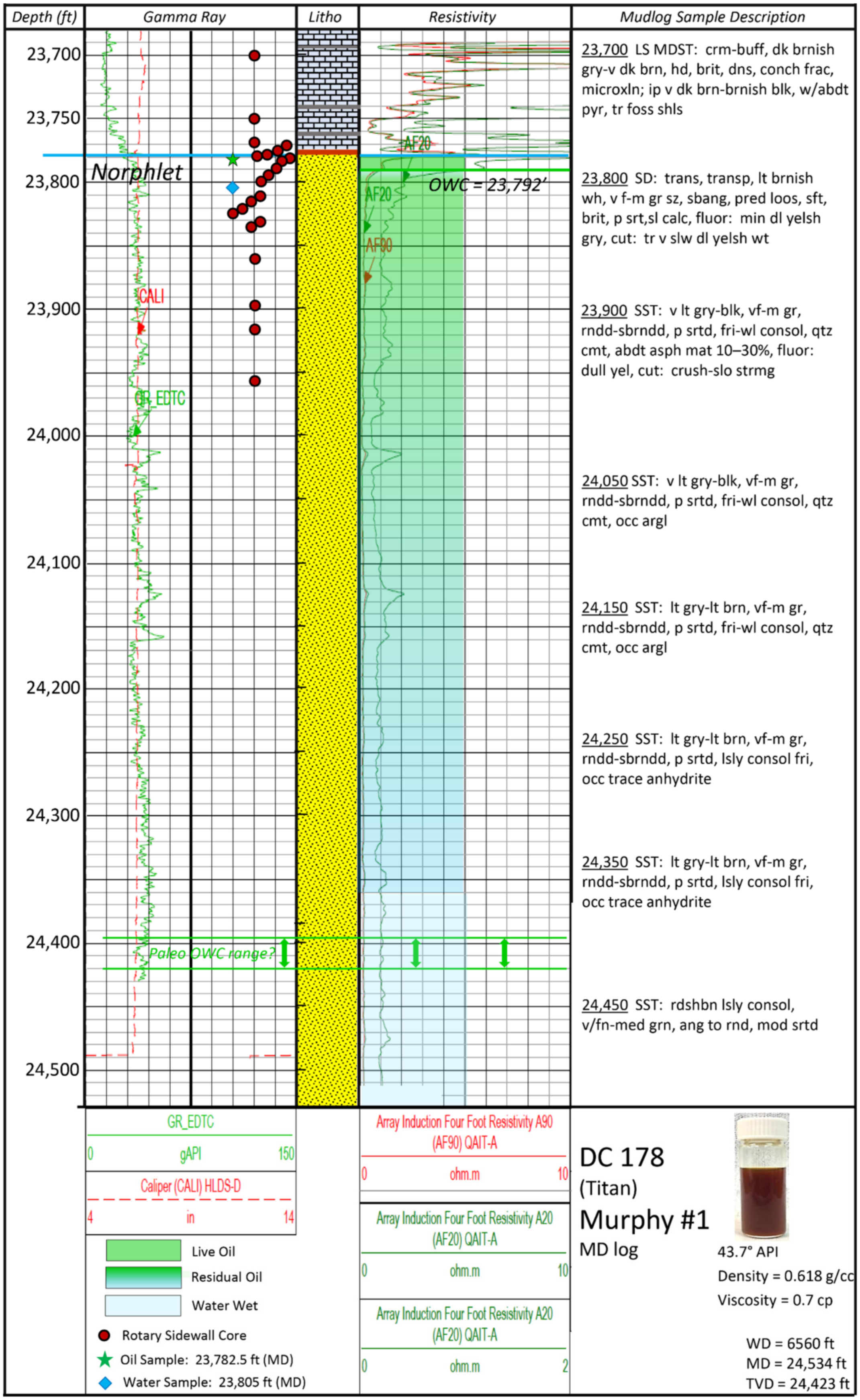

Figure 26. The #1 discovery well at prospect Titan drilled all Norphlet aeolian sandstone and did not penetrate the Louann Salt. The well found a small oil column of about 10 ft (3.05 m). The well drilled gray sandstone to approximately 24,350 ft (7421.9 m) and at 24,450 ft (7452.4 m) the color description changes to red sandstone, where a change to red aeolian sandstones occurred. Several rotary sidewall cores were taken, and the intervals are marked on the log. 100 ft = 30.5 m.

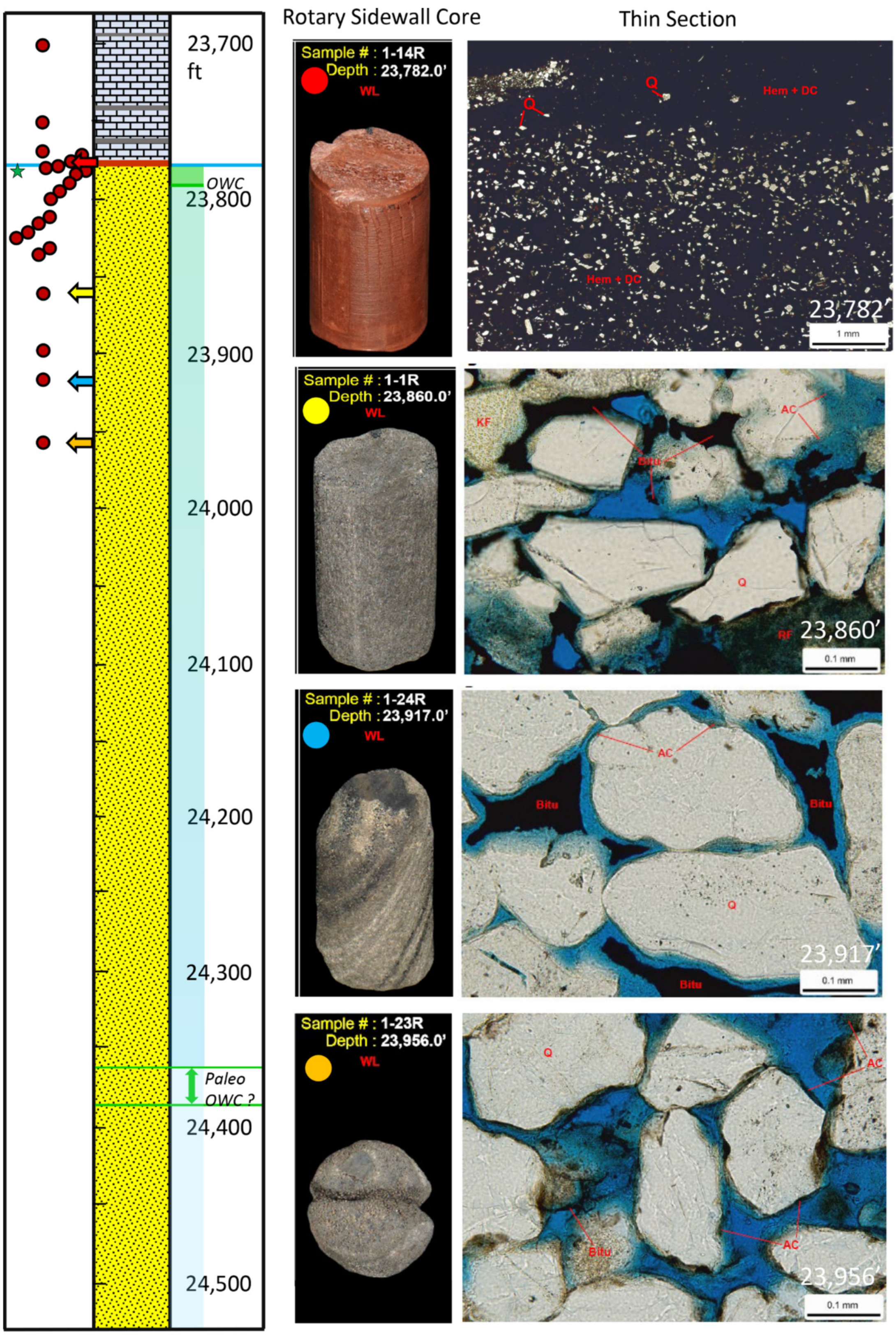

Figure 27. Rotary sidewall cores were taken at depths (MD) in Titan, highlighted on the log by solid red circles. Photomicrographs of 4 thin sections made from these cores are highlighted with 4 color filled circles in the photomicrograph and with the same colored arrows next to the lithology/depth track on the well strip. Photomicrographs: Quartz (Q) (most abundant) with some K feldspar (KF) and plagioclase with rock fragments (RF) as framework grain. Pore filling consists largely of bitumen (Bitu; dead oil or SHC) with chlorite and some mixed layer illite/smectite coating the framework grains. SHC is described as a moderate to common amount in the pores but in the sample at 23,956 ft (7301.8 m) MD as only trace amounts. The residual oil component likely represents a residual amount from an oil saturation in a formerly larger petroleum trap. Blue color is porosity. Bedding laminae defined by variations in grain size. (KF) K feldspar; (AC) authigenic clay-chlorite-illite/smectite; hematite and detrital clay (Hem+DC). 100 ft = 30.5 m.

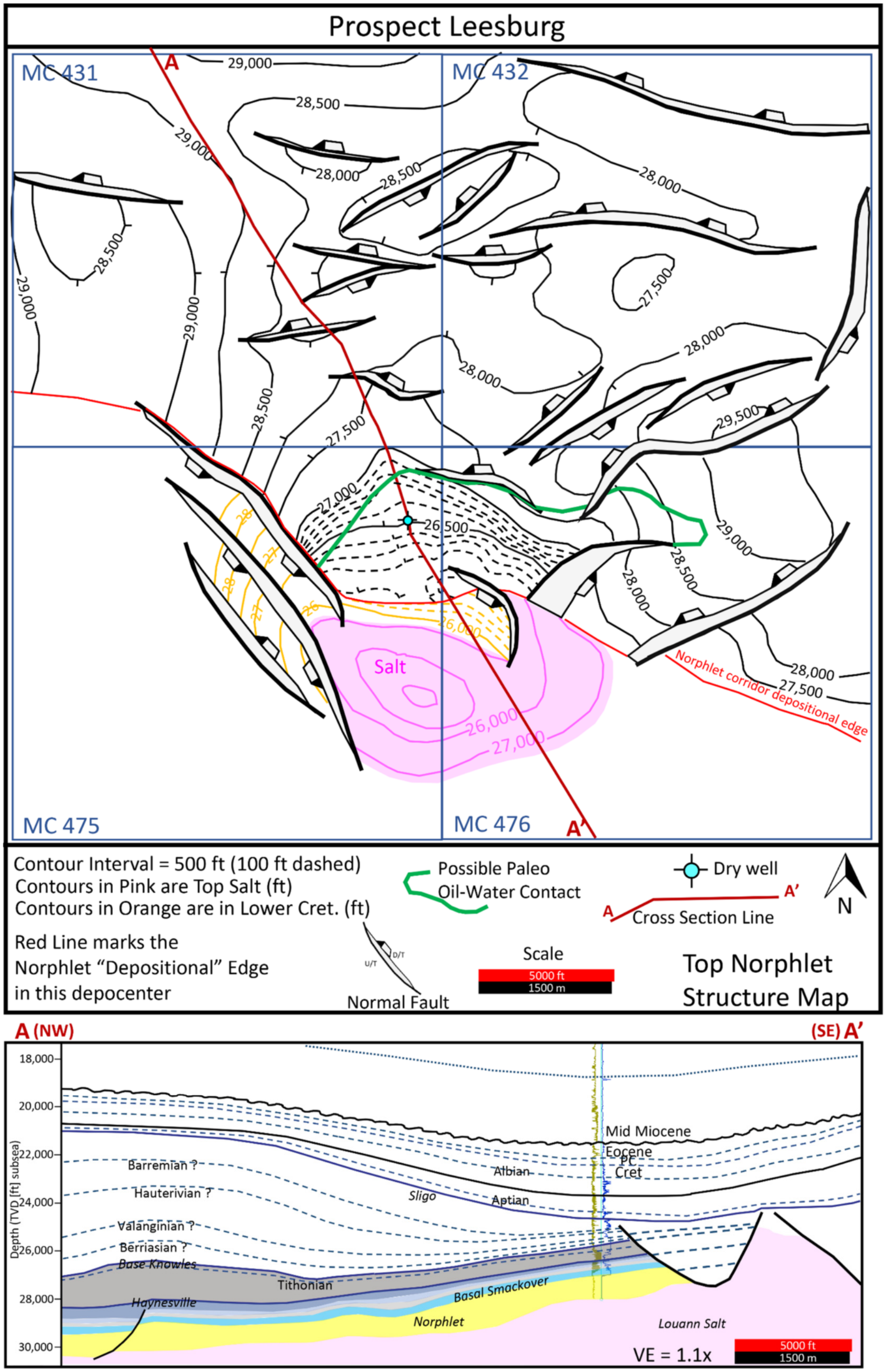

Figure 28. Leesburg structure at the top Norphlet is a three-way dipping structural nose. The trapping elements of Leesburg are the footwall sides of three normal faults against which the closing Norphlet structural contours. In fault juxtaposition with the Norphlet on the hanging wall are rocks of the Haynesville in the eastern fault and of Lower Cretaceous on the western fault. Only in a small crestal area is the Norphlet trapped against salt. There does not appear to be ay trap component of simple closure. The green oil-water contact was marked at a downdip position that corresponded to the likely paleo oil column in the well. Its outlined shape is taken from the isopach of Figure 30 that may have represented the fill level at top Cretaceous time. The column height in the well, is based on the column of gray aeolian sandstone overlying red aeolian sandstone. 2000 ft = 609.6 m.

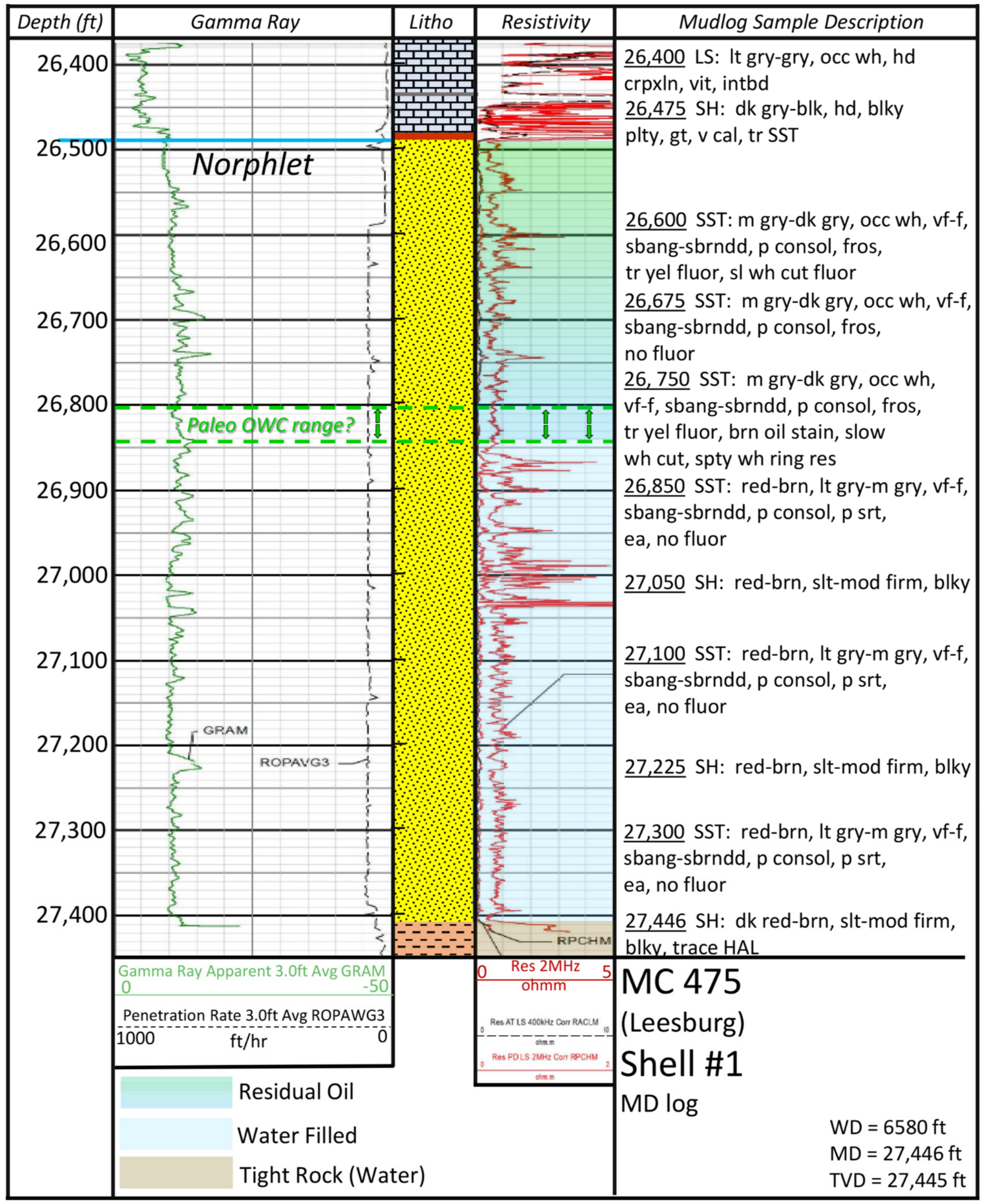

Figure 29. The log of the Norphlet at prospect Leesburg, found 920 ft (280.4 m) TVDT of aeolian sandstone above about 40 ft (12.2 m) TVDT of silty shale before possibly touching top salt. The upper approximately 350 ft (106.7 m) TVDT of Norphlet sand is gray colored with some cut fluorescence and brown oil stain interval. Below this depth is red aeolian sandstone absent of any shows. An assumed 350 ft (106.7 m) TVDT oil column was present in the well at some time past. The column was plotted on the structure map in Figure 28. 100 ft = 30.5 m.

nose was formed like Fredericksburg, as an inverted turtle basin. Also, like Fredericksburg, there is also, an unfaulted four-way simple dip structural closure. The Petersburg structure formed soon after rapid Norphlet deposition that was also undergoing rapid subsidence. The Norphlet structure had already subsided and inverted into a nearly completed turtle structure by middle Smackover deposition. On the cross section (Fig. 33), the middle and upper Smackover doubles in thickness from the north, off structure at ~1200 ft (~365.8 m) to less than 300 ft (91.4 m) over the Norphlet crest. The Norphlet basin evacuated all the Louann Salt as the thickest Norphlet section rested on basement, then began its structural inversion. The entire Petersburg structure was a small Norphlet depobasin, likely bound by salt walls confining Norphlet Formation and creating another example of a “pothole” basin.

The Petersburg well reached a total depth immediately after the measured-while-drilling log first encountered a high spike in resistivity readings and the cutting description indicated Louann Salt had just been entered. The Norphlet facies found in Petersburg are like those in the Fredericksburg well. Both wells have a mix of interbedded red clastic dryland sedimentary rocks. Overall, Petersburg has more silt content than Fredericksburg. At Petersburg, the low angle dips (Fig. 34), in reddish brown mudstone, siltstone and silty sandstone, probably represent the deposition from water by sheetflood events. The thinner sandstone beds may be associated along the flow axis of sheetflows, but also may represent smaller sand dunes that formed after drying out from a waterflood event. The upper 400 ft (121.9 m) of the Norphlet (Fig. 34) contain the thicker sandstone beds which possibly representing this drying upward cycle of small aeolian dunes. The total amount of dune development however is not thick nor very long-lived as the subsidence history would indicate given the rapid subsidence history of this “pothole” basin.

Permeability in all water deposited facies or dune facies modified by a rising water table, have low values for oil to enter the pore system from the overlying source rock. Permeabilities measured from the nuclear magnetic resonance log (Fig. 34) show permeabilities in the entire rarely get above 0.1 md. Several rotary sidewall cores where also taken in Petersburg and had porosity and permeability measured made directly on these sam-

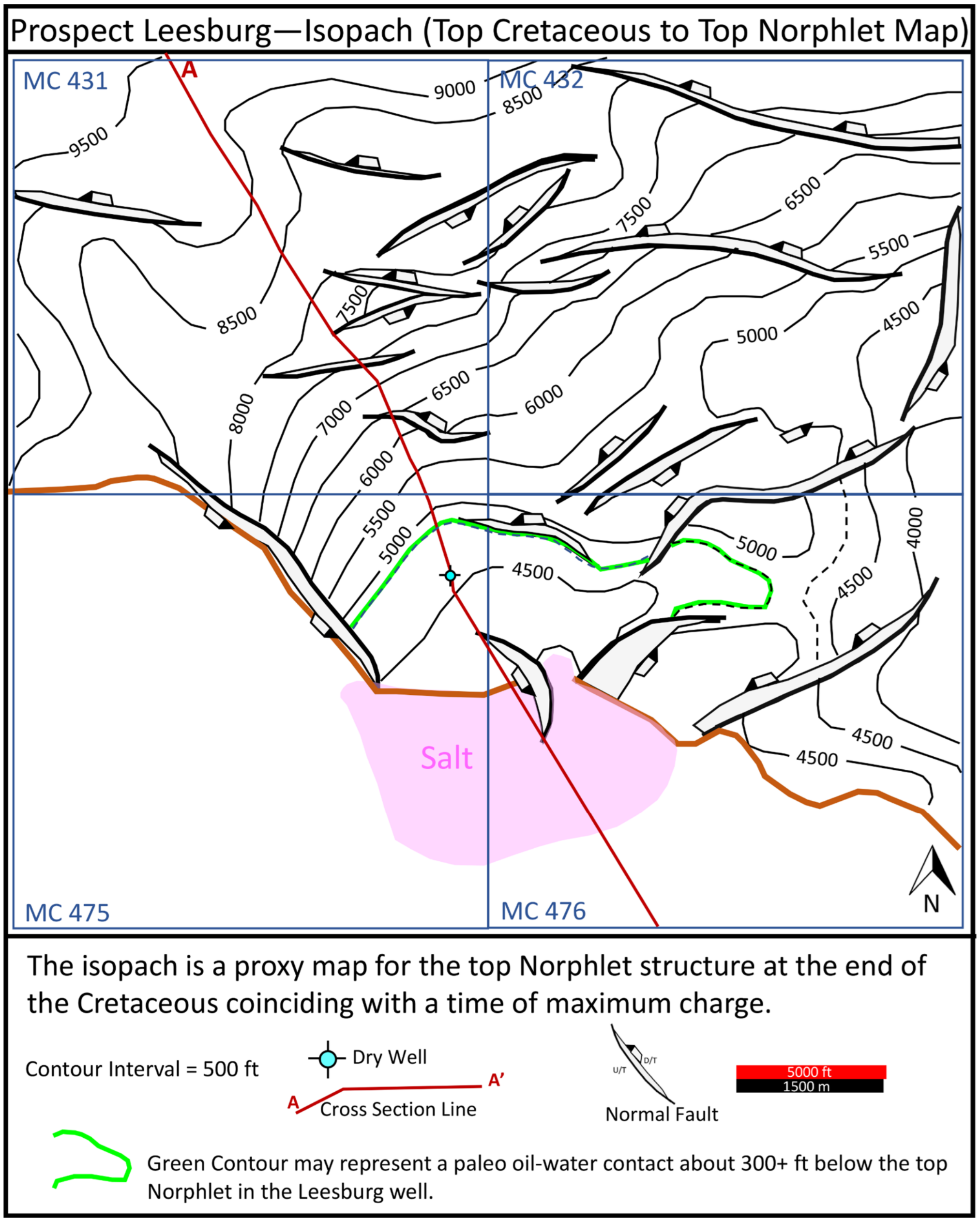

Figure 30. The Cretaceous and Upper Jurassic isopach map was made by subtracting the top Cretaceous map from the top Norphlet map (Fig. 28). The isopach contour lines are thought to represent the structural contours of the top Norphlet at the end of the Cretaceous when peak charge into Leesburg was occurring. The oil column is the 350 ft (106.7 m) TVDT oil column thought to have been found in the well (Fig. 29).

ple (shown as red dots next to the sample log and on the log derived permeability curve). There is a good match to compare the supportive permeability measurements. The porosity values from these rotary cores are not plotted by range in value from about 10 to 20%.

The Smackover log from Petersburg is shown in Figure 35. The total Smackover thickness at Petersburg is one of the thicker sequences of the Norphlet deepwater wells at nearly 1100 ft (335.3 m). The Smackover thickness change seen on the cross section, varies across Petersburg from perhaps 500 ft (152.4 m) to 2000 ft (609.6 m) due to the rapid subsidence off the flanks of the Norphlet turtle structure (Fig. 33). The lithostratigraphy of the Smackover begins with the basal red shale. This bright red shale package was deposited over a flat Norphlet desert devoid of dunes standing above the basin floor. Above this shale package is the sulfide-rich zone primarily of pyrite replacing dolomite, which is present along with anhydrite. Due to the extreme amounts of pyrite, the density log responds with high density readings defining this zone. Correspondingly, the conductivity log is high, and the resistivity values are low. Above the pyrite zone, lies the massive basal carbonate unit deposited in waters with likely high salinity. This high salinity environment prevented the accumulation of microfauna, but, with pulses of fresh water runoff, it allowed algal blooms to flourish temporally. These floating algal mats sank as the fresh water influx waned, thus sinking the mats to the seafloor where they are now microlaminations of source rock. The top of the basal massive carbonate is transitional to the middle Smackover section as an increase in argillaceous content, causes the gamma ray log to read higher and become more serrated in shape.

Smackover source rock richness values are shown in Figure 35 by the total organic content (TOC) and hydrogen index (HI) displays. The source rock is thermally mature with a pyrolysis analyses that yielded Tmax (temperature of release of hydrocarbons from cracking of kerogen during pyrolysis) values having a VRE of 0.8 or greater near the base. Several zones of interest (ZOI) are highlighted in the log that were good oil shows with streaming cut fluorescence. The fluid inclusion report stated that

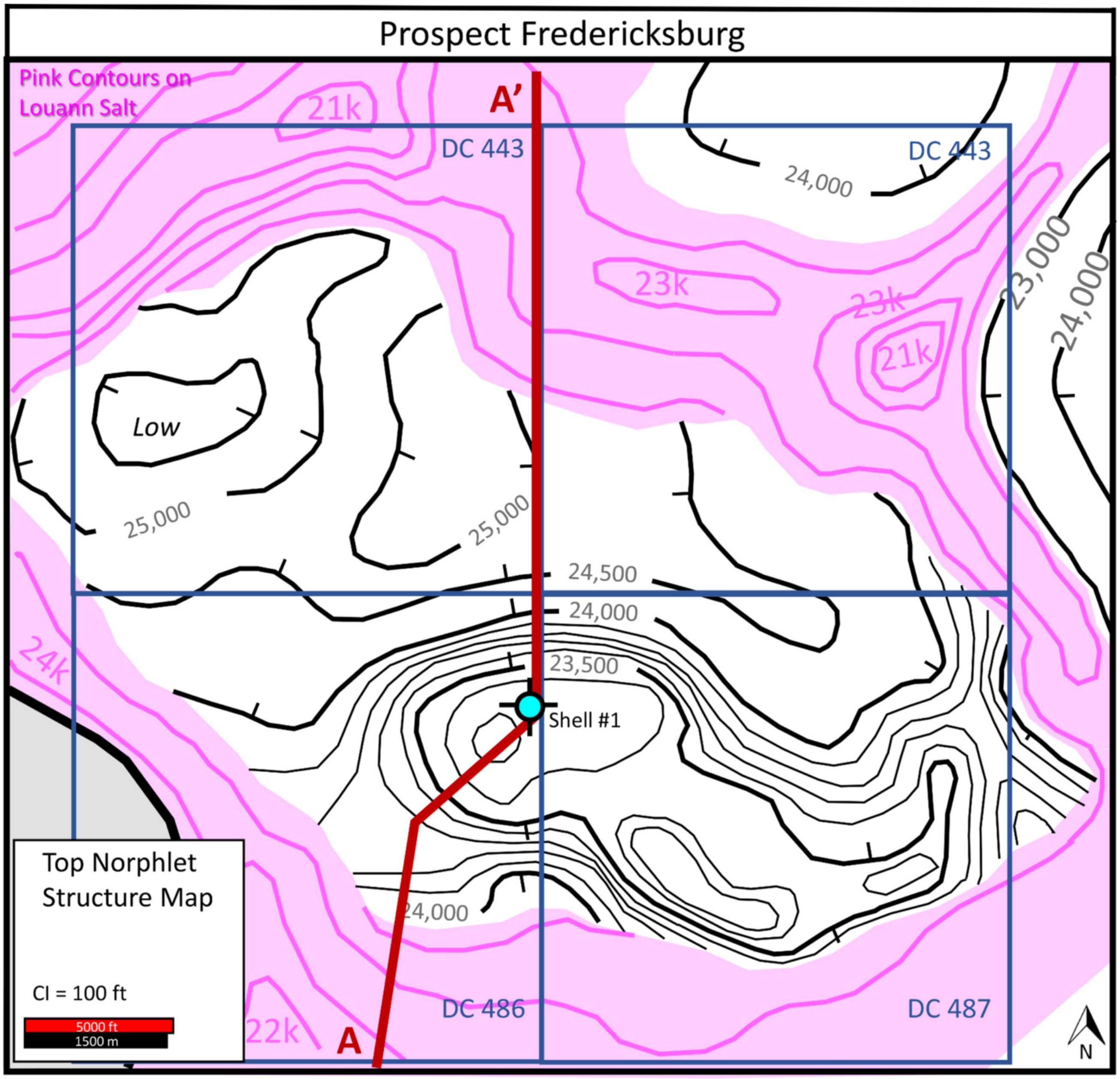

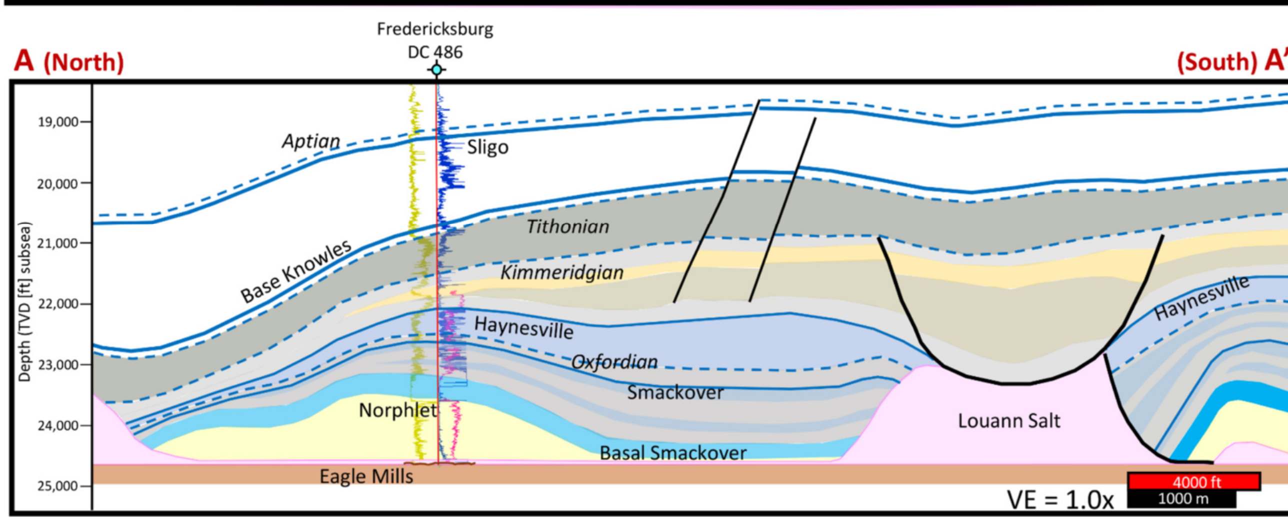

Figure 31. Prospect Fredericksburg is an unfaulted simple four-way dip closure formed as the Norphlet depocenter inverted or "turtled." The cross section show the basal Smackover does not change its thickness significantly across the Norphlet turtle and yet lays flat against the basement on the north side of the basin. 1000 ft = 304.8 m.

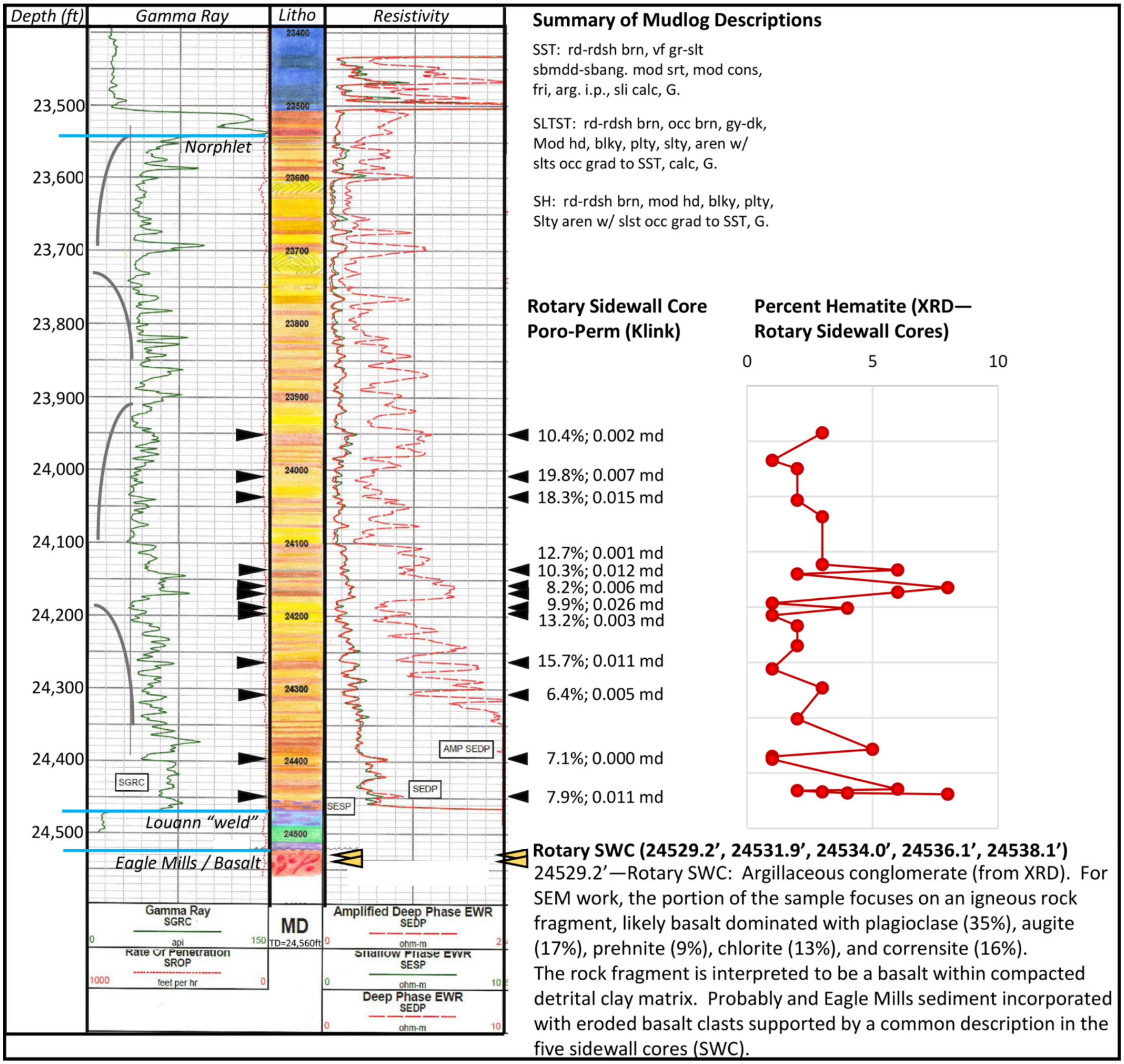

Figure 32. The log of the Norphlet section at Fredericksburg is composed of fluvially dominated shale, siltstone, and sandstone. All these lithologies are red to reddish brown. The plot of hematite from sidewall cores taken in the well are from X–ray diffraction analysis. Very low permeability in the sidewall cores demonstrate how difficult it would be to create any underpressuring relative to the overlying pressures in a maturing source rock. Basement rock is likely composed of basalt rock fragments incorporated into a clay matrix shale. Overlying this basement is what is left of Louann Salt forming a near salt weld. 100 ft = 30.5 ft.

the strongest liquids indications at 25,110–25,400 ft (7653.6–7741.9 m) TVD (in the basal Smackover carbonate).

The source rock was mature at Petersburg even at the structural crest. Yet, the red Norphlet sandstone directly below this source rock are devoid of any hydrocarbon shows, indicating a lack of charge migration. The charge pathway downward into the Norphlet could not be accomplished due to likely high entry pressures in low permeability rock. Oil forced its way upward, because there was no less pressured environment to cause a downward migration into very low permeability rocks. Petersburg and Fredericksburg failures could not be assigned to a failed trap because both were drilled inside of simple four-way dip closures sealed by the basal Smackover. It is this simple trap configuration that holds the remaining accumulations in Shiloh, Antietam and Titan. Also, with the red Norphlet at Petersburg, if there would have been an oil column present, the sandstone would be gray.

SUMMARY

Presented here are the three essential play components required for oil fields to form in the Norphlet sandstone that control

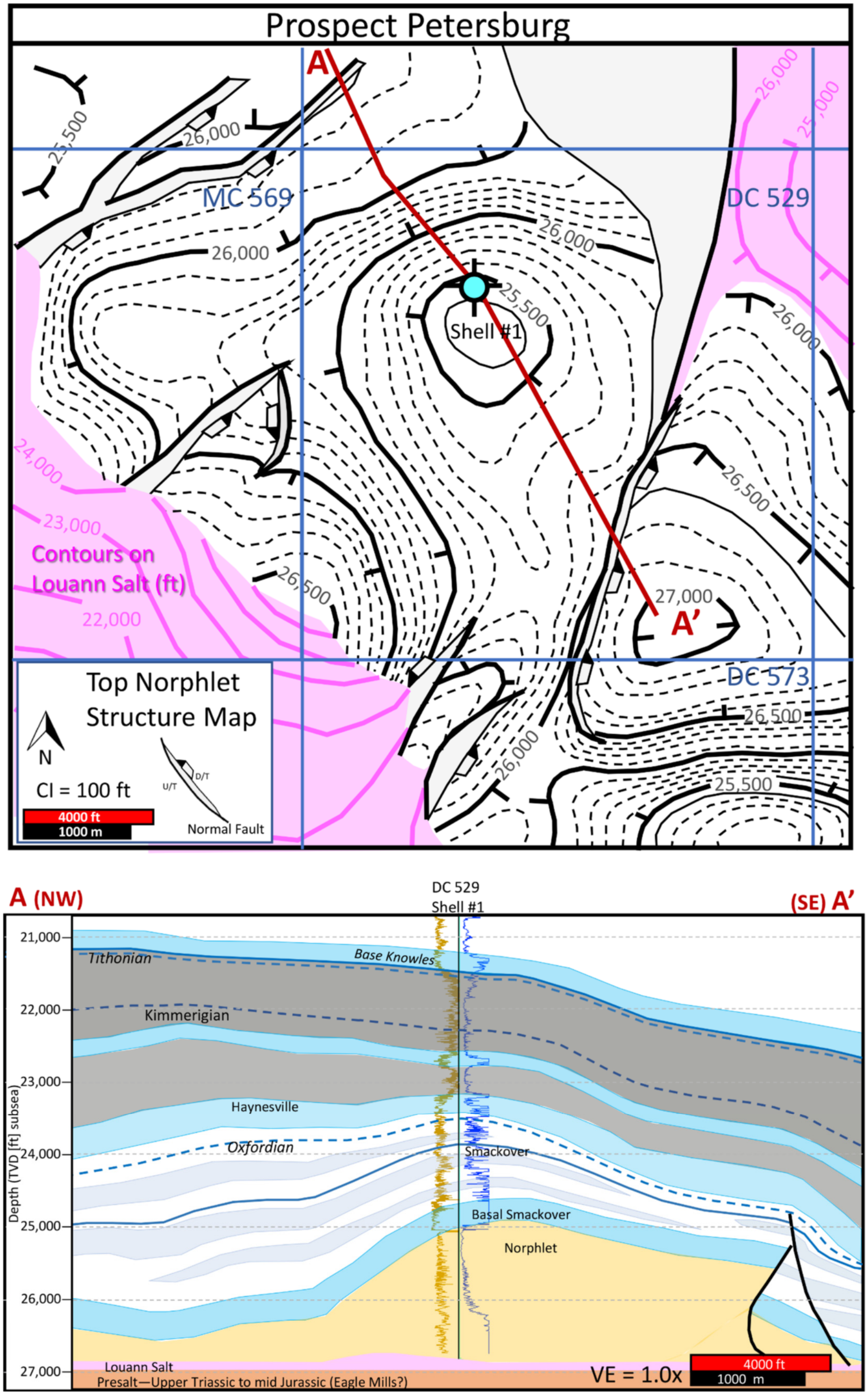

Figure 33. The structural map on the top Norphlet at Petersburg shows the small four-way dipping simple closure on a larger three-way dipping faulted nose structure. Petersburg's structural inversion took place soon after Norphlet deposition. The flanks of the Norphlet structure seen on the cross section, continued to subside during the middle and upper Smackover. The entire Petersburg structure was a small Norphlet depobasin, likely bound by salt walls confining a thick local accumulation Norphlet sediments. 100 ft = 30.5 m.

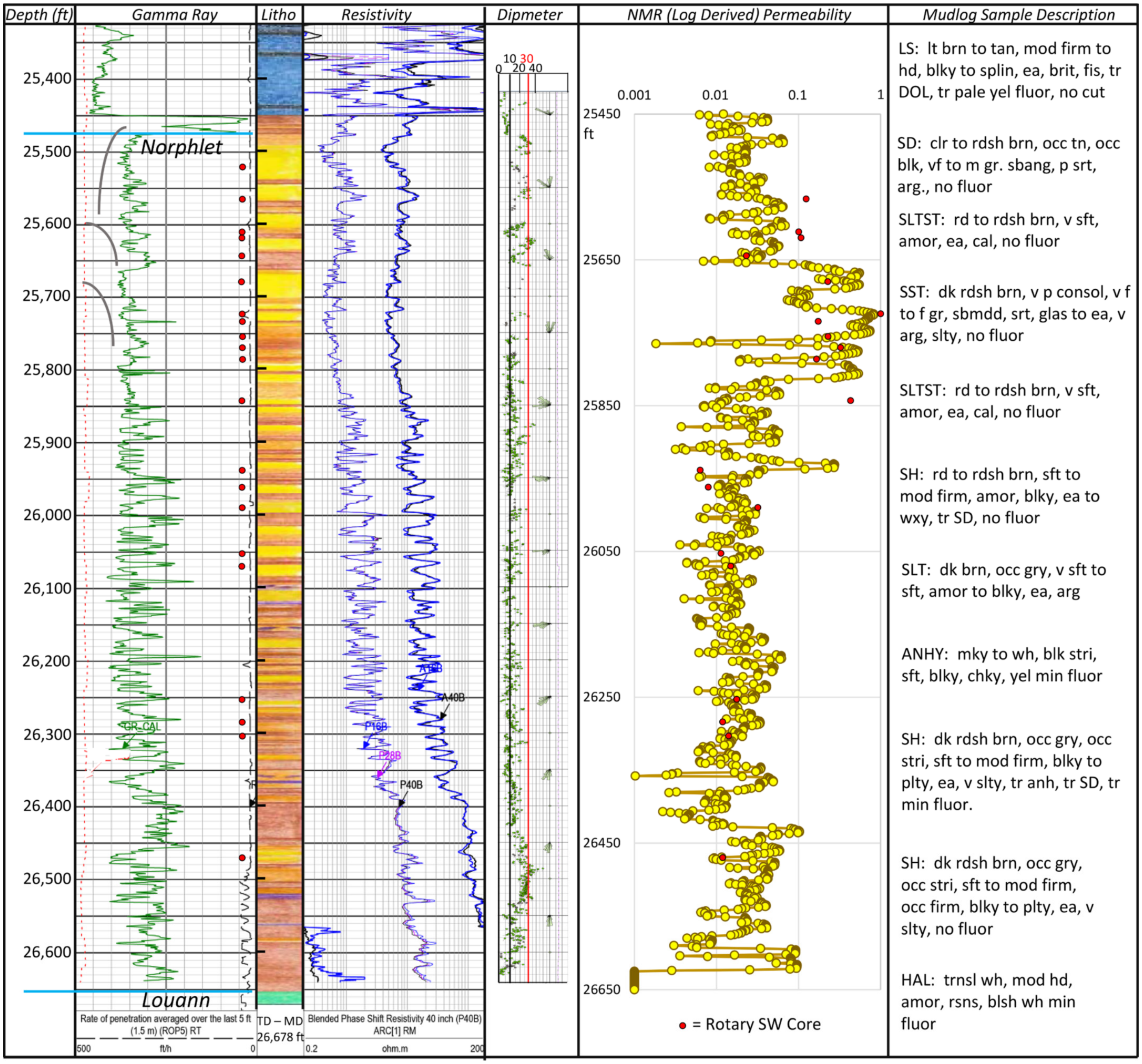

Figure 34. Norphlet sediments at Petersburg are reddish brown mudstones, siltstones and silty sandstones. The low permeabilities in non-aeolian rocks are shown in Petersburg as measured from a nuclear magnetic resonance log. Permeabilities in the entire Petersburg Norphlet section generally do not rise above 0.1 md. Permeabilities from sidewall cores, shown as red dots, compare favorably to the trend of permeabilities as measured from the log. Porosity values as measured from these rotary cores range in value from 10 to 20%. 100 ft = 30.5 m.

the oil field size. Examples are shown in wells that were completely void of hydrocarbons in the Norphlet because one or more of the three components were absent. The three components are here briefly summarized. Component one, is finding the aeolian dune facies of the Norphlet. Only dune facies have the required preserved permeability enough to create a pressure "sink" in today's subsurface. A "sink" is a permeable sandstone with significant lateral continuity that it is less pressured relative to its bounding stratigraphy. The Norphlet sandstone pressure sink provides the outlet for oil to enter from the overlying and over pressured maturing Smackover source rocks. Component two is having a high enough or threshold level of thermal maturity of the Smackover source rocks measured by the VRE level. A VRE level of 0.9 is found to be a minimal level of maturity needed for oil migration to effectively fill a trap to an economic amount. Smaller "fetch area" can also affect smaller volumes especially at lower maturity levels. Higher maturity levels more effectively "squeeze out" Smackover oil creating more robust oil volumes charged downward into the permeable Norphlet reservoir. The third component is the timing of expulsion and migration from the source rock. The critical moment of Smackover source rock migration must occur from the recent, but no older than 15 to 20 million yr ago. Otherwise, older formed traps will leak, leaving only residual oil.

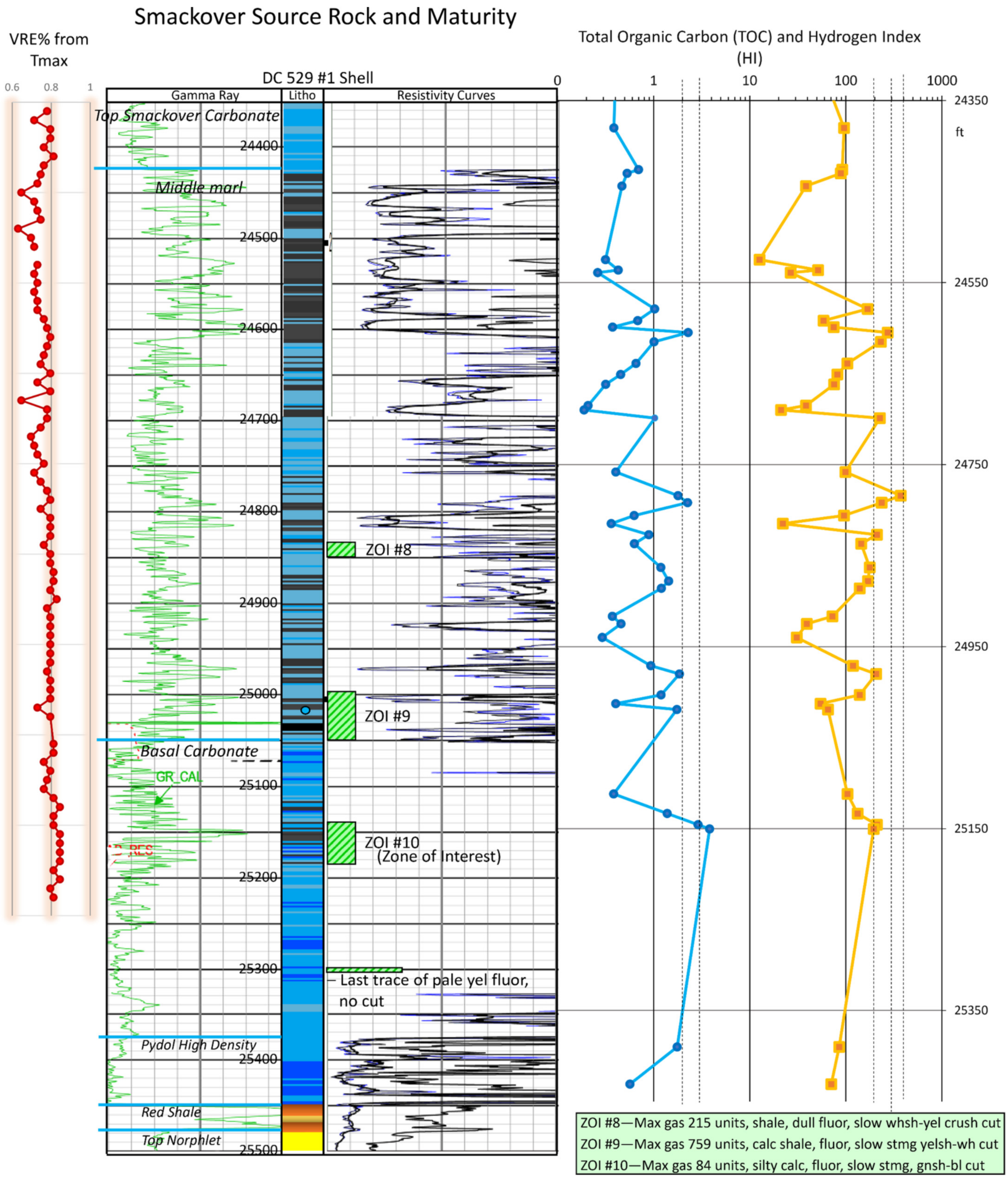

Figure 35. The Smackover MD log at Petersburg illustrates the lithostratigraphy of the Smackover. At the base is the basal red shale with a typical thickness found across low desert areas devoid of topographical sand dunes. Above the red shale is the sulfide-rich zone primarily of pyrite replacing dolomite, present along with anhydrite. Above the pyrite zone lies the massive basal carbonate unit. This massive carbonate is transitional to the overlying middle Smackover section with increasing argillaceous content. Source rock richness's are shown as measured from the total organic content (TOC) and hydrogen index (HI) displays. The source rock is thermally mature with a pyrolysis analyses that yielded Tmax values having a vitrinite reflectance equivalent (VRE) of 0.8 or greater near the base. Several zones if interest (ZOI) are highlighted in the log that were good oil shows with streaming cut fluorescence. 100 ft = 30.5 m.

ACKNOWLEDGMENTS

The author is honored to present this paper at the annual convention for GCAGS. The author wishes to thank and acknowledge TGS (Tomlinson Geophysical Services) for their permission to use the three seismic examples at Antietam, Shiloh, and Titan. I thank Murphy Oil Company management, for the time and data and encouragement to write this paper. A special thanks to Murphy's technical staff for discussions and consultations. The geologists Kyle Day, Alex Blacque, and Craig Farley, along with the exceptional geochemical expert, Fausto Mosca, and detailed petrophysical analyses by Brian LeCompte, made this a better paper. A very special thanks goes to them. Much gratitude is extended to Robyn McAllister who formatted the figures. To Shell Oil, thank you for the opportunity to have been involved in exploring the Norphlet in deepwaters from our start in 1999 and continuing with your dogged tenacity to never give up. The Bureau of Safety and Environmental Enforcement (BSEE) provided all the data used which is publicly available but extended to me prompt and courteous correspondence and help. Thank you all again.

REFERENCES CITED

Aase, N. E., P. A. Bjorkum, and P. H. Nadeau, 1996, The effect of grain-coating microquartz on preservation of reservoir porosity: American Association of Petroleum Geologists Bulletin, v. 80, p. 1654–1673, <https://doi.org/10.1306%2F64eda0f0-1724-11d7-8645000102c1865d>.

Abraham, H., 1960, Asphalts and allied substances: Their occurrence, modes of production, uses in the arts and methods of testing, 6th ed.: D. Van Nostrand Company, Inc., Princeton, New Jersey, 432 p., <https://doi.org/10.1002/jctb.5000573407>.

Ahlbrandt, T. S., 1979, Textural parameters in eolian deposits, *in* E. D. McKee, ed., A study of global sand seas: U.S. Geological Survey Professional Paper 1052, p. 21–52, <https://doi.org/10.3133/pp1052>.

Ajdukiewicz, J. M., P. H. Nicholson, and W. L. Esch, 2010, Prediction of deep reservoir quality from early diagenetic process models in the Jurassic eolian Norphlet Formation, Gulf of Mexico: American Association of Petroleum Geologists Bulletin, v. 94, p. 1189–1227, <https://doi.org/10.1306/04211009152>.

Aplin, A. C., and S. R. Larter, 2005, Fluid flow, pore pressure, wettability, and leakage in mudstone cap rocks, *in* P. Boult and Kaldi, eds., Evaluating fault and cap rock seals: American Association of Petroleum Geologists Hedberg Series 2, Tulsa, Oklahoma, p. 1–12, <https://doi.org/10.1306/1060752H23158>.

Aydin, A., and A. M. Johnson, 1978, Development of faults as zones of deformation bands and as slip surfaces in sandstones: Pure and Applied Geophysics, v. 116, p. 931–942, <https://doi.org/10.1007/bf00876547>.

Banham, S. G., and N. P. Mountney, 2013, Evolution of fluvial systems in salt-walled mini-basins: A review and new insights; Sedimentary Geology, v. 296, p. 142–166, <https://doi.org/10.1016/j.sedgeo.2013.08.010>.

Beaubouef, B., 2018, Shell keeps deepwater viable with Appomattox project: Offshore Magazine, January 2 issue, <https://www.offshore-mag.com/articles/print/volume-77/issue-12/top-offshore-projects/shell-keeps-deepwater-viable-with-appomattox-project.html>.

Berner, R. A., 1969, Goethite stability and the origin of red beds: *Geochimica et Cosmochima Acta*, v. 33, p. 267–273, <https://doi.org/10.1016/0016-7037(69)90143-4>.

Brand, J., 2016, Stratigraphy and Mineralogy of the Oxfordian lower Smackover Formation in the eastern Gulf of Mexico, *in* C. Lowery, J. W. Snedden, and N. C. Rosen, eds., Mesozoic of the Gulf Rim and beyond: New progress in science and exploration of the Gulf of Mexico Basin: Proceedings of the 35th Annual Gulf Coast Section of the Society of Economic Paleontologists and Mineralogists Foundation Perkins-Rosen Research Conference, Houston, Texas, p. 14–35.

Bureau of Safety and Environmental Enforcement (BSEE), 2019, Well information, <https://www.data.bsee.gov/Main/Well.aspx>.

Chan, M. A., W. T. Parry, and J. R. Bowman, 2000, Diagenetic hematite and manganese oxides and fault-related fluid flow in Jurassic sandstones, southeastern Utah: American Association of Petroleum Geologists Bulletin, v. 84, p. 1281–1310, <https://doi.org/10.1306/a9673e82-1738-11d7-8645000102c1865d>.

Crone, A. J., 1975, Laboratory and field studies of mechanically infiltrated matrix clay in arid fluvial sediments: Ph.D. Thesis, University of Colorado at Boulder, 162 p.

Crossey, L. J., R. C. Surdam, and R. Lahann, 1986, Application of organic/inorganic diagenesis to porosity prediction, *in* D. L. Gautier, ed., Roles of organic matter in sediment diagenesis: Society of Economic Paleontologists and Mineralogists Special Publication 38, Tulsa, Oklahoma, p. 147–156, <http://dx.doi.org/10.2110/pec.86.38.0147>.

Cunningham, R., J. W. Snedden, I. O. Norton, H. C. Olson, T. L. Whitaker, and J. W. Virdell, 2016, Upper Jurassic Tithonian-centered source mapping in the deepwater northern Gulf of Mexico: Interpretation, v. 4, p. SC97–SC123, <https://doi.org/10.1190/INT-2015-0093.1>.

Dixon, S. A., D. M. Summers, and R. C. Surdam, 1989, Diagenesis and preservation of porosity in Norphlet Formation (Upper Jurassic), southern Alabama: American Association of Petroleum Geologists Bulletin, v. 73, p. 707–728, <https://doi.org/10.1306/44b4a24e-170a-11d7-8645000102c1865d>.

Dobson, L. M., and R. T. Buffler, 1997, Seismic stratigraphy and geologic history of Jurassic rocks, northeastern Gulf of Mexico: American Association of Petroleum Geologists Bulletin, v. 81, p. 100–120, <https://doi.org/10.1306/522b42a3-1727-11d7-8645000102c1865d>.

Douglas, S. W., 2010, The Jurassic Norphlet Formation of the deepwater eastern Gulf of Mexico: A sedimentologic investigation of aeolian facies, their reservoir characteristics, and their depositional history: M.S. Thesis, Baylor University, Waco, Texas, 59 p.

Dutton, S. P., W. A. Ambrose, R. G. and Loucks, 2016, Diagenetic controls on reservoir quality in deep Upper Wilcox sandstones of the Rio Grande Delta system, South Texas: Gulf Coast Association of Geological Societies Journal, v. 5, p. 95–110, <https://www.gcags.org/Journal/2016.GCAGS.Journal/2016.GCAGS.Journal.v5.06.p95-110.Dutton.et.al.pdf>.

Folk, R. L., 1976. Reddening of desert sands: Simpson Desert, N. T., Australia: Journal of Sedimentary Research, v. 46, p. 604–615, <http://dx.doi.org/10.1306/212f6fff-2b24-11d7-8648000102c1865d>.

Fossen, H., and A. Bale, 2007, Deformation bands and their influence on fluid flow: American Association of Petroleum Geologists Bulletin, v. 91, p. 1685–1700, <https://doi.org/10.1306/07300706146>.

French, M. W., and R. H. Worden, 2012, Microcrystalline quartz generation and the preservation of porosity in sandstones: Evidence from the Upper Cretaceous of the Subhercynian Basin, Germany: Journal of Sedimentary Research, v. 82, p. 422–434, <https://doi.org/10.2110/jsr.2012.39>.

Fryberger, S. G., A. M. Al-Sari, and T. J. Clisham, 1983, Eolian dune, interdune, sand sheet, and siliclastic sediments of an offshore prograding sand sea, Dharan area, Saudi Arabia: American Association of Petroleum Geologists Bulletin, v. 67, p. 280–312, <https://doi.org/10.1306/03b5acff-16d1-11d7-8645000102c1865d>.

Frydl, P., 1989, Reservoir heterogeneity in the Keg River "AA" pool, Rainbow Field, Alberta, *in* P. Aukes, ed., Geology and reservoir heterogeneity: Canadian Society of Petroleum Geologists 1989 Core Conference, Calgary, Alberta, Canada, p. 1–1 to 1–36 <http://archives.datapages.com/data/cspg_sp/data/CSPG-SP-012/012001/i_cspgsp12i.htm>.

Galloway, W. E., 2008, Chapter 15—Depositional evolution of the Gulf of Mexico sedimentary basin: Sedimentary basins of the World, v. 5, p. 506–549, <https://doi.org/10.1016/S1874-5997(08)00015-4>.

Giannetta, L. G., N. D. Webb, S. K. Butler, and N. P. Grigsby, 2016, Using clay microporosity to improve formation evaluation in potential ROZs: Cypress Sandstone, Illinois Basin: Illinois State Geological Survey, Champaign, 24 p. <http://www.isgs.illinois.edu/sites/isgs/files/files/2016_Giannetta_ESAAPG.pdf>.

Goddard, E. N., P. D. Trask, R. K. Deford, O. N. Rove, J. T. Singewald, and R. M. Overbeck, 1948, [also reprinted in 1951, 1963, 1970, 1975, 1979 and 1980:], Rock-color chart, Munsell color: Geological Society of America, Boulder, Colorado.

Godo, T., 2006, Norphlet aeolian dunes in the deep-water Gulf of Mexico: Houston Geological Society Bulletin, v. 49, no. 2, p. 11.

Godo, T. J., E. Chuparova, and D. E. McKinney, 2011, Norphlet aeolian sand fairway established in the deep-water Gulf of Mexico: American Association of Petroleum Geologists Search and Discovery Article 90124, Tulsa, Oklahoma, 1 p., <http://www.searchanddiscovery.com/abstracts/html/2011/annual/abstracts/Godo.html>.

Godo, T., 2017, The Appomattox Field: Norphlet aeolian sand dune reservoirs in the deep-water Gulf of Mexico, *in* R. K. Merrill and C. A. Sternbach, eds., Giant fields of the decade 2000–2010: American Association of Petroleum Geologists Memoir 113, Tulsa, Oklahoma, p. 29–54, <https://doi.org/10.1306/13572000M113368https0>.

Gomes, S. W., A. Weislogel, and S. Kuehn, 2018, Evaluation of downward hydrocarbon migration model in Smackover-Norphlet petroleum system in Mobile Bay, Alabama using trace element analysis of pyrite: American Association of Petroleum Geologists Annual Convention and Exposition, May 20–23, 2018, Salt Lake City, Utah, 1 p. <https://www.researchgate.net/publication/321544307_Evaluation_of_Downward_ Hydrocarbon_Migration_Model_in_Smackover-Norphlet_Petroleum_System_in_Mobile_Bay_Alabama_Using_Trace_Element_Analysis_of_Pyrite/link/5a26f3cd4585155dd4241013/download>.

Goteti, R., S. J. Ings, and C. Beaumont, 2012, Development of salt minibasins initiated by sedimentary topographic relief: Earth and Planetary Science Letters, v. 339, p. 103–116, <https://doi.org/10.1016/j.epsl.2012.04.045>.

Harding, A., L. Walker, S. Ehlinger, and T. Chapman, 2016, The siliciclastic Upper Cretaceous play of eastern Mississippi Canyon, *in* C. Lowery, J. W. Snedden, and N. C. Rosen, eds., Mesozoic of the Gulf Rim and beyond: New progress in science and exploration of the Gulf of Mexico Basin: Proceedings of the 35th Annual Gulf Coast Section of the Society of Economic Paleontologists and Mineralogists Foundation Perkins-Rosen Research Conference, Houston, Texas, p. 215–231, <https://doi.org/10.5724/gcs.15.35.0215>.

Harris, D. W., and M. K. McGowan, 1987, Influence of differential sediment loading on salt tectonics in the East Texas Basin, *in* I. Lerche and J. J. O'Brien, eds., Dynamic geology of salt and related structures: Elsevier Ltd., p. 77–128, <https://doi.org/10.1016/b978-0-12-444170-5.50008-7>.

Hartman, J. A., 1968, The Norphlet sandstone, Pelahatchie Field, Rankin County, Mississippi: Gulf Coast Association of Geological Societies, Transactions, v. 18, p. 2–11, <https://doi.org/10.1306/5d25c511-16c1-11d7-8645000102c1865d>.

Hermanrud, C., H. M. Nordgard Bolas, and G. M. G., Teige, 2005, Seal failure related to basin-scale processes, *in* P. Boult and J. Kaldi, eds., Evaluating fault and cap rock seals: American Association of Petroleum Geologists Hedberg Series 2, Tulsa, Oklahoma, p. 13–22, <https://doi.org/10.1306/1060753H23159>.

Hesthammer, J., and H. Fossen, 2001, Structural core analysis from the Gullfaks area, northern North Sea: Marine and Petroleum Geology, v. 18, p. 411–439, <https://doi.org/10.1016/s0264-8172(00)00068-4>.

Hudec, M. R., I. O. Norton, M. P. A. Jackson, and F. J. Peel, 2013a, Jurassic evolution of the Gulf of Mexico salt basin; American Association of Petroleum Geologists Bulletin, v. 97, p. 1683–1710, <https://doi.org/10.1306/04011312073>.

Hudec, M. R., I. O. Norton, M. P. A. Jackson, and F. J. Peel, 2013b, Influence of deep Louann structure on the evolution of the northern Gulf of Mexico: American Association of Petroleum Geologists Bulletin, v. 97, p. 1711–1755, https://doi.org/10.1306/04011312074>.

Hughes, D. J., 1968, Salt tectonics as related to several Smackover fields along the northeast rim of the Gulf of Mexico Basin: Gulf Coast Association of Geological Societies Transactions, v. 18, p. 320–330.

Hunt, B., 2013, Regional Norphlet facies correlation, analysis and implications for paleostructure and provenance, eastern Gulf of Mexico: Master's Thesis, University of Alabama, Tuscaloosa, 102 p.

Hunt, B., D. M. Robinson, A. L. Weislogel, and R. C. Ewing, 2017, Sediment source regions and paleotransport of the Upper Jurassic Norphlet Formation, eastern Gulf of Mexico; American Association of Petroleum Geologists Bulletin, v. 101, p. 1519–1542, <https://doi.org/10.1306/10171615156>.

Hunt, J. M., F. Stewart, and P. A. Dickey, 1954, Origin of hydrocarbons of Uinta Basin, Utah: American Association of Petroleum Geologists Bulletin, v. 38, p. 1671–1698, <https://doi.org/10.1306/5ceae01c-16bb-11d7-8645000102c1865d>.

Hurst, A. and P. H. Nadeau, 1995, Clay microporosity in reservoir sandstones: An application of quantitative electron microscopy in petrophysical evaluation, American Association of Petroleum Geologists Bulletin, v. 79, p. 653–573, <https://doi.org/10.1306/8d2b1598-171e-11d7-8645000102c1865d>.

Ings, S. J., and C. Beaumont, 2010, Shortening viscous pressure ridges, a solution to the enigma of initiating salt "withdrawal" minibasins: Geology, v. 38, p. 339–342, <https://doi.org/10.1130/G30520.1>.

Jackson, J. B., and P. M. Harris, 1982, Jurassic petroleum geology of Southwestern Clarke County, Mississippi: Gulf Coast Association of Geological Societies Transactions, v. 32, p. 45–57.

Jackson, M. P. A., and W. E. Galloway, 1984, Structural and depositional styles of Gulf Coast tertiary continental margins: Application to hydrocarbon exploration: American Association of Petroleum Geologists Continuing Education Course Note Series 25, Tulsa, Oklahoma, 226 p.

Jacob, H., 1989, Classification, structure, genesis and practical importance of natural solid oil bitumen ("migrabitumen"): International Journal of Coal Geology, v. 11, p. 65–79, <https://doi.org/10.1016/0166-5162(89)90113-4>.

Knipe, R. J., Q. J. Fisher, M. R. Clennell, A. B. Farmer, A. Harrison, B. Kidd, E. McAllister, J. R. Porter, and E. A. White, 1997, Fault seal analysis: Successful methodologies, application and future directions, *in* P. Møller-Pedersen and A. G. Koestler, eds., Hydrocarbon seals: Importance for exploration and production: Norwegian Petroleum Society Special Publication 7, Oslo, p. 15–38, <https://doi.org/10.1016/S0928-8937(97)80004-5>.

Kocurek, G., and K. Havholm, 1993, Eolian sequence stratigraphy—A conceptual framework, *in* P. Weimer and H. Posamentier, eds., Recent advances in and applications of siliciclastic sequence stratigraphy: American Association of Petroleum Geologists Memoir 58, Tulsa, Oklahoma, p. 393–409, <https://doi.org/10.1306/0c9b03eb-1710-11d7-8645000102c1865d>.

Kugler, R. L., and A. E. McHugh, 1990, Regional diagenetic variation in Norphlet sandstone: Implications for reservoir quality and the origin of porosity: Gulf Coast Association of Geological Societies Transactions, v. 40, p. 411–423, <https://doi.org/10.1306/20b23147-170d-11d7-8645000102c1865d>.

Kugler, R. L., and R. M. Mink, 1998, Depositional and diagenetic history and petroleum geology of the Jurassic Norphlet Formation of the Alabama coastal waters area and adjacent Federal waters area, *in* G. Dellagiarino, L. A. Miller, and S. Doenges, eds., Fourth symposium on studies related to continental margins—A summary of year–9 and year–10 activities, November 16–19, 1997, Corpus Christi, Texas: Minerals Management Service, Association of American State Geologists, and Bureau of Economic Geology, p. 100–116, <https://doi.org/10.1080/106411999273909>.

Langmuir, D., and D. O. Whittemore, 1971, Variations in the stability of precipitated ferric oxyhydroxides, *in* J. D. Hem, ed., Nonequilibrium systems and processes in natural water chemistry, a symposium: Advances in Chemistry, v. 106, p. 209–234, <https://doi.org/10.1021/ba-1971-0106.ch008>.

Lawton, T. F., and B. J. Buck, 2006, Implications of diapir-derived detritus and gypsic paleosols in Lower Triassic strata near the Castle Valley salt wall, Paradox Basin, Utah: Geology, v. 34, p. 885–888, <https://doi.org/10.1130/g22574.1>.

Levandowski, D. W., M. E. Kaley, S. R. Silverman, and R. G. Smalley, 1973, Cementation in Lyons sandstone and its role in oil accumulation, Denver Basin, Colorado: American Association of Petroleum Geologists Bulletin, v. 57, p. 2217–2244, <https://doi.org/10.1306/83d912db-16c7-11d7-8645000102c1865d>.

Lindquist, S. J., 1983, Nugget Formation reservoir characteristics affecting production in the overthrust belt of S.W. Wyoming: Journal of Petroleum Technology, v. 35, p. 1355–1365, <https://doi.org/10.1016/0037-0738(88)90059-0>.

Lomando, A. J., 1992, The influence of solid reservoir bitumen on reservoir quality: American Association of Petroleum Geologists Bulletin, v. 76, p. 1137–1152, <https://doi.org/10.1306/bdff8984-1718-11d7-8645000102c1865d>.

Lupe, R., and T. S. Ahlbrandt, 1979, Sediments of the ancient eolian environment—Reservoir inhomogeneity, *in* E. D. McKee, ed., A study of global sand seas: U.S. Geological Survey Professional Paper 1052, p. 241–252, <https://doi.org/10.1306/bdff8984-1718-11d7-8645000102c1865d>.

Macgregor, D. S., 1996, Factors controlling the destruction or preservation of giant light oilfields: Petroleum Geoscience, v. 2, p. 197–217, <https://doi.org/10.1144/petgeo.2.3.197>.

Mancini, E. A., R. M. Mink, B. L. Bearden, and R. P. Wilkerson, 1985, Norphlet Formation (Upper Jurassic) of southwestern and offshore Alabama: Environments of deposition and petroleum geology: American Association of Petroleum Geologists Bulletin, v. 69. p. 881–898, <https://doi.org/10.1306/ad462b14-16f7-11d7-8645000102c1865d>.

Mankiewicz, P. J., R. J. Pottorf, M. G. Kozar, and P. Vrolijk, 2009, Gas geochemistry of the Mobile Bay Jurassic Norphlet Formation: Thermal controls and implications for reservoir connectivity: American Association of Petroleum Geologists Bulletin, v. 93, p. 1319–1346, <https://doi.org/10.1306/05220908171>.

Martin, R. G., 1978, Northern and eastern Gulf of Mexico continental margin: Stratigraphic and structural framework; 1. The setting: Stratigraphic and structural framework, *in* A. H. Bouma, G. T. Moore, and J. M. Coleman, eds., Framework, facies, and oil trapping characteristics of the upper continental margin: American Association of Petroleum Geologists Studies in Geology 7, Tulsa, Oklahoma, p. 21–42, <https://doi.org/10.1017/s0016756800044599>.

Marton, G. L., and R. T. Buffler, 2016, Jurassic-Cretaceous tectonic evolution of the southeastern Gulf of Mexico, constraints on the style and timing of Gulf of Mexico rift-drift development: American Association of Petroleum Geologists Search and Discovery Article 41945, Tulsa, Oklahoma, 24 p., <http://www.searchanddiscovery.com/pdfz/documents/2016/41945marton/ndx_marton.pdf.html>.

Marzano, M. S., G. M. Pense, and P. Andronaco, 1988, A comparison of the Jurassic Norphlet Formation in Mary Ann Field, Mobile Bay, Alabama to onshore regional Norphlet trends: Gulf Coast Association of Geological Societies Transactions, v. 38, p. 85–100, <https://doi.org/10.1306/703c9889-1707-11d7-8645000102c1865d>.

Matlack, K. S., D. W. Houseknecht, and K. R. Applin, 1989, Emplacement of clay into sand by infiltration: Journal of Sedimentary Petrology, v. 59, p. 77–87, <https://doi.org/10.1306/212f8f21-2b24-11d7-8648000102c1865d>.

McBride, E. F., 1981, Diagenetic history of Norphlet Formation (Upper Jurassic), Rankin County, Mississippi: Gulf Coast Association of Geological Societies Transactions, v. 31, p. 347–351, <https://doi.org/10.1306/a1adda54-0dfe-11d7-8641000102c1865d>.

McBride, E. F., L. S. Land, L. E. Mack, 1987, Diagenesis of eolian and fluvial feldspathic sandstones, Norphlet Formation (Upper Jurassic), Rankin County, Mississippi, and Mobile County, Alabama: American Association of Petroleum Geologists Bulletin, v. 71, p. 1019–1033, <https://doi.org/10.1306/703c7dea-1707-11d7-8645000102c1865d>.

McDonough, J., R. T. Murphy, R. S. Pilcher, and C. Burke, 2008, A deepwater frontier in the north-eastern Gulf of Mexico: The Jurassic Norphlet sandstone oil play: American Association of Petroleum Geologists Search and Discovery Article 471347, Tulsa, Oklahoma, 1 p., <http://www.searchanddiscovery.com/abstracts/html/2008/intl_capetown/abstracts/471347.htm>.

Miller, D. N., and R. L. Folk, 1955, Occurrence of detrital magnetite and ilmenite in red sediments: New approach to the significance of red beds: American Association of Petroleum Geologists Bulletin, v. 39, p. 338–345, <https://doi.org/10.1306/5ceae157-16bb-11d7-8645000102c1865d>.

Miller, R. G., 1992, The global oil system: The relationship between oil generation, loss, half-life, and the world crude oil resource: American Association of Petroleum Geologists Bulletin, v. 76, p. 489–500, <https://doi.org/10.1306/bdff8844-1718-11d7-8645000102c1865d>.

Moulton, G. F., 1926, Some features of redbed bleaching: American Association of Petroleum Geologists Bulletin, v. 10, p. 304–311, <https://doi.org/10.1306/3d932715-16b1-11d7-8645000102c1865d>.

Net, L. I., 2003, Linking diagenetic styles to reservoir quality: The Eolian Nugget Sandstone (Jurassic), SW Wyoming: American Association of Petroleum Geologists Search and Discovery Article 90013, Tulsa, Oklahoma, 3 p., <http://www.searchanddiscovery.com/pdfz/abstracts/pdf/2003/annual/extend/ndx_79975.PDF.html>.

Parry, W. T., M. A. Chan, and B. P. Nash, 2009, Diagenetic characteristics of the Jurassic Navajo Sandstone in the Covenant Oil Field, Central Utah Thrust Belt: American Association of Petroleum Geologists Bulletin, v. 93, p. 1039–1061, <https://doi.org/10.1306/04270908170>.

Peel, F. J., 2014, How do salt withdrawal minibasins form? Insights from forward modelling, and implications for hydrocarbon migration: Tectonophysics, v. 630, p. 222–235, <https://doi.org/10.1016/j.tecto.2014.05.027>.

Pepper, A. S., and P. J. Corvi, 1995, Simple kinetic models of petroleum formation. Part I: Oil and gas generation from kerogen, Marine and Petroleum Geology, v. 12, p. 291–319, <https://doi.org/10.1016/0264-8172(95)98381-e>.

Picard, M. D., 1965, Iron oxides and fine-grained rocks of Red Peak and Crow Mountain Sandstone members, Chugwater (Triassic) Formation, Wyoming: Journal of Sedimentary Petrology, v. 35, p.464–479, <https://doi.org/10.1306/74d712ad-2b21-11d7-8648000102c1865d>.

Pilcher, R. S., R. T. Murphy, and J. M. Ciosek, 2014, Jurassic raft tectonics in the northeastern Gulf of Mexico: Interpretation, v. 2, p. SM39–SM55, <https://doi.org/10.1190/int-2014-0058.1>.

Pittman, E. D., 1979, Porosity, diagenesis, and productive capability of sandstone reservoirs, *in* P. A. Scholle and P. R. Schluger, eds., Aspects of diagenesis: Society of Economic Paleontologists and Mineralogists Special Publication 26, Tulsa, Oklahoma, p. 159–173, <https://doi.org/10.2110/pec.79.26.0159>.

Pudlo, D., D. Albrecht, G. Leonhard, R. Gauppa, B. Kohlheppa, B. Meyerc, V. Reitenbachb, and J. Wienandb, 2011, Petrophysical, facies and mineralogical-geochemical investigations of Rotliegend sandstones from the Altmark Natural Gas Field in central Germany: *Energy Procedia*, v. 4, p. 4648–4655, <https://doi.org/10.1016/j.egypro.2011.02.425>.

Rainoldi, A. L., M. Franchini, D. Beaufort, P. Mozley, A. Giusiano, et al., 2015, Mineral reactions associated with hydrocarbon paleomigration in the Huincul High, Neuquen Basin, Argentina: Geological Society of America Bulletin, Geological Society of America, v. 127, p. 1711–1729, <https://doi.org/10.1130/b31201.1>.

Rarey, P. J., 1990, Sedimentological and reservoir characteristics of the upper Sespe Formation at Sockeye Field, offshore

California, *in* M. Keller and M. McGowen, eds., Miocene and Oligocene petroleum reservoirs of the Santa Maria and Santa Barbara–Ventura basins, California: Society of Economic Paleontologists and Mineralogists Core Workshop 14, Tulsa, Oklahoma, p. 12–18, <https://doi.org/10.2110/cor.90.14.0012>.

Rogers, M. A., J. D. McAlary, and N. J. L. Bailey, 1974, Significance of reservoir bitumens to thermal maturation studies, western Canada Basin: American Association of Petroleum Geologists Bulletin, v. 58, p. 1806–1824, <https://doi.org/10.1306/83d919b6-16c7-11d7-8645000102c1865d>.

Rice, D. D., C. J. Schenk, J. W. Schmoker, J. E. Fox, J. L. Clayto, T. S. Dyman, D. K. Higley, C. W. Keighin, B. E. Law, and R. M. Pollastro, 1997, Deep natural gas resources in the eastern Gulf of Mexico: U.S. Geological Survey Bulletin 2146, p. 219–229.

Sassen, R., 1988, Geochemical and carbon isotopic studies of crude oil destruction, bitumen precipitation, and sulphate reduction in the deep Smackover Formation: Organic Geochemistry, v. 12, p. 351–361, <https://doi.org/10.1016/0146-6380(88)90009-5>.

Sawyer, D. S., R. T. Buffler, and R. H. Pilger, Jr., 1991, The crust under the Gulf of Mexico Basin, *in* Salvador, A. ed., The geology of North America, v. J: The Gulf of Mexico Basin: Geological Society of America, Boulder, Colorado, p. 53–72, <https://doi.org/10.1130/dnag-gna-j.53>.

Schenk, C. J., 1981, Porosity and textural characteristics of eolian stratification: American Association of Petroleum Geologists Bulletin, v. 65, p. 986.

Schenk, C. J., 1983, Textural and structural characteristics of some experimentally formed eolian strata, *in* M. E. Brookfield and T. S. Ahlbrandt, eds., Eolian sediments and processes: Developments in Sedimentology, v. 38, p. 41–49, <https://doi.org/10.1016/s0070-4571(08)70787-8>.

Schenk, C. J., and J. W. Schmoker, 1993, Role of halite in the evolution of sandstone porosity, Upper Jurassic Norphlet Formation, Mississippi Salt Basin: Gulf Coast Association of Geological Societies Transactions, v. 43, p. 357–362.

Shammari, S., S. Franks, and O. Soliman, 2011, Depositional and facies controls on infiltrated/inherited clay coatings: Unayzah sandstones, Saudi Arabia: American Association of Petroleum Geologists Search and Discovery Article 50459, Tulsa, Oklahoma, 24 p., <http://www.searchanddiscovery.com/documents/2011/50459shammari/ndx_shammari.pdf>.

Sigsby, R. J., 1976, Paleoenvironmental analysis of the Big Escambia Creek–Jay–Blackjack Creek Field area: Gulf Coast Association of Geological Societies Transaction, v. 26, p. 258–270.

Sofer, Z., 1988, Biomarkers and carbon isotopes of oils in the Jurassic Smackover Trend of the Gulf Coast States, U.S.A.: Organic Geochemistry, v. 12, p. 421–432, <https://doi.org/10.1016/0146-6380(88)90152-0>.

Steier, A., 2018, Jurassic-Cretaceous stratigraphic and structural evolution of the northern Yucatan margin, Gulf of Mexico Basin: Master's Thesis, University of Houston, Texas, 69 p.

Surdam, R. C., Z. S. Jiao, and D. B. MacGowan, 1993, Redox reactions involving hydrocarbons and mineral oxidants: A mechanism for significant porosity enhancements in sandstones: American Association of Petroleum Geologists Bulletin, v. 77, p. 1509–1518, <https://doi.org/10.1306/bdff8ed4-1718-11d7-8645000102c1865d>.

Taylor, T., R. Stancliffe, C. Macaulay, and L. Hathon, 2004, High temperature quartz cementation and the timing of hydrocarbon accumulation in the Jurassic Norphlet sandstone offshore Gulf of Mexico, USA, *in* J. M. Cubitt, W. A. England, and S. Larter, eds., Understanding petroleum reservoirs: Towards an integrated reservoir engineering and geochemical approach: Geological Society (London) Special Publications, v. 237, p. 257–278, <https://doi.org/10.1144/gsl.sp.2004.237.01.15>.

Taylor, T. R., M. R. Giles, L. A. Hathon, T. N. Diggs, N. R. Braunsdorf, G. V. Birbiglia, M. G. Kittridge, C. I. Macaulay, and I. S. Espejo, 2010, Sandstone diagenesis and reservoir quality prediction: Models, myths, and reality. American Association of Petroleum Geologists Bulletin, v. 94, 1093–1132, <https://doi.org/10.1306/04211009123>.

Thomson, A., 1979, Preservation of porosity in the deep Woodbine/Tuscaloosa trend, Louisiana: Gulf Coast Association of Geological Societies Transactions, v. 29, p. 1156–1162, <https://doi.org/10.1306/2f918810-16ce-11d7-8645000102c1865d>.

Thomson, A., and R. J. Stancliffe, 1990, Diagenetic controls on reservoir quality, eolian Norphlet Formation, South State Line Field, Mississippi, *in* J. H. Barwis, J. G. McPherson, and J. R. J. Studlick, eds., Sandstone petroleum reservoirs: Springer-Verlag, New York, p. 205–224, <https://doi.org/10.1007/978-1-4613-8988-0_10>.

Tissot, B. P., and D. H. Welte, 1984, Petroleum formation and occurrence, 2nd ed.: Springer-Verlag, New York, 699 p., <https://doi.org/10.1007/978-3-642-87813-8>.

Trudgill, B. D., 2011, Evolution of salt structures in the northern Paradox Basin: Controls on evaporite deposition, salt wall growth and supra-salt stratigraphic architecture: Basin Research, v. 23, p. 208–238, <https://doi.org/10.1111/j.1365-2117.2011.00522.x>.

Tucker, C. F., 2013, Solving for paleo porosity: Volumetric fractions of solid and liquid phases using NMR, density, and TOC measurements from logs and core: Society of Petrophysicists and Well Log Analysts Paper SPWLA–2013–BBBB, Houston, Texas, 11 p.

Turner, P., 1974, Origin or red beds in the Ringerrike Group (Silurian) of Norway: Sedimentary Geology, v. 12, p. 215–235, <https://doi.org/10.1016/0037-0738(74)90011-6>.

Turner, P., 1980, Continental red beds: Elsevier Scientific Publishing Company, Amsterdam, Netherlands, 562 p., <https://doi.org/10.1016/s0070-4571(08)x7013-x>.

Turner, P., M. Jones, D. J. Prosser, G. Williams, and A. Searl, 1993, Structural and sedimentological controls on diagenesis in the Ravenspurn North gas reservoir, UK Southern North Sea: Geological Society (London) Petroleum Geology Conference Series, v. 4; , p. 771–785, <https://doi.org/10.1144/0040771>.

Van Houten, F. B., 1961, Climatic significance of red beds, *in* A. E. M. Nairn, ed., Descriptive paleoclimatology: Interscience Pub., Inc., New York, p. 89–139.

Van Houten, F. B., 1973, Origin of red beds: A Review—1961–1972: Annual Review of Earth and Planetary Sciences, v. 1, p. 39–61, <https://doi.org/10.1146/annurev.ea.01.050173.000351>.

Walderhaug, O., 1996, Kinetic modeling of quartz cementation and porosity loss in deeply buried sandstone reservoirs: American Association of Petroleum Geologists Bulletin, v. 80, p. 731–745, <https://doi.org/10.1306/64ed88a4-1724-11d7-8645000102c1865d>.

Walker, T. R., 1967, Formation of red beds in modern and ancient deserts: Geological Society of America Bulletin, v. 78, p. 353–368, <https://doi.org/10.1130/0016-7606(1967)78[353:forbim]2.0.co;2>.

Walker, T. R., and R. M. Honea, 1969, Iron content of modern deposits in the Sonaran desert —A contribution to the origin of red beds: Geological Society of America Bulletin, v. 80, p. 535–543, <https://doi.org/10.1130/0016-7606(1969)80[535:icomdi]2.0.co;2>.

Walker, T. R., 1974, Formation of red beds in moist tropical climates: A hypothesis: Geological Society of America Bulletin, v. 85, p. 633–638, <https://doi.org/10.1130/0016-7606(1974)85<633:FORBIM>2.0.CO;2>.

Walker, T. R., and Crone, A. J., 1974, Mechanically-infiltrated clay matrix in desert alluvium: Geological Society of America Abstracts with Programs, v. 6, no. 7, p. 998.

Walker, T. R., 1976, Diagenetic origin of continental red beds, *in* Horst Falke, ed., The continental Permian in west, central and south Europe: Nato Advanced Study Institutes Series (Series C—Mathematical and Physical Sciences), v. 22, p. 240–282, <https://doi.org/10.1007/978-94-010-1461-8_20>.

Walker, T. R., L. J. Suttner, and G. H. Mack, 1978, Paleoclimate interpretation from a petrographic comparison of Holocene Sands and the Fountain Formation (Pennsylvanian) in the Colorado Front Range: A discussion: Journal of Sedimentary Petrology, v. 48, p. 1011–1013, <https://doi.org/10.1306/212f75ea -2b24-11d7-8648000102c1865d>.

Walker, T. R., 1979, Red colour in eolian sand, *in* E. D. McKee, ed., A study of global sand seas: U.S. Geological Survey Professional Paper 1052, p. 62–81, <https://doi.org/10.3133/pp1052>.

Weber, R. D., and B. W. Parker, 2016, Pre-Albian biostratigraphical and paleoecological observations from the De Soto Canyon area; Gulf of Mexico, USA, *in* C. Lowery, J. W. Snedden, and N. C. Rosen, eds., Mesozoic of the Gulf Rim and beyond: New progress in science and exploration of the Gulf of Mexico Basin: Proceedings of the 35th Annual Gulf Coast Section of the Society of Economic Paleontologists and Mineralogists Foundation Perkins-Rosen Research Conference, Houston, Texas, p. 154–172, <https://doi.org/10.5724/gcs.15.35.0154>.

Weimer, P., E. Zimmermann, R. Bouroullec, S. Cumella, J. Adson, W. Gutterman, T. Payeur, B. Snyder, H. Hirsh, D. Bettinger, 2016a, Litho- and biostratigraphic evolution of the Upper Jurassic through top Cretaceous section, northern deepwater Gulf of Mexico: Preliminary results: Gulf Coast Association of Geological Societies Transactions, v. 66, p. 569–582.

Weimer, P., R. Bouroullec, V. Matt, T. Lapinski, A. van den Berg, and J. G. Roesink, 2016b, Petroleum geology of the Mississippi Canyon, Atwater Valley, western DeSoto Canyon western Lloyd areas, northern deepwater Gulf of Mexico: Source rocks, generation, and accumulation: Gulf Coast Association of Geological Societies Transactions, v. 66, p. 601–624.

Weimer, P., et al., 2017, Atlas of fields and discoveries, central Mississippi Canyon, Atwater Valley, northwestern Lloyd Ridge, and western DeSoto Canyon protraction areas, northern deepwater Gulf of Mexico: American Association of Petroleum Geologists Bulletin, v. 101, p. 995–1002 <https://doi.org/10.1306/bltnfieldatlas070815>.

Weimer, R. J., K. W. Porter, and C. B. Land, 1985, Depositional modeling of detrital rocks. Lyons Sandstone: Society of Economic Paleontologists and Mineralogists Core Workshop 8, Tulsa, Oklahoma, p. 232–237.

Wilson, K. L., 2011, The origin and development of the Tampa Embayment: Implications for the tectonic evolution of the Eastern Gulf of Mexico, Master's thesis, The University of Alabama, Tuscaloosa, Alabama, 57 p.

Zuluaga, L. F., A. Rotevatn, E. Keilegavlen, and H. Fossen, 2016, The effect of deformation bands on simulated fluid flow within fault-propagation fold trap types: Lessons from the San Rafael monocline, Utah: American Association of Petroleum Geologists Bulletin, v. 100, p. 1523–1540, <https://doi.org/10.1306/04151614153>.